Master Thesis in Geographical Information Science nr 47

Development of a method for mapping the highest coastline in Sweden using breaklines extracted from high resolution digital elevation models

Anna Lundgren

2016
Department of
Physical Geography and Ecosystem Science
Centre for Geographical Information Systems
Lund University
Sölvegatan 12
S-223 62 Lund
Sweden

Anna Lundgren (2016). Development of a method for mapping the highest coastline in Sweden using breaklines extracted from high resolution digital elevation models.
Master degree thesis, 30 credits in Master in Geographical Information Sciences
Department of Physical Geography and Ecosystem Science, Lund University

Development of a method for mapping the highest coastline in Sweden using breaklines extracted from high resolution digital elevation models

Anna Lundgren
Master thesis, 30 credits, in Geographical Information Sciences

Tore Påsse
Geological Survey of Sweden

Harry Lankreijer
Lund University

Abstract

Anna Lundgren

Development of a method for mapping the highest coastline in Sweden using breaklines extracted from high resolution digital elevation models

The geospatial position of the highest coastline (HCL) defines the boundary between subaquatic and supra-aquatic deposited sediments. Today the HCL is located at different elevations throughout Sweden, a few m.a.s.l. in southern Scania to around 289 m.a.s.l. at the coast of Ångermanland, due to the glacio-isostatic rebound. High quality data of the HCL is of interest e.g. in land-use and spatial planning and when reconstructing historical sea levels and events within the Baltic Sea Basin.

In this study the use of land surface parameter (LSP) breakline extraction methods applied on high resolution DEMs for automating mapping of the HCL in wave washed areas in Sweden was investigated. Appropriate scale dimensions for enhancing breaklines of interest was estimated by testing a range of moving window sizes for the LSP computations. Four semi-automated mapping methods based on curvature breakline extraction was developed in ESRI's ArcGIS 10.2.2 for Desktop and applied on two pilot areas in Sweden. The methods consist of a common breakline extraction step and individual breakline classification steps with differing grade of automation. To compare the HCL maps generated by the developed methods with HCL maps manually mapped from high resolution hillshade maps and with the current HCL data supplied by the Geological Survey of Sweden (SGU) classification accuracies and elevation errors were computed using a reference data set.

A 22x22m moving window size was found successful for the extraction of curvature breaklines related to wave washed features and glacial flow lineation features used to map the HCL within the pilot areas under investigation. The accuracy assessment indicates that three of the developed methods generate HCL maps with accuracies above the current HCL data provided by SGU and accuracies similar to or above HCL maps based on manually mapped HCL data points. Higher accuracies were found for the methods using a manual classification of the extracted breaklines than for the methods using an automated classification of the extracted breaklines.

This study found that, by applying curvature breakline extraction methods on high resolution DEMs, HCL mapping in wave washed areas can be made more automated, structured and reproducible while still reaching similar accuracies as manual hillshade mapping methods.

Keywords: Physical Geography and Ecosystem analysis, GIS, the highest coastline, Geological Survey of Sweden, SGU, high resolution digital elevation model, LiDAR, land surface parameter, curvature, breakline extraction, geomorphological mapping

Advisor: **Tore Påsse (SGU) and Harry Lankreijer (LU)**
Master degree project 30 credits in Master in Geographical Information Sciences, 2016
Department of Physical Geography and Ecosystem Science, Lund University.
Thesis nr 47

Sammanfattning

Anna Lundgren

Utveckling av en metod för att kartera högsta kustlinjen i Sverige med hjälp av brytlinjer extraherade från högupplösta höjdmodeller

Högsta kustlinjens (HK) geografiska läge i landskapet markerar gränsen mellan subakvatiskt och supraakvatiskt avsatta sediment. Idag varierar HKs höjd över havet från några få m.ö.h. i Skåne till omkring 289 m.ö.h. i Ångermanland på grund av den glacialisostatiska landhöjningen. Högkvalitativ HK-data är av intresse bland annat vid markanvändnings- och samhällsplanering och vid rekonstruktion av historiska havsnivåer och händelser i Östersjöns havsbassäng.

Den här studien har undersökt möjligheten att använda brytlinjer i terrängen, extraherade från så kallade ”land surface parameters” (LSPs) som genererats ur högupplöst höjddata, för att automatisera karteringen av HK i svallade områden i Sverige. För att uppskatta lämpliga skaldimensioner som framhäver terrängbrytlinjer av intresse för studien testades ett intervall av fönsterstorlekar för terrängparameterberäkningarna. Fyra stycken semi-automatiserade metoder för att extrahera brytlinjer baserade på markytans krökning utvecklades i ESRIs ArcGIS 10.2.2 for Desktop och tillämpades på två pilotområden i Sverige. Metoderna är uppbyggda av ett gemensamt steg där brytlinjerna extraheras och ett individuellt steg där brytlinjerna klassificeras med olika grad av automation. För att jämföra HK-kartorna genererade från de utvecklade metoderna med HK-kartor som manuellt karterats från högupplösta terrängskuggningskartor och med HK-data som idag finns tillgänglig hos Sveriges geologiska undersökning (SGU) beräknades klassificeringsnoggrannhet och höjdfel för samtliga kartor i förhållande till referensdata.

Studien fann att en 22x22m fönsterstorlek var framgångsrik för att extrahera brytlinjer av markytans krökning relaterad till strandvallar och glaciala lineationer som används för att kartera HK i pilotområdena. Noggrannhetsutvärderingen indikerar att tre av de utvecklade metoderna genererar HK-kartor med högre noggrannhet än SGUs HK-data, och liknande till högre noggrannhet än HK-kartor baserade på HK-punkter manuellt karterade från högupplösta terrängskuggningskartor. Metoderna som använder en manuell klassificering av brytlinjerna visade en högre noggrannhet än metoderna som använder en automatiserad klassificering av brytlinjerna.

Denna studie visar att brytlinjer av markytans krökning genererade från högupplösta höjdmodeller kan användas för att göra kartering av HK i svallade områden mer automatiserad, strukturerad och reproducerbar samtidigt som man uppnår liknande noggrannhet som vid manuell kartering baserad på terrängskuggningskartor.

Nyckelord: naturgeografi och ekosystemvetenskap, GIS, högsta kustlinjen, Sveriges geologiska undersökning, SGU, högupplöst höjdmodell, LiDAR, terrängparameter, krökning, brytlinje-extraktion, geomorfologisk kartering

Handledare: **Tore Påsse (SGU) och Harry Lankreijer (LU)**
Masterexamensarbete 30 högskolepoäng i Master i geografisk informationsvetenskap, 2016
Institutionen för naturgeografi och ekosystemvetenskap, Lunds universitet.
Uppsats nr 47

Table of contents

1 Introduction 1
1.1 Project aim 1
1.2 Project initiation 2
2 Background 3
2.1 The highest coastline in Sweden 3
2.2 High resolution DEMs 3
2.3 Automated image interpretation methods 3
2.4 How can landforms be described by LSPs? 4
2.5 Scale 4
2.6 LSP and scale dimensions used in other studies 5
3 Methods and material 7
3.1 Preparation phase 9
3.1.1 Data 9
3.1.2 Pre-study 10
3.1.3 Study area 10
3.1.4 Literature study 12
3.2 Development phase 12
3.2.1 Method idea and development 12
3.2.2 LSP generation and scale assessment 13
3.2.3 Visual evaluation of LSP rasters 14
3.2.4 Extract breaklines for pilot area 14
3.2.5 Breakline classification and HCL identification 15
3.2.6 Type1 model method 16
3.2.7 Type3 model method 18
3.2.8 Type4 model method 18
3.2.9 Type4top model method 18
3.2.10 Interpolate HCL 19
3.2.11 Ground truth data 19
3.3 Evaluation phase 19
3.3.1 Error matrix 20
3.3.2 HCL boundary classification accuracy – “buffer method” 22
3.3.3 Elevation error evaluation using 100 random samples 26
4 Result 29
4.1 LSP and scale dimension evaluation 29
4.2 Breakline extraction result for 11x11cell window 35

4.3 Model method classification of breaklines and resulting HCL point generation 41
4.3.1 Type1 model method 41
4.3.2 Type3 model method 46
4.3.3 Type4 model method 48
4.3.4 Type4top model method 50
4.3.5 Manual model method HCL points 52
4.3.6 Agrell model method HCL points 53
4.4 Resulting HCL maps – surfaces and boundaries 54
4.5 Map evaluation results – accuracy estimations 57
4.5.1 Error matrix result for interpolated HCL-surface 57
4.5.2 HCL boundary classification accuracy – “buffer method” 62
4.5.3 Elevation error for model methods 64
5 Discussion 67
5.1 Result 67
5.1.1 Error matrix 67
5.1.2 Completeness 67
5.1.3 Correctness 68
5.1.4 Quality 68
5.1.5 Redundancy 68
5.1.6 Elevation error 69
5.2 Method 70
5.2.1 Method choice 70
5.2.2 Choice of LSP for HCL landform extraction 70
5.2.3 Scale dimension 70
5.2.4 Breakline classification using coarse scale LSP and object attributes 71
5.2.5 Interpolation method 73
5.2.6 Processing time 74
5.3 Sources of error 76
5.3.1 Input data 76
5.3.2 Interpreter bias 76
5.3.3 Parameter settings and tool functionality 77
5.4 Future work 77
6 Conclusions 79
7 Acknowledgements 81
8 References 83
9 Appendices 89

9.1 Appendix A 89
9.2 Appendix B 91
9.3 Appendix C 106
9.4 Appendix D 110
9.5 Appendix E 112
9.6 Appendix F 115

Abbreviation list

Abbreviation	*Full name*
ALS	Airborne Laser Scanning
BSB	the Baltic Sea Basin
DEM	Digital Elevation Model
ESRI	Environmental Systems Research Institute
GIS	Geographic Information System
HCL	the Highest Coastline
IDW	Inverse Distance Weigthed
LiDAR	Light Detection and Ranging
LSP	Land Surface Parameter
MRS	Multi Resolution Segmentation
NMAD	Normalized Median Absolute Deviation
OBIA	Object Based Image Analysis
SGU	the Geological Survey of Sweden

1 Introduction

The geospatial position of the highest coastline (HCL) is of interest when mapping quaternary deposits since it defines the boundary between subaquatic and supra-aquatic deposited sediments, information of high importance in e.g. land-use and spatial planning (Peterson and Smith 2013, Ojala et al. 2013). The position of the HCL in Sweden is also useful when reconstructing historical sea levels and events within the Baltic Sea Basin (BSB) (Ojala et al. 2013, Jakobsson et al. 2007, Påsse and Andersson 2005). Detailed information of the historical development of the BSB can further be important components in climate and ocean circulation modeling (Jakobsson et al. 2007).

The HCL has been mapped and its position and linkage to the historical events in the BSB discussed by many researchers throughout the past starting in the late nineteen century (see e.g. Lundqvist G. 1961, Agrell 1976, Påsse 1983, Björck 1995, Lundqvist J. 2002, Påsse and Andersson 2005, and Berglund 2012).

The Geological Survey of Sweden (SGU) provides a database of HCL locations with shifting spatial accuracies (horizontally around 50 m and vertically around ±2 m) compiled by Agrell (2001) from historical HCL studies (SGU 2015d).

The national high resolution digital elevation model (DEM) offers the opportunity to generate a database of HCL locations with accuracies matching the DEMs (horizontal resolution of 2 meters and a vertical resolution of minimum ±0.5 meter, Lantmäteriet 2015). Hillshade maps generated from high resolution DEM are excellent support for manual mapping of HCL locations and other geomorphological landforms (Ojala et al. 2013, Roering et al. 2013, Dowling et al. 2012, Smith et al. 2006). Manual mapping of the HCL using hillshade maps is however time consuming and the method (as other operator driven methods) susceptible to interpreter bias (Peterson and Smith 2013, Roering et al. 2013, Seijmonsbegen et al. 2011).

By automating the process of mapping the HCL using the high resolution DEM data, objective and standardized HCL data can be received with a more consistent quality. By using breaklines extracted from land surface parameters (LSP) (Rutzinger et al. 2012; 2011; 2007, Seijmonsbegen et al. 2011) generated from the DEM data together with breakline classification procedures the identification of landforms connected to the HCL can be automated. This information can further be used to automate manual HCL mapping methods which are based on the identified landforms.

1.1 Project aim

The main aim of this study is to investigate the possibilities of automating the mapping of the highest coastline (HCL) in wave washed areas in Sweden by utilizing topographic information extracted from the national high resolution DEM.

Project objectives:

- Incorporate geology expert knowledge used in hillshade based manual mapping of the highest coastline (HCL) in wave washed areas in Sweden into an automated mapping methodology.
- Generate land surface parameters (LSP) at appropriate scale dimensions from the DEM data that enhance the geomorphological landforms used to identify the HCL in wave washed areas.
- Develop, test (put into practice), and evaluate potential automated mapping method workflows which could be used to identify locations of the HCL in wave washed areas.

- Compare the developed method(s) with the manual mapping method and data present in SGU's HCL database.
- Suggest method(s) for updating SGU's database of existing wave washed HCL locations in Sweden to match the national high resolution DEM.

1.2 Project initiation

The project was initiated in 2014 by Tore Påsse at the Geological Survey of Sweden (SGU) (SGU 2015h). The final goal is to update SGU's database of HCL locations (SGU 2015d) to match the national high resolution DEM provided by the Lantmäteriet (Lantmäteriet 2015). This master thesis is a sub-project with the aim to structure and automate the mapping process of the HCL using the high resolution DEM with focus on mapping procedures in wave washed areas.

Project motivation:

- To gain knowledge of how to identify the HCL in Sweden in high resolution DEMs.
- To gain knowledge of how to incorporate geological expert knowledge of manual mapping methods of the HCL in wave washed areas into more automated methods.
- To provide an alternative workflow of mapping the HCL using the national high resolution DEM with accuracies comparable to the manual method but which is structured and repeatable independent of operator i.e. less susceptible to interpreter bias.
- In the long term, provide users and researchers with high quality HCL data with resolution updated against the high resolution DEM.

2 Background

2.1 The highest coastline in Sweden

The highest coastline (HCL) in Sweden is remnants of the highest positioned shoreline developed during the final stages of the deglaciation of the last ice age called Weichsel (about 10 000 years ago) (Fredén 2002, SGU 2015a). When the ice retreated, large parts of the land, depressed from the weight of the ice sheet, were taken in by the sea, a transgression took place (Fredén 2002, SGU 2015b). The HCL marks the maximum extent of the transgression and can today be located by e.g. identifying geomorphological formations such as relict shorelines, wave washed till, till capped heights, glaciofluvial plains, and supra-aquatic erosion marks (Agrell 1976, Påsse 1983, SGU 2015c). Today the HCL is located at different elevations throughout Sweden (a few m.a.s.l in southern Scania to around 289 m.a.s.l at the coast of Ångermanland) due to the glacio-isostatic rebound (Fredén 2002, SGU 2015d). The relative location of the HCL is also revealed by the quaternary deposits of a region: sub-aquatic deposits and reworked deposits represent areas under the HCL or areas in a former ice dammed lake and supra-aquatic deposits represent areas above the HCL (SGU 2015b, Ojala et al. 2013, Fredén 2002, Agrell 1976).

2.2 High resolution DEMs

The influence of LiDAR derived high resolution DEM data on geomorphological mapping and other geospatial mapping has been studied, discussed and reviewed by many researchers e.g. Tarolli (2014), Roering et al. (2013), Ojala et al. (2013), Dowling et al. (2013), Seijmonsbergen et al. (2011), and Liu (2008), Slatton et al. (2007). LiDAR is short for light detection and ranging and is also referred to as airborne laser scanning (ALS) in the literature. Major advantages of using LiDAR DEMs are:

- the overall higher detail compared to the earlier generation of DEMs based on aerial photographs and field measurements, making it possible to study small-scaled local phenomena,
- the revolutionary increased resolution in forested areas due to the LiDAR techniques' ability to penetrate trough vegetation making it possible to produce full detailed images of the earth's surface,
- it has become a cost and time effective alternative due to increased availability of LiDAR data mainly because of decreased acquisition cost sprung from the rapid technical developments (Roering et al. 2013, Dowling et al. 2013, Drăguţ and Eisank 2011,Liu 2008, Slatton et al. 2007).

The dense data that LiDAR generated DEMs provide can be overwhelming to visually interpret without training or refining of the data, a challenge pointed out by Dowling et al. (2013). The amount of data generated by LiDAR data is also computer memory demanding and computational analysis can therefore result in long processing times (Sailer et al. 2014, Dowling et al. 2013, Seijmonsbergen et al. 2011, Lang 2008, Blaschke 2010).

2.3 Automated image interpretation methods

To facilitate and automate the interpretation of high resolution DEM data digital image interpretation analysis can be applied (Lillesand et el. 2008). Cell based multivariate classification uses a composite image of different land surface parameters (LSPs) layers generated from the DEM data or other data in a supervised or unsupervised classification to classify each cell into classes (Seijmonsbergen et al. 2011). The method can be used to produce maps over geomorphological classes on the cell level much like different bands from remote sensing images are used when classifying land cover

(Seijmonsbergen et al. 2011, Lillesand et al. 2008). With the increasing availability of high resolution DEMs the question of the applicability of the traditional cell based classification methods compared to object based image analysis (OBIA) have arisen (for discussion see e.g. Blaschke 2010, Drăguț and Eisank 2011). In summary, OBIA includes a single or more often multi-resolution segmentation/clustering of cells into discrete objects followed by classification of the discrete objects (Seijmonsbergen et al. 2011, Blaschke 2010, Lillesand et al. 2008). Spatial filters can be used on image data (e.g. DEM data) to enhance local information of interest for the application (e.g. local relief, local curvature, and local roughness) (Lillesand et al. 2008). Structure line or breakline extraction can be achieved using local edge preserving filters to enhance linear features at a certain scale (Rutzinger et al. 2011, Lillesand et al. 2008). The accuracy of breaklines extracted from high resolution DEM depends on the accuracy and resolution of the raw LiDAR data and the final DEM in combination with the scale dimension of the mapped feature (Rutzinger et al. 2012).

2.4 How can landforms be described by LSPs?

The physical characteristics of geomorphological landforms can be described using land surface parameters (LSPs) derived from DEM data (Rutzinger et al. 2012, Seijmonsbergen et al. 2011, Minár and Evans 2008). Seijmonsbergen et al. (2011) divides LSP into three main groups: 1) basic LSPs, 2) LSPs connected to hydrology, and 3) LSPs connected to climate modeling. Basic LSPs are further divided by Seijmonsbergen et al. (2011) into local (e.g. slope, aspect, and curvature), regional (e.g. catchment area, slope length, and relative relief), and statistical (e.g. terrain roughness, complexity, and anisotropy). LSPs can thus be used to enhance certain properties or parts of geomorphological landforms e.g. flat areas and steep areas using the LSP slope (Seijmonsbergen et al. 2011), the location of concave and convex surfaces of landforms using the LSP curvature (Rutzinger et al. 2012; 2011; 2007, Cavalli and Marchi 2008) or to distinguish rough surfaces from smooth surfaces using the LSP roughness (McKean and Roering 2004, Tarolli 2014). LSPs can be used in land surface segmentation analysis (Rutzinger et al. 2012; 2011; 2007, Minár and Evans 2008,) by enhancing linear structure of geomorphological landforms also called breaklines or in classification of land surface character using cell-based classification (Seijmonsbergen et al. 2011, Minár and Evans 2008) (see section 2.3 for more detail on automated image interpretation methods).

2.5 Scale

The original DEM resolution, together with the size of the neighboring surrounding area (i.e. scale dimension of the moving window) included in the computation of local LSP, governs what scale of landforms that are enhanced (Tarolli 2014, Berti et al. 2013, Rutzinger et al. 2012; 2007, McKean and Roering 2004) – e.g. large scale landforms like major valley and hill topography (km scale) or small scale landforms like relict beach ridge (a few m to 100 m scale (Påsse 1983)). When computing local LSP in a GIS environment a moving window is used sized after the scale dimensions of the sought feature (ESRI 2015a). Future challenge in earth surface analysis pointed out by Tarolli (2014) is the concept of scale and feature size. The scale dimension used must match the scale of the feature or process aimed to be enhances in the local morphology (Tarolli 2014). The practice of using a trial and error approach to find appropriate scale dimensions due to lacking conventional methods is also highlighted in the studies of e.g. Berti et al. (2013), Rutzinger et al. (2012; 2007), Minár and Evans 2008, and McKean and Roering (2004). The major studies of scale and feature size have been in landslide research according to Tarolli (2014).

2.6 LSP and scale dimensions used in other studies

Small scaled local roughness LSPs (scale dimension of a few meters) have successfully been used to map landslides, taking advantage of the land surface within a landslide being significantly rougher at this scale than the land surface surrounding the landslide (McKean and Roering 2004, Tarolli 2014).

Rutzinger et al. (2012; 2011; 2007) used curvature LSP raster generated from LiDAR DEM with 1 m resolution for a range of scale dimensions (moving window size) to investigate the automation of breakline extraction of natural and anthropogenic linear structures. Rutzinger et al. (2012) found that small window sizes (e.g. 3x3 cells) used on high resolution DEM (cell size: 1 m) for breakline extraction using a curvature LSP, are sensitive to the detailed variation and noise present in the dataset while large window sizes (25x25 cells) only enhance major features smoothing details under a certain scale.

Cavalli and Marchi (2008) used shaded relief together with the LSPs plan curvature and roughness generated from high resolution LiDAR DEM (2m) to map the morphology of an alpine alluvial fan. Cavalli and Marchi (2008) used moving window sizes corresponding to the feature sizes (22 m) they wanted to smooth out when generating a plan curvature map. A moving window of 5x5 cells was used to generate roughness index describing the topographical variable over the length scale 2m (cell size) to 10 m (moving window size).

Berti et al. (2013) compared ten roughness algorithms ability to map landslides within two 10 km^2 study areas in Bologna, Italy. Berti et al. (2013) applied the roughness algorithms using scale dimensions 3x3 cells to 31x31 cells on a 1 m resolution LiDAR DEM. The study of Berti et al. (2013) show no major difference between the tested roughness algorithms and they conclude that de-trending of input data and size of moving window affect the resulting accuracies more than type of roughness algorithm.

3 Methods and material

The method development is based on data available to this project (section 3.1.1), expert knowledge in the HCL field gathered in the pre-study (section 3.1.2), and methods used to solve similar problems supported by the literature study (section 3.1.4). The main steps involved in this project (Figure 1) can be divided into three phases: the preparation phase, the development phase, and the evaluation phase which are described in detail in section 3.1, 3.2, and 3.3 respectively.

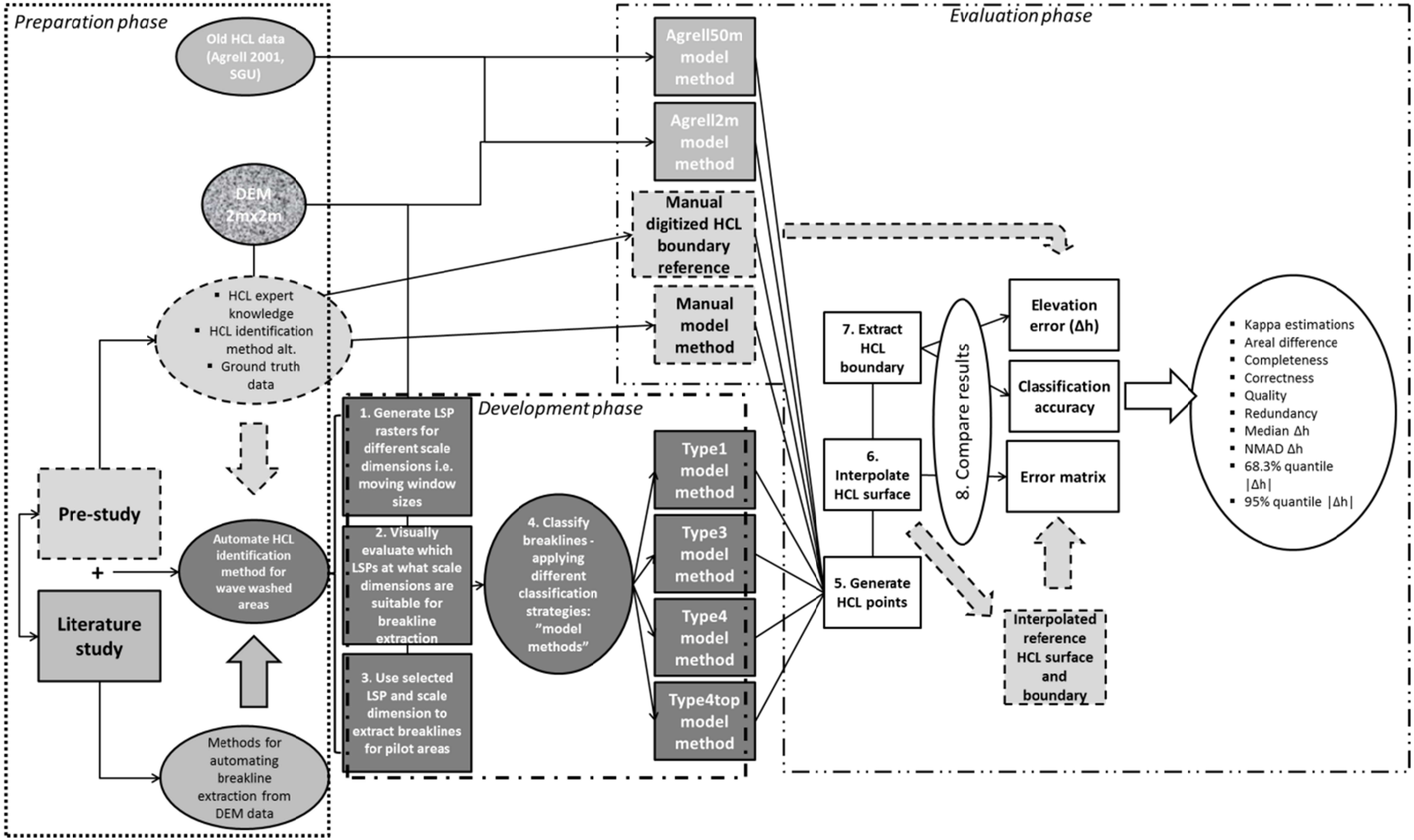

Figure 1 Workflow sketch over main steps involved in the different phases: preparation phase, development phase, and evaluation phase; of the project.

3.1 Preparation phase

In this section the data available to the study, the pre-study, the study area, and the literature study are presented.

3.1.1 Data

Table 1 presents the data used in the pre-study and in this project.

Table 1 Data used in the project.

Data	**DEM:**			**Ancillary data:**		
Data set	*DEM Sweden*	*DEM Västerbotten pilot area*	*DEM Gästrikland pilot area (incl. test run1)*	*Old HCL point data*	*Old HCL surface*	*Quaternary maps*
Source	Lantmäteriet	Lantmäteriet	Lantmäteriet	SGU	SGU	SGU
Data provider	SGU spring 2014	SGU spring 2014	SGU spring 2014	SGU spring 2014	SGU spring 2014	SGU spring 2014
Data type	raster	raster	raster	point	polygon	polygon, polyline, point
Technique	generated from LiDAR data	generated from LiDAR data	generated from LiDAR data	compiled from available studies of the HCL	generated from the old HCL point data set (SGU) and a 50 m resolution DEM (Lantmäteriet)	varying *
Horizontal resolution	2 m	2 m	2 m	varying approx. 50 m, data based on different studies	50 m	varying approx. 25m to 200m **
Vertical resolution	average vertical error of max. 0.5 m	average vertical error of max. 0.5 m	average vertical error of max. 0.5 m	varying, based on different studies	average vertical error of around 2 m	---
Spatial reference	SWEREF99_TM	SWEREF99_TM	SWEREF99_TM	SWEREF99_TM	SWEREF99_TM	SWEREF99_TM
Height system	RH2000	RH2000	RH2000	RH2000	RH2000	---
Extent	Sweden	Top: 7225852 Left: 737698 Right: 763013 Bottom: 7200537	Top: 6773804 Left: 568406 Right: 594625 Bottom: 6673535	Sweden	Sweden	Sweden
Scan area(flight-line no.)		See ***	See ****			
Scanning date	2009 and ongoing	20100805-20100907	20090529-20120526			
Classification level 1, 2 or 3		2	2 and 3			
Update	no updates planned	no updates planned	no updates planned	no updates planned	no updates planned	successive update *****
Data reference	Lantmäteriet 2015	Lantmäteriet 2015	Lantmäteriet 2015	SGU 2015d, Agrell 2001	SGU 2015d, Agrell 2001	SGU 2015e-g

* varying mapping technique e.g. comprehensive mapping in field, image interpretation of aerial photos and/or high resolution DEMs, ** depending on mapping technique indicated by map-type index 2, 3, 4, and 5, *** 09G016(15-27, 29-30), 09G017(23), 09G018(2-24), 09G026(1,31), **** 09D022(18-31), 09D029(22-36), 09P001(1-13, 22-24), 09P002(1-28), 10C043(16-21, 23-24), 10C044(1-17, 23-24), 11E007(1-13, 15), ***** successive update of map-type 4 and 5 to map-type 2 and 3. Update follows SGUs yearly survey plan.

3.1.2 Pre-study

In the pre-study to the current study presented in this report the HCL in Sweden was studied in hillshade maps generated from the high resolution DEM using methods similar to the methods used by Ojala et al. (2013) for shoreline identification. The aim of the pre-study was to gather knowledge of how to identify landforms in hillshade maps connected to the HCL and define where the actual HCL boundary is positioned in relation to the landforms. The pre-study found that two major HCL landform classes can be identified in hillshade maps: deltas and wave washed features were the latter gives a clearer indication of the HCL boundary. The current study presented in this report attempts to automatize the method used to map the HCL in areas with wave washed features. The ideal environment to locate the HCL boundary in a hillshade map using this method is where glacial flow lineation features are broken up by wave washed features (Figure 2). This gives a clear picture of land area not processed by wave washing (where glacial landforms are preserved) and land area processed by wave washing (glacial landforms are "washed away") and thus produces a distinct HCL boundary. Another aim of the pre-study was to generate reference data near ground truth accuracy (Smith et al. 2006) to be used in the accuracy assessment of the resulting HCL-maps produced through this project.

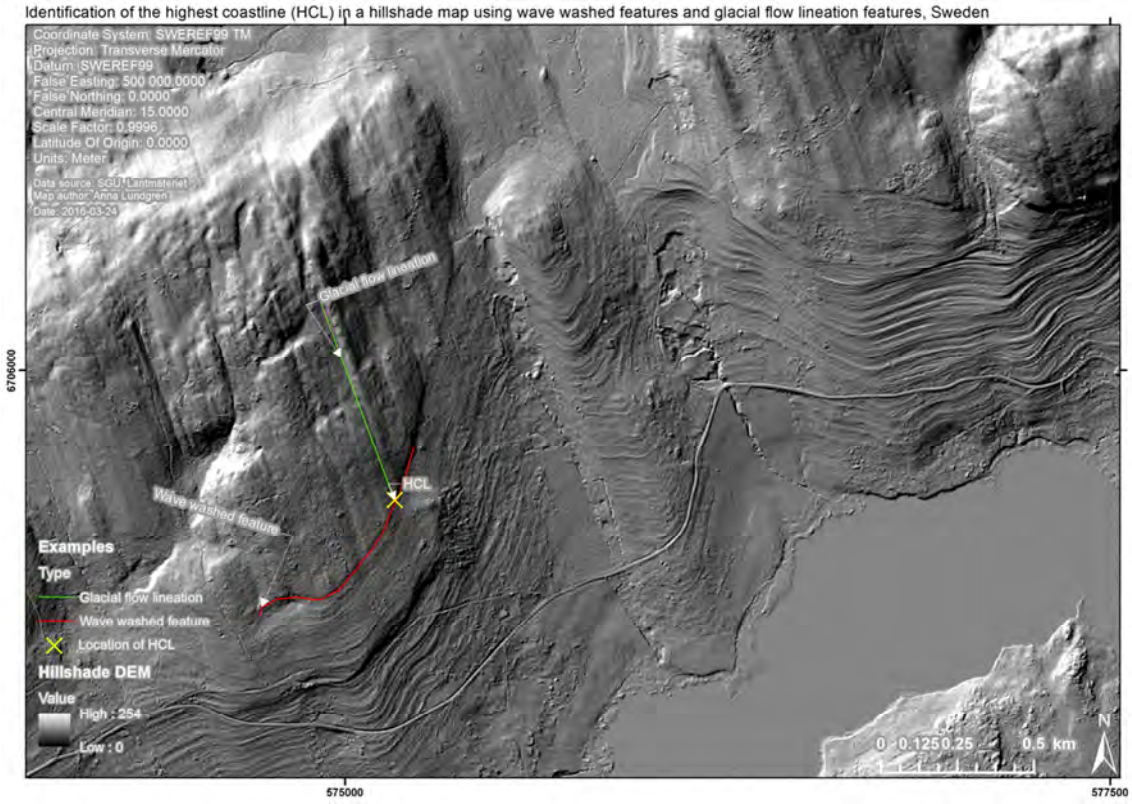

Figure 2 Identification of the HCL in hillshade map generated from high resolution (2 m) DEM using glacial lineation features and wave washed features.

3.1.3 Study area

The HCL locations and landform types identified and manually digitized in the pre-study are presented in Figure 3 together with the two pilot areas used in this study. Two wave washed dominated areas are used as pilot areas for the development of an more automated version of the manual method: *the Gästrikland pilot area* and *the Västerbotten pilot area*. The method(s) were developed using data in a smaller area: *Test run 1 area*, within the Gästrikland pilot area and then applied to the Västerbotten pilot area as a whole for further development and evaluation (Figure 3). The final results have not been applied to the Gästrikland pilot area as a whole due to the time frame of the project.

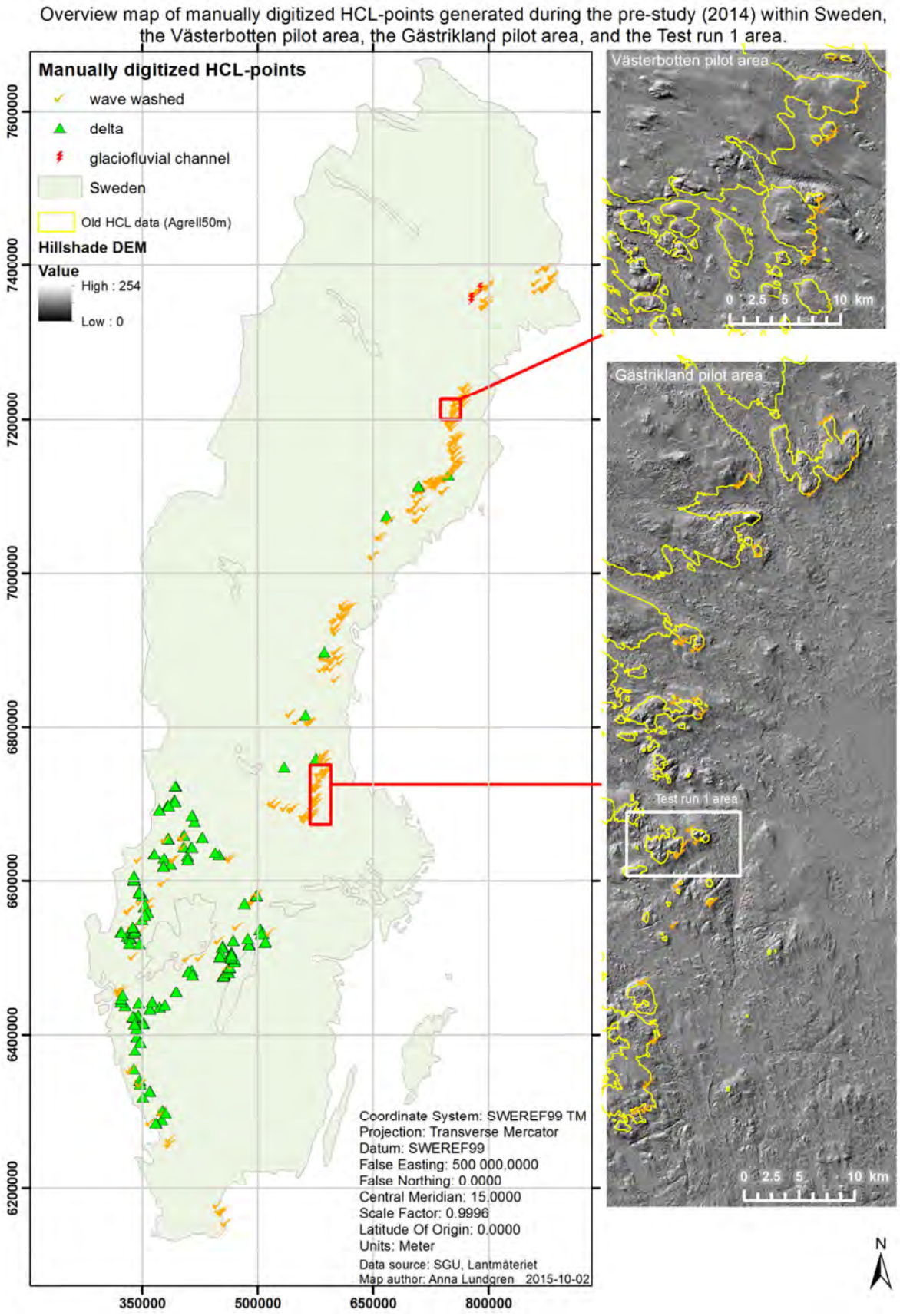

Figure 3 HCL locations of delta type, wave washed type, and glaciofluvial channel type in Sweden, manually digitized using hillshade maps during the pre-study (2014) of this project. The location of the wave washed dominated pilot areas Västerbotten pilot area and Gästrikland pilot area are indicated with red frames. The Test run 1 area lies within the white frame in the Gästrikland pilot area.

3.1.4 Literature study

A literature study was executed in order to find appropriate methods for the extraction of breaklines formed by the wave washed features and glacial flow lineation features present in HCL locations. Important references included in the literature study are presented in Table 2.

Table 2 Important references included in the literature study used to find appropriate methods for the extraction of breaklines formed by the wave washed features and glacial flow lineation features.

Litterature study	
Important reference	***Description***
Tarolli (2014)	Review of recent important literature on high-resolution topographic analysis.
Eisank et al. (2014)	Study of the use of multi resolution segmentation (MRS) on DEM data to delimitate drumlins.
Sailer et al. (2014)	Study investigating the magnitude of error for topographic change calculations using DEMs with different resolution generated from multi-temporal airborne laser scanning (ALS) images.
Berti et al. (2013)	Comparative analysis of surface roughness algorithms for landslide detection.
Rutzinger et al. (2012)	Investigation of accuracy of automatic geomorphological breakline extraction from LiDAR data.
Cracknell et al. (2013)	Study using methods for enhancement and extraction of curvature lineaments.
Rutzinger et al. (2011)	Presentation of a method for automatic extraction of linear structures from high resolution digital terrain models.
Lillesand et al. (2008) chapter 7	The chapter addresses spatial filtering and edge enhancement usable for image preparation and interpretation.
Cavalli and Marchi (2008)	Study applying topographic analysis on LiDAR data studying alluvial fan morphology.
Liu (2008)	Highlights critical issues of DEM generation using LiDAR data.
Rutzinger et al. (2007)	Investigation of the detection and extraction of linear lineaments in laser scanning data.
Nyborg (2007)	Investigation of the use of LiDAR data for lineament detection.
McKean and Roering (2004)	Investigation of landslide detection and surface morphology mapping using LiDAR data.

3.2 Development phase

In this section the steps and methods involved in the actual development of the HCL extraction method models are described.

3.2.1 Method idea and development

The suggested method is to find areas where glacial flow lineation features are broken by lineation formed by beach ridges in wave washed zones connected to the highest coastline (HCL) (see Figure 2). By finding where these two features intersect, HCL locations can be identified. The method is automated by:

1. automating the extraction of wave washed features and glacial flow lineation features from the high resolution DEM data,
2. automating the classification of extracted features to successfully separate wave washed features from glacial flow lineation features,
3. automating an elongation of the glacial flow lineation features to find the nearest intersection with the wave washed features.

The literature study suggests a number of methods to automate the extraction and classification of features using DEM data as input e.g. breakline extraction using curvature LSPs (Rutzinger et al. 2012; 2011; 2007, Cavalli and Marchi 2008), object-oriented (OBIA) approaches using multi

resolution segmentation (MRS) with one or several LSPs as input (Eisank et al. 2014, d'Oleire-Oltmanns et al. 2013) or automatically mapping of landform complexes and landform units using local roughness LSPs (Berti et al. 2013, McKean and Roering 2004). The method suggested in this study is based on methods described in the studies of Cracknell et al. (2013), Rutzinger et al. (2012; 2011; 2007), Lillesand et al. (2008), and Cavalli and Marchi (2008). In summary the method extracts feature breaklines by classifying land surface parameter (LSP) rasters (LSP ex. are roughness index, residual DEM, and curvature) generated from the DEM raster data into extreme classes to enhance the breaklines of features and then converts the breaklines into line vector data. In the attempt to automate the classification and separation of breaklines representing wave washed features and glacial flow lineation features for larger study areas coarse scaled LSP rasters are applied of de-trended type. A de-trended LSP is computed from a DEM where the mean elevation trend for a certain scale has been removed also called a residual DEM (Lillesand et al. 2008). For example a coarse scaled roughness index layer can be used to divide the landscape into rougher areas characterized by higher elevation than its surrounding and flatter smoother areas located in lower areas. This could be used in an attempt to separate smoother low-lying wave washed land areas from rougher land area with higher lying obstacles (e.g. mountains and hills) with preserved glacial flow lineation features. The *ArcGIS 10.2* tool *Extend Line* (ESRI 2015b) is used together with other steps in the *ArcGIS 10.2 Modelbuilder* (ESRI 2015c) environment to automate the elongation of glacial flow lineation feature breaklines to the nearest intersection with a wave washed feature breakline.

The challenges of the suggested method are:

- to use appropriate scale dimensions on the moving window to extract relevant breakline data (corresponding to the features of interest) a challenge pointed out in similar studies by e.g. Tarolli (2014), Sailer et al. (2014), Berti et al. (2013), Rutzinger et al. (2012; 2007), and McKean and Roering (2004);
- to develop an accurate selection analysis methodology to separate wave washed feature areas from glacial flow lineation feature areas and to filter away unwanted noisy information that will interfere with the elongation and intersection procedures of the suggested method workflow.

3.2.2 LSP generation and scale assessment

For the Test run 1 area, roughness index rasters and curvature rasters were generated from the DEM data for 23 moving window sizes. 20 moving window sizes from 3x3 cells to 41x41 cells adding 2 cells for each new size and 3 additional moving window sizes: 75x75 cells, 99x99 cells, and 199x199 cells. A curvature raster was also computed using the raw DEM as input (see curvature generation section below for explanation). The different sized windows were applied to find the appropriate scale dimensions to use for the detection and extraction of the linear features (referred to as breaklines in this report) formed by wave washed beach ridges and the glacial flow within the DEM data. Instead of using a range of grid resolution on the input DEM a range of moving-window sizes was used.

To test a wide range of moving-window sizes was of interest in this study due to:

- meager guidelines in the literature on moving window sizes in relation to the scale dimensions of a sought feature (Tarolli 2014) and the pronounced use of trial and error approaches in similar studies (Rutzinger et al. 2012; 2007, Berti et al. 2013, McKean and Roering 2004),

- the scale dimensions of the features under investigation not being well established and also varying to some degree from location to location,

- a shortage of knowledge on what information of potential interest to this project that can be produced by generating LSPs at different scales.

Roughness (McKean and Roering 2004, Berti et al. 2013, Cavalli and Marchi 2008, Lillesand et al. 2008) and curvature (Cracknell et al. 2013, Rutzinger et al. 2012; 2011, Cavalli and Marchi 2008) rasters can be computed using different methods and algorithms. For this study a roughness index method described in Cavalli and Marchi (2008) was applied where a low-pass filtered image (smoothed image) of the DEM is subtracted from the original DEM generating a high-pass filter image of the DEM (referred to as a residual DEM in this report) (Cavalli and Marchi 2008, Lillesand et al. 2008). Finally the standard deviation is calculated for the residual DEM to produce a roughness index LSP raster. The ArcGIS tool *Focal Statistics* with statistic setting MEAN (ESRI 2015d) was used to generate low-pass filtered (smoothed) DEM images for all window sizes. The ArcGIS tool *Focal Statistics* was also used to compute the standard deviation for the residual DEM using statistic setting STD and the same moving window size used to produce the input raster. The ArcGIS tool *Raster Calculator* was used in the subtraction step (ESRI 2015e).

"Mean/normal" curvature, plan curvature, and profile curvature rasters were generated using the ArcGIS *Curvature* tool (ESRI 2015f). The ArcGIS *Curvature* tool calculates the second derivative of the input surface data. Using a DEM as input surface will produce an output which describes the change of slope i.e. the curvature of the DEM surface. The profile curvature is a measure of the curvature in the direction of the steepest slope, the plan curvature is a measure of the curvature perpendicular to the steepest slope, and the "mean/normal" curvature measure is a combination of the profile and plan curvature. Since the window size cannot be changed for the *Curvature* tool in ArcGIS 10.2 the curvature rasters were generated from the low-pass filtered DEM images (smoothed images) used in the intermediate step in the roughness index raster generation. A curvature raster with the raw DEM (i.e. unsmoothed DEM) as input was also generated. For detailed information of the workflow used in ArcGIS 10.2 for the LSP raster generation see Appendix D Figure D1.

3.2.3 Visual evaluation of LSP rasters

The resulting roughness index and curvature LSP rasters from test run1 were visually analyzed and compared to estimate their use to reach the aim of this project and to find appropriate scale dimensions (moving-window sizes) suitable for the extraction of the wave washed and glacial flow lineation feature breaklines. According to Tarolli's (2014) review of the subject of high resolution topographic analyses, there is no conventional method for testing the ideal scale dimensions for the features sought, so a trial and error approach is often the solution together with knowledge of the landform size. This matter is also highlighted in other studies e.g. Rutzinger et al. (2012; 2007), Berti et al. (2013), McKean and Roering (2004). The LSP rasters for scale dimensions of the original DEM (2m) up to 13x13 cells for the Test run 1 area were further processed through the breakline extraction steps of the suggested workflow (for details see Appendix D Figure D2) to support the visual evaluation of scale dimensions.

3.2.4 Extract breaklines for pilot area

Following the results from the Test run area 1 the "normal/mean" curvature, profile curvature, and plan curvature LSPs for scale dimension 11x11 cells were used for breakline extraction in the Västerbotten pilot area using the workflow described in Appendix D Figure D2.

The main steps of the workflow for extracting breaklines (Appendix D Figure D2) are explained below.

Reclassify into extreme values: The “normal/mean”, profile, and plan curvature LSP rasters for the scale dimension 11x11 cells were reclassify into 3 classes using curvature thresholds enhancing maximum values for positive and negative curvature. Threshold values suggested in similar studies (Cracknell et al. 2013, Rutzinger et al. 2011; 2007) were used as starting point and then adjusted to separate cell values representing valleys and crests of the enhanced features. Important is not to set the thresholds for the maximum and minimum curvature classes too narrow as connectivity between the cells forming the sought breaklines risk being lost. For the Västerbotten pilot area the following curvature threshold values were used: curvature <-0.1 = class 1, curvature -0.1 to 0.1 = class 0, and curvature >0.1 = class 3.

Majority filter: A majority filter using 3x3 cell window (i.e. the 8 nearest neighboring cells is used in the filter) was applied twice on the reclassified curvature rasters to fill in gaps and make the linear features more continues (ESRI 2015g).

Reclassify max. and min. curvature into separate layers: The “normal/mean”, plan, and profile curvature rasters were further converted into one raster layer containing the maximum positive curvature values (curvature >0.1 = class 3) and one raster layer containing the maximum negative curvature values (curvature <-0.1 = class 1). This to make the thinning step more effective by processing positive and negative curvature values separately. Reducing the density of the extracted curvature cells and removing the connectivity of positive and negative curvature values by processing them in separate rasters will produce a clearer thinning result.

Thinning step: raster cell areas representing the extreme “normal/mean”, plan, and profile curvature values were thinned using the ArcGIS tool *Thin* (ESRI 2015h) Setting used for the *Thin* tool: corners=SHARP, maximum_thickness=DEFAULT (ten times the cell size i.e. 2m*10=20m).

Raster to polyline: The thinned curvature breakline raster features were converted into non-simplified 2D polyline features using the *Raster to Polyline* tool in ArcGIS (ESRI 2015i). The non-simplified polyline option was used to minimize the number of modification steps of the original data.

3.2.5 Breakline classification and HCL identification

Extracted curvature polylines corresponding to road and other infrastructure were removed before the classification of the breaklines. This was done manually for the Västerbotten pilot area, but for larger areas infrastructure data sets are preferable used as filters.

Four workflows were developed for the classification of the extracted curvature polyline breaklines and the identification of potential HCL points:

1. **Type1 model method** is an attempt to apply as objective model as possible by using breakline attributes and terrain information for the classification of the extracted curvature polylines into wave washed feature breaklines and glacial flow lineation feature breaklines and by applying an automated elongation of the glacial flow lineation breaklines.
2. **Type3 model method** applies manual classification of breaklines and automated elongation of the glacial flow lineation breaklines. (Type2 model method was abandoned and developed into Type 3 model method).
3. **Type4 model method** utilizes only breaklines representing the uppermost wave washed features adjacent to the HCL (from the manual classification) and does not use glacial flow lineation information at all.
4. **Type4top model method** is a version of Type4 model method using only the one uppermost breakline representing wave washed features adjacent to the HCL.

3.2.6 Type1 model method

The aim of the *Type1 model method* is to objectively classify the extracted curvature polylines into breaklines representing the wave washed features and the glacial flow lineation features using length, mean orientation, and sinuosity attributes together with topographic location determined by terrain information extracted from coarse scale dimensioned LSP rasters. Sinuosity (*S*) is computed using the formula given by Rutzinger et al. (2012):

$$\mathbf{S} = \frac{\mathbf{l_a}}{\mathbf{l}} \quad (1)$$

where l_a is the actual path length between the starting point and the end point of the curvature polyline and l is the length of curvature polyline.

The main steps of the workflow used in the Type1 model method are explained below. A detailed workflow schedule of the steps executed in ArcGIS 10.2 can be found in Appendix D Figure D3.

3.2.6.1 Select by attribute

Certain attribute criteria were set for the extracted curvature polylines to be classified as wave washed feature breaklines or glacial flow lineation feature breaklines. The attribute criteria values were obtained from samples of the extracted curvature polylines manually classified into wave washed feature breaklines and glacial flow lineation breaklines for each input layer (both negative and positive "normal/mean", profile, and plan curvature). Only well-defined curvature polylines easy to classify into the breakline classes were used in the samples (see Figure 4 for an example of manually classified glacial flow lineation). Knowledge gained from manual hillshade mapping during the pre-study was applied in the classification of the samples. Curvature polylines with diffuse classification were not included in the samples.

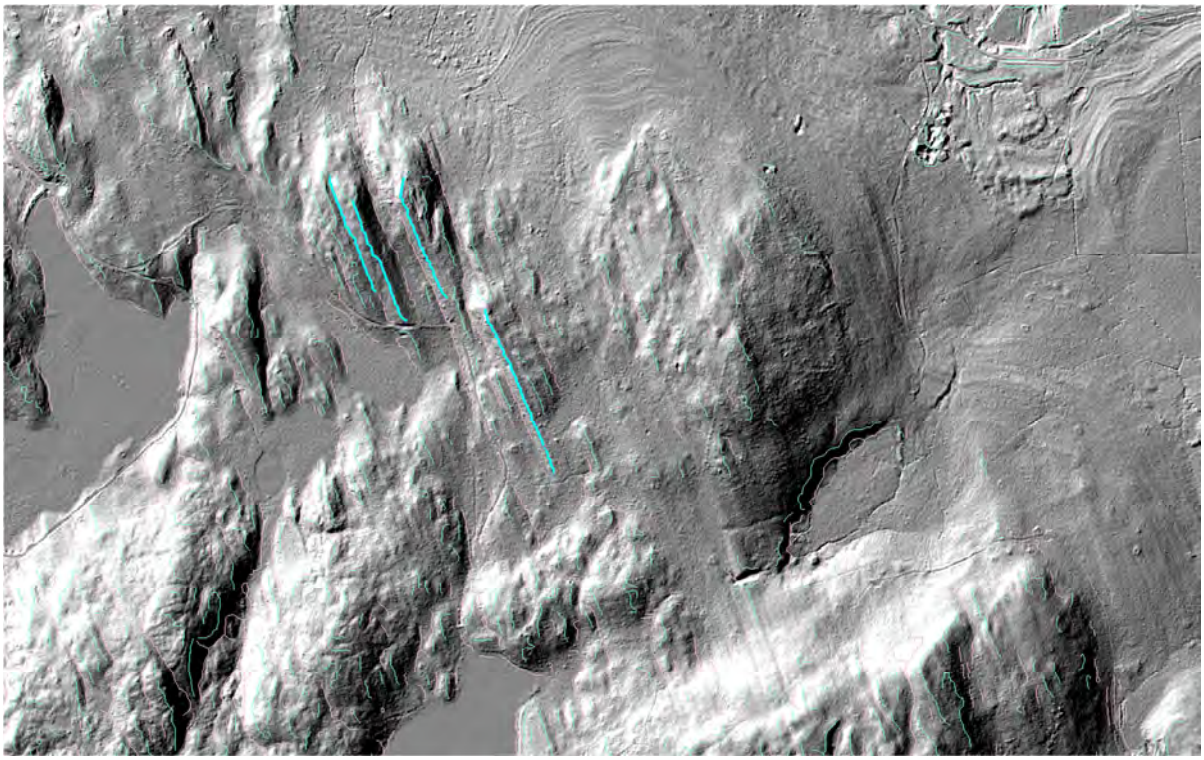

Figure 4 Well-defined glacial flow lineation polylines (highlighted in blue) extracted from the curvature data (example from Test run 1 area within the Gästrikland pilot area).

The following curvature polyline attributes were used:

- The *length attribute* was used to filter away curvature polylines too short to be classified as a glacial flow line of importance.
- The *mean orientation attribute* was used to select curvature polylines with certain mean orientation e.g. corresponding to the regional glacial flow orientation and thus helpful in the separation of wave washed features from glacial flow lineation features. The mean orientation attribute for each curvature polyline was added using the ArcGIS tool *Linear Directional Mean* (ESRI 2015j) setting the case field setting to the polyline unique identity field i.e. *ARCID*. The tool creates a new shapefile with vectors representing the mean orientation values for each polyline present in the input file. The attribute containing the orientation information was joined to the input curvature polyline layer. The mean glacial flow orientation for the pilot areas was acquired by calculating the *Linear Directional Mean* (ESRI 2015j) for the manually classified glacial flow lineation breakline samples. An alternative is to use other glacial flow directional data with the risk of introducing unknown errors.
- The *sinuosity attribute* was used to filter away polylines too excessively curved to be glacial flow lineation features (Figure 5).

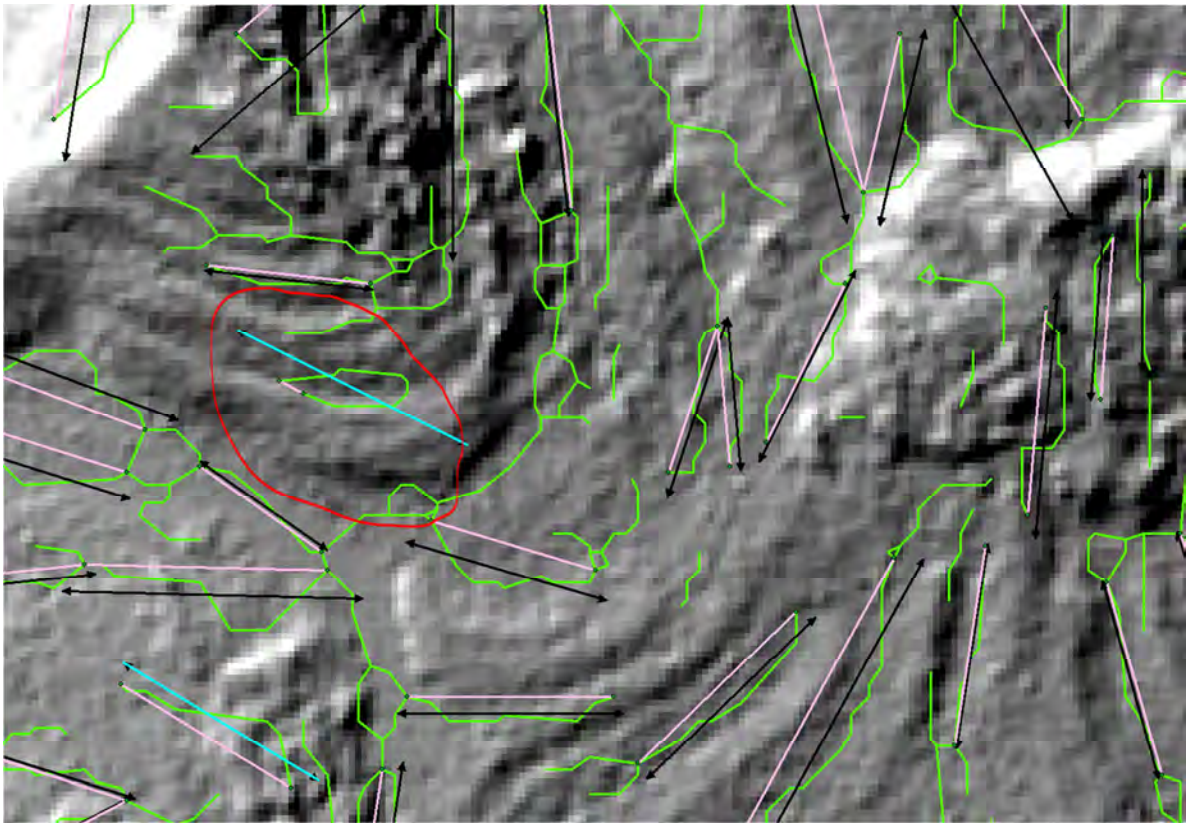

Figure 5 The green polylines represent extracted curvature breaklines, the black and blue vectors represent the extracted curvature polylines' mean directions and length (len), and the pink vectors represents the actual path length (alen) between the starting point and the end point of the curvature polyline. The sinuosity of the curvature polylines (Eq. 1) can be used to filter away polylines too excessively curved (see example encircled in red).

3.2.6.2 Select by location

The use of residual DEM (Lillesand et al. 2008), roughness index (Cavalli and Marchi 2008), curvature (ESRI 2015e), and relative topographic position (Cooly 2015) LSP rasters with coarse scale dimensions varying from 99x99 cells to 2999x2999 cells for a spatial classification of areas dominated

by wave washed features and areas dominated by glacial flow lineation features was investigated using an iterative process of: generating LSP rasters for a certain scale dimension, setting classification thresholds, and visual evaluation.

The classification result of the positive and negative "normal/mean", profile and plan curvature breaklines data sets were visually inspected to only include curvature breakline data sets that enhance wave washed features and glacial flow lineation features in further steps of the Type1 model method (see Results chapter).

3.2.6.3 Elongation

In preparation for the elongation procedure, mean orientation vectors (generated by the *Linear Directional Mean* ArcGIS tool, ESRI 2015j) representing the curvature polylines classified as glacial flow lineation breaklines were merged with the polylines classified as wave washed breaklines (see workflow for Type 1 model method Appendix D Figure D3). This was required for the ArcGIS *Extend Line* tool (ESRI 2015b), used in the elongation procedure, to elongate the extracted glacial flow lineation breaklines in mean glacial flow orientation to the first intersection with a wave washed feature breakline which is the objective of the Type1 model method. Due to the large amount of data the elongation procedure was automated using the *Modelbuilder* environment in ArcGIS 10.2 (ESRI 2015c). The *Extend Line tool* was modified in the *Modelbuilder* environment to function according to Type1 model method (see Appendix A for details).

3.2.6.4 Intersection

The final step in the Type1 model method executes the intersection between the elongated glacial flow lineation breakline vectors and the wave washed feature breaklines to generate potential HCL points.

3.2.7 Type3 model method

The Type3 model method is based on the same method as the Type1 model method i.e. identifying HCL location points by finding where wave washed features intersect glacial flow lineation features by elongating glacial flow lineation vectors. Instead of applying automated methods for a more objective classification (as in the Type1 model method) the extracted curvature polylines are manually classified into glacial flow lineation feature breaklines and wave washed feature breaklines by interpreting the features in hillshade maps. The elongation procedure is also executed manually in the Type3 model (partly due to the bug in the ArcGIS 10.2 *Extend Line* tool increasing processing time, see Appendix A) which gives the operator the possibility to choose which vectors to elongate thus increasing the quality by filtering away errors at this stage. The Type3 model method is applied to show the potential the Type1 model method would have if an objective classification of breaklines is successful in the sense that manual interpretation of hillshade maps is assumed to be the truth.

3.2.8 Type4 model method

The Type4 model method deserts the method idea of identifying HCL location points by finding the intersection of glacial flow lineation features by wave washed features used in Type1 model method and Type3 model method. Instead the Type4 model method uses the vertices of the two uppermost extracted curvature polylines manually classified as wave washed feature breaklines as HCL location points (see Figures 23-24 in the Results chapter).

3.2.9 Type4top model method

The Type4top model method is a variation of the Type4 model method were only the vertices of the uppermost extracted curvature polylines manually classified as wave washed feature breaklines are used as HCL location points (see Figures 25-26 in the Results chapter).

3.2.10 Interpolate HCL

Elevation data was extracted from the DEM data set to the HCL points generated by the model methods. HCL surfaces were interpolated for each model method using the HCL points with the elevation information as input. The interpolation was executed with ArcGIS 10.2 software using the inverse distance weighted (IDW) method setting cell size: 2m (snapped to the DEM data set), power: 2, and search radius: variable with number of points set to the default: 12 (ESRI 2015k). The search radius was set variable for a complete surface to be generated. To find the HCL boundary the interpolated HCL surface was subtracted from the original elevation surface i.e. the DEM. The resulting deviation raster was reclassified into two classes: class 1 = cell values ≤ 0 which is land area under the HCL and class 2 = cell values > 0 which is land area over the HCL. The HCL data sets were vectorized into polygons representing the two land area classes (land area under and over the HCL) and polylines representing the HCL boundary for each model method: Type1, Type3, Type4, and Type4top.

HCL surface and HCL boundary data sets were also generated for the manually mapped HCL location points digitized in the pre-study, *Manual model method*, and the old HCL data points, *Agrell50m and Agrell2m model method*, within the Västerbotten pilot area for comparison. The Agrell50m model method is the HCL surface data set present in SGU's HCL database at the initiation of this project and it is generated from DEM with cell size 50 m (SGU 2015d). The Agrell2m model method uses the same HCL data points as the Agrell50m but the HCL surface is generated from the high resolution DEM with cell size 2m.

3.2.11 Ground truth data

To evaluate the interpolated HCL surfaces and HCL boundaries generated by the model methods a HCL surface was interpolated from reference data (see Appendix E). The reference data used for the interpolation of the HCL reference data sets (HCL surface and boundary) in the Västerbotten pilot area is a detailed manually digitized HCL boundary clearly identified by wave washed features in hillshade maps generated from the high resolution DEM, and is thus assumed to have similar accuracy as ground truth acquired in field (Smith et al. 2006). The reference HCL boundary is digitized as a line following the valley of the uppermost wave washed feature. The HCL location points manually digitized during the pre-study are part of the HCL boundary line reference data set. Elevation data was extracted for each cell in the DEM intersected by the HCL boundary line reference. The intersection points were used to generate the interpolated HCL reference data sets using the same method and settings described for the generation of the model method HCL data sets (see section 3.2.10 above).

3.3 Evaluation phase

The following section presents the methods used to estimate the accuracies of the developed model methods.

The accuracies of the HCL surface and boundary maps generated from the different model methods (Manual, Type1, Type3, Type4, Type4top, Agrell2m, and Agrell50m) for the Västerbotten pilot area were estimated using the following three approaches:

1. Constructing error matrices for different sized evaluation areas around the digitized HCL boundary reference data to evaluate the classification of land area under (class 1) and over (class 2) the generated HCL boundaries.
2. Estimating line classification accuracy by applying the "buffer method" (Heipke et al. 1997) to compute completeness, correctness, quality, and redundancy measures for the HCL boundaries generated by the model methods.

3. Evaluating the elevation error (Δh) for each model method compared to the reference data for 100 random sample points along the HCL boundary by computing the median, 68.3 % quantile, 95% quantile, and the normalized median absolute deviation (NMAD) of the elevation error (Δh).

3.3.1 Error matrix

To estimate the accuracy of the model methods: Manual, Type1, Type3, Type4, Type4top, Agrell2m, and Agrell50m, error matrices (Lillesand et al. 2008, Mårtensson and Pilesjö 2004) were constructed for different sized evaluation areas (buffers with radius of 11m, 50m, 100m, and 1500m as well as the 'whole area', Figure 6) around the HCL boundary reference data. Areal difference (A_d), Overall Kappa ($\hat{\kappa}$), and individual Kappa ($\hat{\kappa}_i$) were computed from the error matrices for each evaluation area using the following formulas:

$$A_d = \frac{C-B}{B} \quad (2)$$

$$\hat{\kappa} = \frac{Nd-q}{N^2-q} \quad (3)$$

$$\hat{\kappa}_i = \frac{Nd_i-q_i}{NB_i-q_i} \quad (4)$$

where B is the number of ground truth points, C is the number of map data points, N is the total number of points, d is the sum of correctly mapped points, q is the sum of the products between B and C, d_i is the sum of correctly mapped points for class i, and q_i is the product of B and C in class i (Mårtensson and Pilesjö 2004). Different sized areas were evaluated to compare accuracy assessments of the modeled HCL boundaries at different scales. All classified cells (class 1 = under HCL and class 2 = over HCL) from the model methods for each evaluation area within the Västerbotten pilot area were included in the Kappa and areal difference computations. The idea of including all cells for different evaluation areas instead of a number of random sample points is based on that it is the actual HCL boundary that is to be evaluated and not the land area of class 1 and class 2 per se.

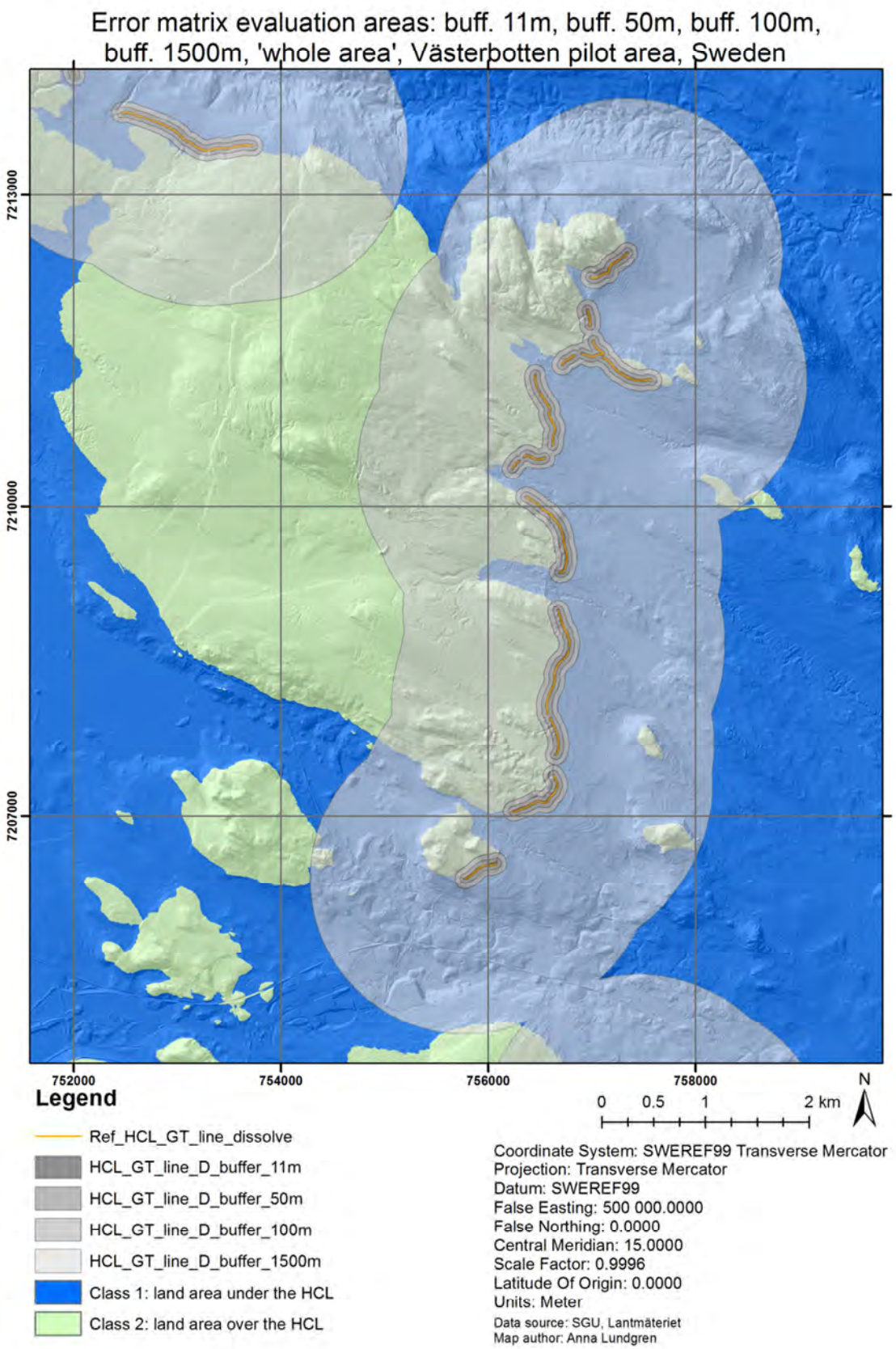

Figure 6 Example of the evaluation areas around the HCL reference data: buffer 11m, 50m, 100m, 1500m, and 'whole area', used in the error matrix accuracy assessment of the model methods.

3.3.2 HCL boundary classification accuracy – "buffer method"

To evaluate the classification accuracy the HCL boundary lines generated from the interpolated HCL-surfaces for the different model methods are compared with the HCL boundary line interpolated from the HCL boundary reference data. The comparison is done for the generated HCL boundary lines:

- as a whole (total HCL-boundary within the Västerbotten pilot area) and,
- adjacent (within about a 200 m flat buffer) to the manually digitized HCL boundary reference data available for the Västerbotten pilot area.

Completeness (*C*), correctness (*Cr*), quality (*Q*), and redundancy (*R*) were calculated as measures for the HCL boundary classification accuracy following the "buffer method" described by Heipke et al. (1997):

$$C = \approx \frac{"TP"}{"TP"+FN} \quad (5)$$

$$Cr = \frac{TP}{TP+FP} \quad (6)$$

$$Q = \frac{TP}{TP+FP+FN} \quad (7)$$

$$R = \frac{TP-"TP"}{TP} \quad (8)$$

where *"TP"* is the length of matched reference which is approximately the same as the *TP* if redundancy (*R*) is low, *TP* = true positive is the length of matched extraction here the modeled HCL boundary line, *FN* = false negative is the length of unmatched reference, *FP*= false positive is the length of unmatched extraction here the modeled HCL boundary line, *qq* is the sum of the length of extracted data (*TP + FP*) and the length of unmatched reference (*FN*), and *rr* = length of matched extraction minus length of matched reference (*TP – "TP"*) (Figure 7).

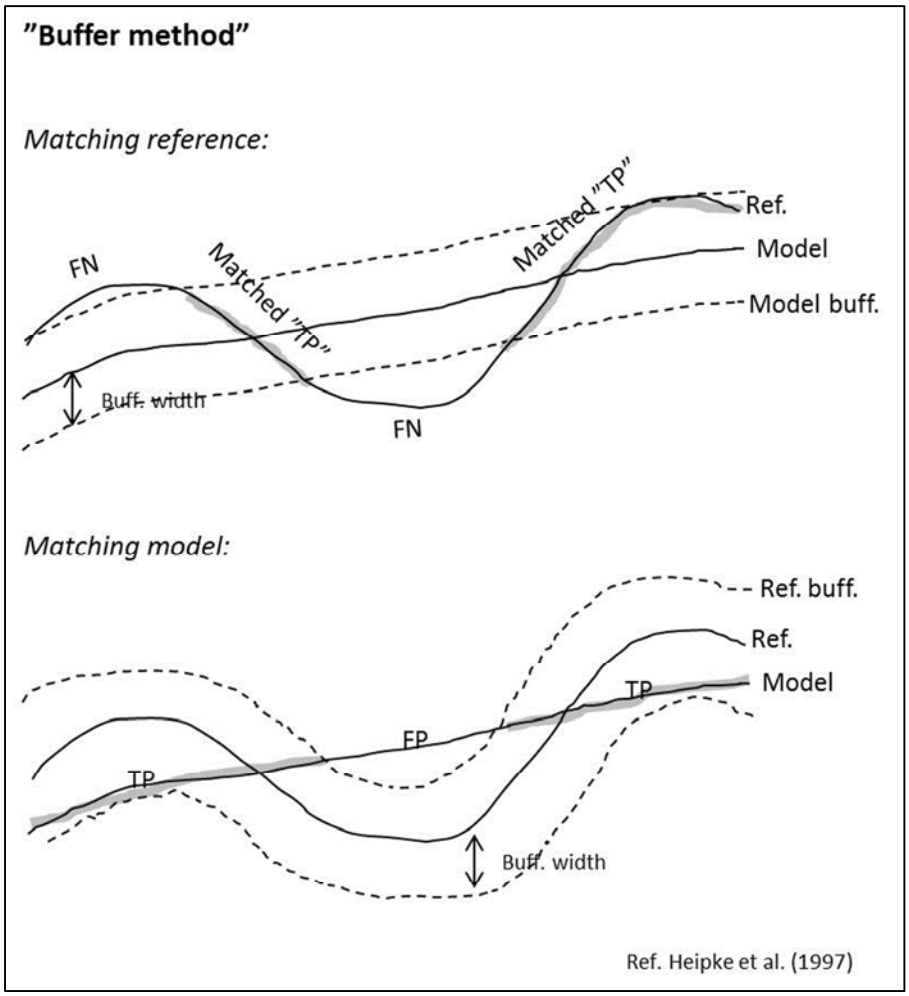

Figure 7 Sketch over the "buffer method" principle used for estimating the accuracy of the HCL boundary classification. Figure modified from Heipke et al. (1997).

A 6.25 m buffer around the modeled HCL boundary and reference HCL boundary corresponding to the scale dimensions of the extracted crest or valley of a wave washed HCL feature is used for the calculations (Rutzinger et al. 2012, Heipke et al. 1997). Heipke et al. (1997) suggests a buffer width of approximately half the extracted objects width. The width/wavelength of a wave washed feature at the HCL boundary in the Västerbotten pilot area varies approximately between 15 m and 35 m. The concave part or the convex part of the wave washed HCL-features corresponds to approximately half the width/wavelength (7.5-17.5 m) which gives a mean buffer of 6.25 m (Figure 8).

"Buffer method" parameters used for the HCL boundary classification accuracy assessment - matching reference step, Västerbotten pilot area, Sweden

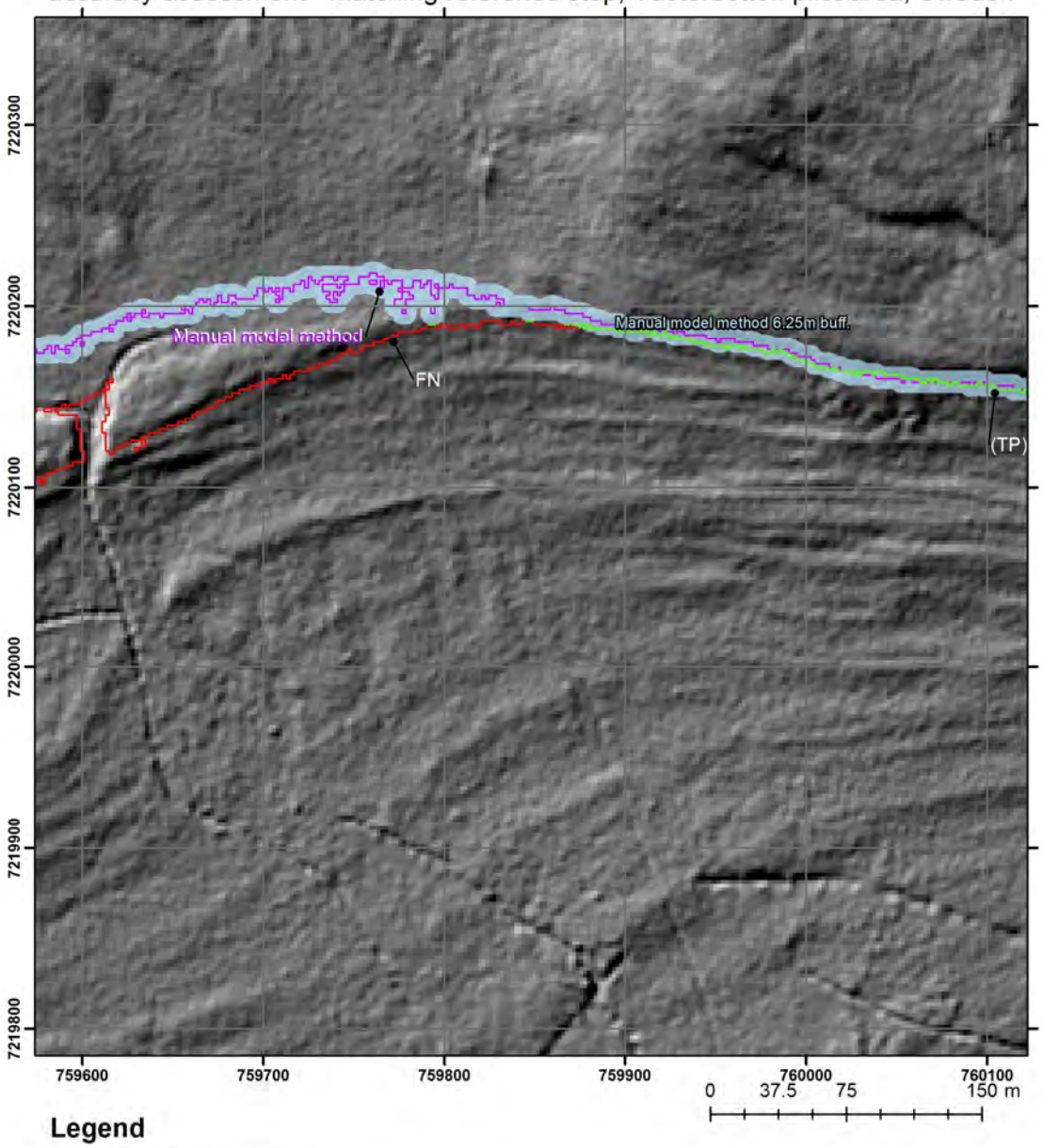

Legend

Manual model method

Manual model method 6.25 m buff.

Ref. matched to manual model method

(TP) - matched

FN - not matched

Hillshade_dem_h315

Value

High : 254

Low : 0

Coordinate System: SWEREF99 Transverse Mercator
Projection: Transverse Mercator
Datum: SWEREF99
False Easting: 500 000.0000
False Northing: 0.0000
Central Meridian: 15.0000
Scale Factor: 0.9996
Latitude Of Origin: 0.0000
Units: Meter

Data source: SGU, Lantmäteriet
Map author: Anna Lundgren
Date: 2016-04-20

N

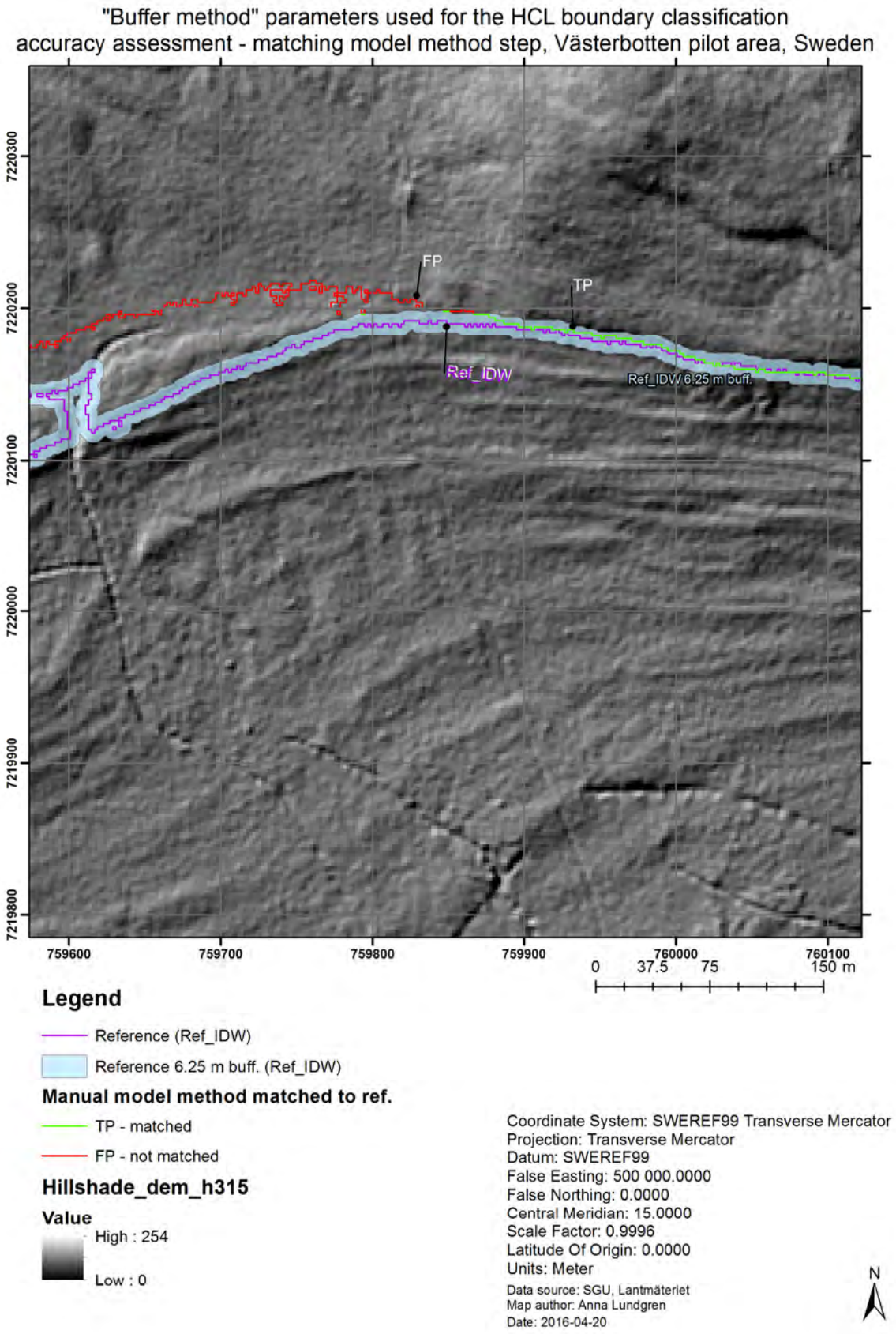

Figure 8 Sketch describing the lengths: TP, FP, "TP" (matched reference), and FN and the buffers used in the HCL boundary classification accuracy assessment for the matching reference step (top image) and the matching model method step (bottom image) (figure modified from Heipke et al. 1997).

Different methods for matching linear extracted data to linear reference data exists (Heipke et al. 1997). Heipke et al. (1997) states that the “buffer method” is a simple approach concerning the fact that topological differences between the datasets most likely are present but points out the method is sensitive to high redundancy. Rutzinger et al. (2012) applies the “buffer method” on 1 m interval spaced points along extracted breaklines and compares with reference data manually digitized from shaded relief maps. In Rutzinger et al. (2012) work the number of *TP*, *FP*, and *FN* points instead of lengths are used to calculate the completeness, correctness and quality.

3.3.3 Elevation error evaluation using 100 random samples

100 random sample points were generated along the HCL boundary line reference data (manually digitized from shaded relief maps) to serve as evaluation points for the elevation error of the model methods (Manual, Type1, Type3, Type4, Type4top, Agrell2m, and Agrell50m). Elevation data for the HCL reference data was extracted from the DEM to each random sample point as well as elevation data for corresponding point along the HCL boundary generated by the model methods. The corresponding point was identified as the point perpendicular to the random sample points along the reference data (Figure 9).

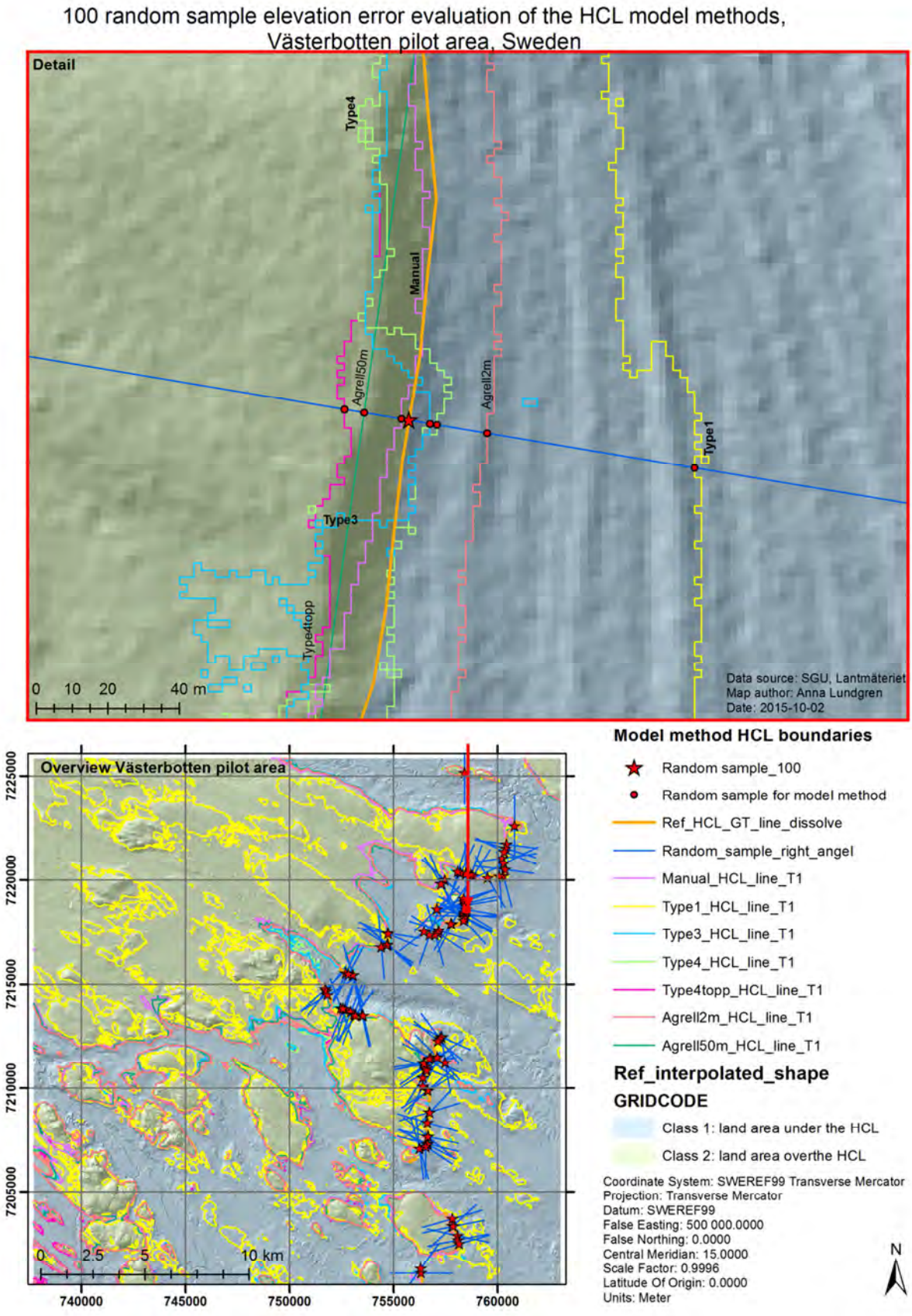

Figure 9 Location of 100 random samples along the digitized HCL boundary reference data and the modeled HCL boundaries used for evaluating elevation errors of the model methods.

Elevation difference between random evaluation points for the model method data and the reference data are defined as the elevation error and were calculated as follows:

$$\Delta h_{m_i} = h_{m_i} - h_{r_i} \quad (9)$$

where $h_{m_i}$is the model method elevation value for random sample i, $h_{r_i}$is the reference elevation value for random sample i, and $\Delta h_{m_i}$is the elevation error for model method m at random sample i.

The distributions of the elevation error data sets for each model method (Δh_m) were visually investigated using a Normal Quantile plot method (Höhle and Höhle 2009).

The elevation error for each model method (E_m) was estimated by calculating the median (50% quantile) and the normalized median absolute deviation (NMAD, Eq. 10) for the signed elevation errors (Δh_m), and the 68.3 % quantile and the 95% quantile for the absolute elevation errors ($|\Delta h_m|$) which are robust accuracy measures suggested by Hasan et al. (2012) and Höhle and Höhle (2009) for non-normal error distributions (see Normal Quantile plots result).

$$NMAD = 1.4826 \times median(|\Delta h_{m_i} - m_{\Delta h_m}|) \quad (10)$$

where $m_{\Delta h_m}$is the median of elevation errors for model method m and $\Delta h_{m_i}$is the elevation error for model method m at random sample i (see Hasan et al. 2012 and Höhle and Höhle 2009 for details).

4 Result

In this chapter the resulting decisions from the visual evaluation of the investigated LSPs and scale dimensions for the Test run1 area and the Västerbotten pilot area are presented in section 4.1, the resulting breakline extractions within the Västerbotten pilot area are presented in section 4.2, the model methods breakline classifications and HCL point generations within the Västerbotten pilot area are presented in section 4.3, the HCL surface and boundary maps generated for the Västerbotten pilot area by the model methods are presented in section 4.4, and finally the accuracy of the HCL boundary data generated by the model methods are presented in section 4.5. For further discussion of the results see chapter 0.

4.1 LSP and scale dimension evaluation

The visual comparison of the LSP rasters (roughness index and curvature) generated for the Test run 1 area within the Gästrikland pilot area for the 23 scale dimensions revealed that the curvature LSP was useful for extraction of linear breakline features related to wave washed areas and areas with glacial flow lineation (Figure 10).

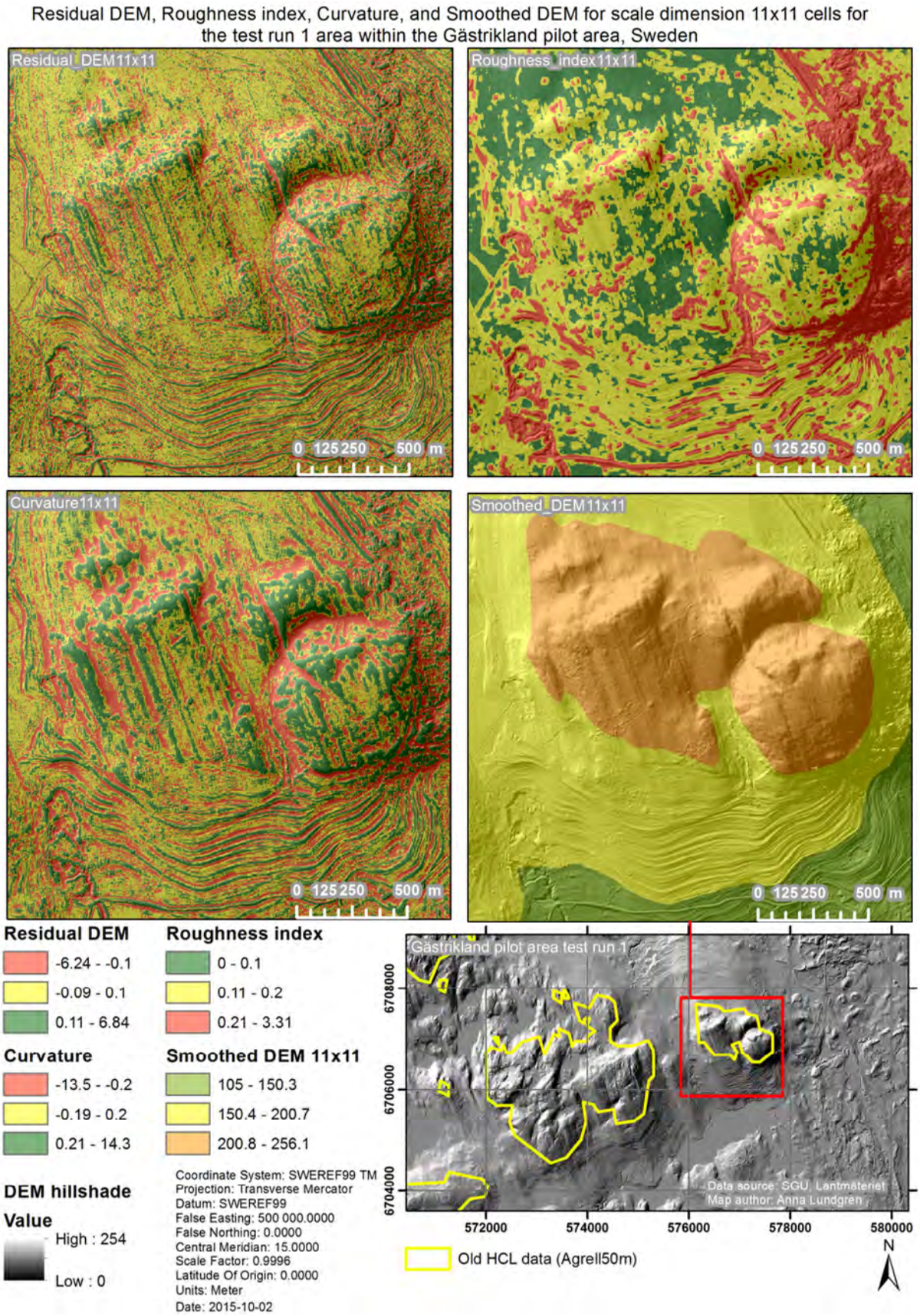

Figure 10 Examples of residual DEM, roughness index, curvature, and mean DEM (i.e. smoothed DEM) LSP rasters for scale dimension 11x11 cells within Test run 1 area in the Gästrikland pilot area.

The visual evaluation of suitable scale dimension using the curvature LSP conducted in the Test run 1 area concluded that a moving window size of 11x11 cells enhances breaklines related to wave washed features and glacial flow lineation features satisfactory. Figure 11 presents a comparison of breaklines extracted from “normal/mean” curvature, profile curvature, and plan curvature LSP rasters using scale dimension 11x11 cells on the moving window within the Test run 1 area in the Gästrikland pilot area.

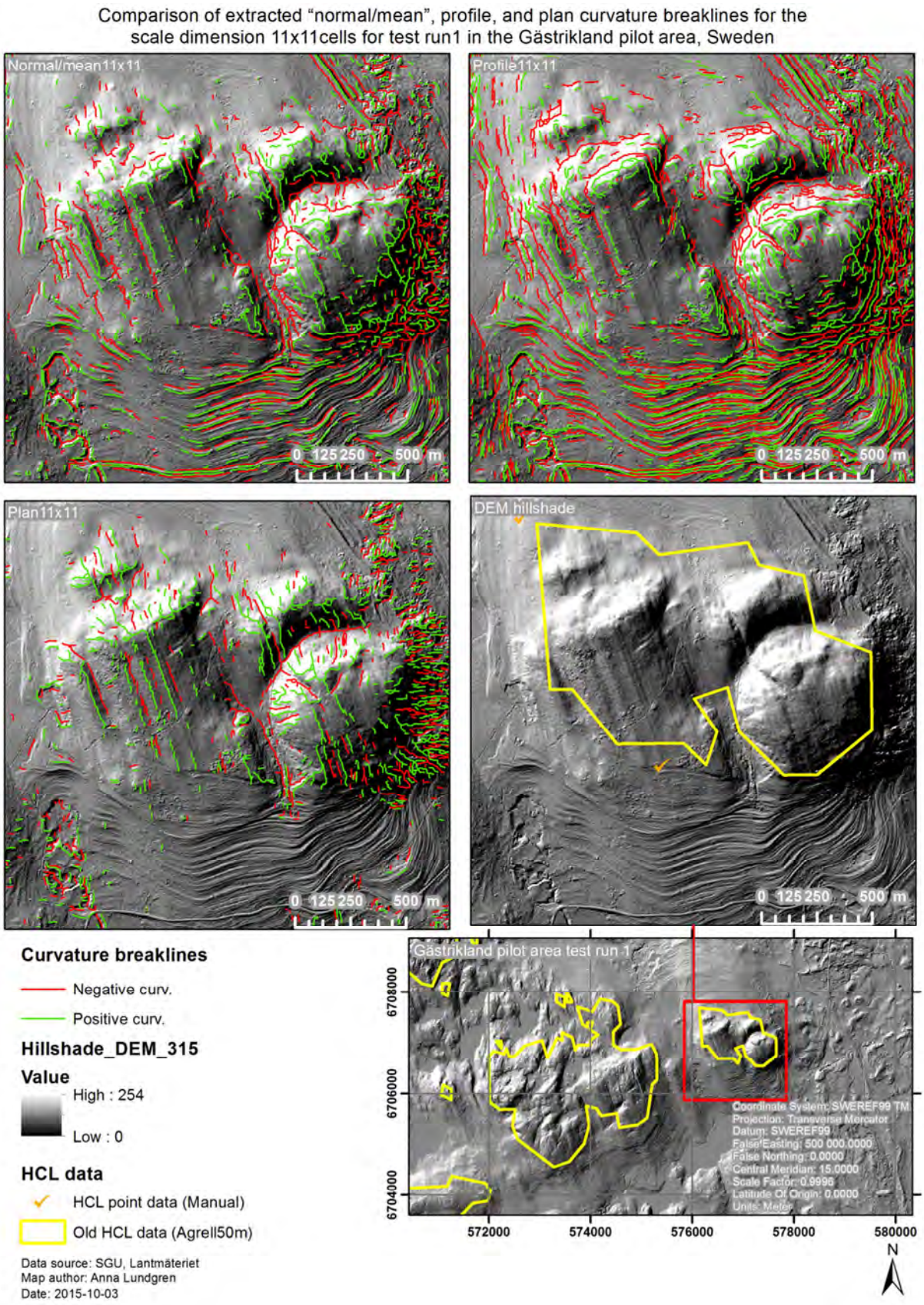

Figure 11 Comparison of breaklines extracted from "Normal/mean", profile, and plan curvature LSP rasters with scale dimension 11x11 cells within the Test run 1 area located in the Gästrikland pilot area.

A window size of 11x11 cells was also determined to be an appropriate scale dimension for extracting breaklines related to wave washed feature and glacial flow lineation in the Västerbotten pilot area. For a comparison of extracted “normal/mean” curvature polylines for scale dimension (moving window size) of the original DEM (2x2 meters) up to 19x19 cells for an area within the Västerbotten pilot area see Appendix B Figures B1-B3.

The roughness index LSP for coarse scale dimensions (around 99x99 cells) was useful in the separation of wave washed feature breaklines from glacial flow lineation feature breaklines within the Test run 1 area in the Gästrikland pilot area (Figure 12) and thus was a candidate for the *Select By Location*-step in the Type1 model method (see section 3.2.6 and Appendix D Figure D3 for details on the Type1 model method).

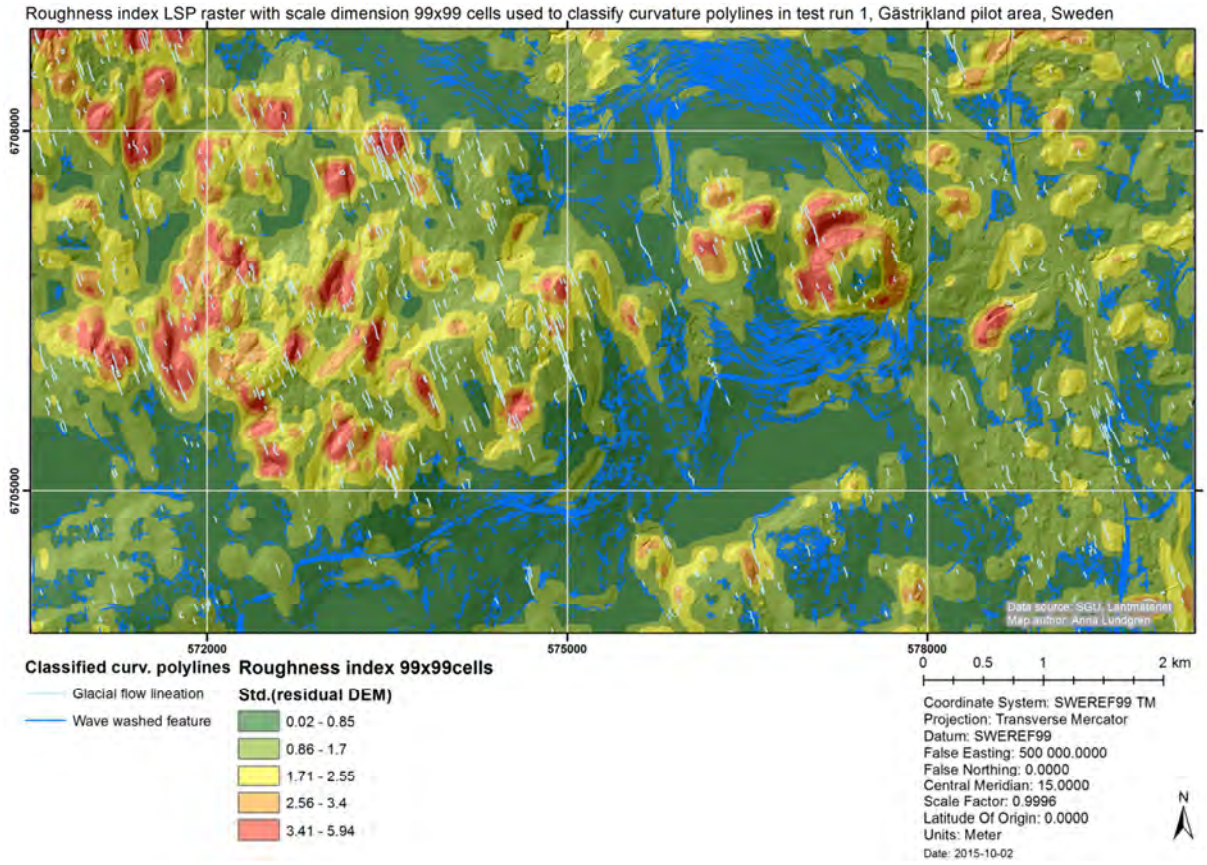

Figure 12 99x99 cell dimensioned roughness index LSP raster applied in the classification of wave washed feature breaklines and glacial flow lineation feature breaklines in the Test run 1 area in the Gästrikland pilot area.

Coarse scale dimensioned residual DEM LSP rasters generated from a high-pass filter with moving window size around 2999x2999 cells was visually evaluated as useful for the separation of wave washed feature breaklines and glacial flow lineation feature breaklines in the Västerbotten pilot area (Figure 13) and applied in the *Select By Location*-step of the Type1 model method (see section 3.2.6 and Appendix D Figure D3 for details on the Type1 model method).

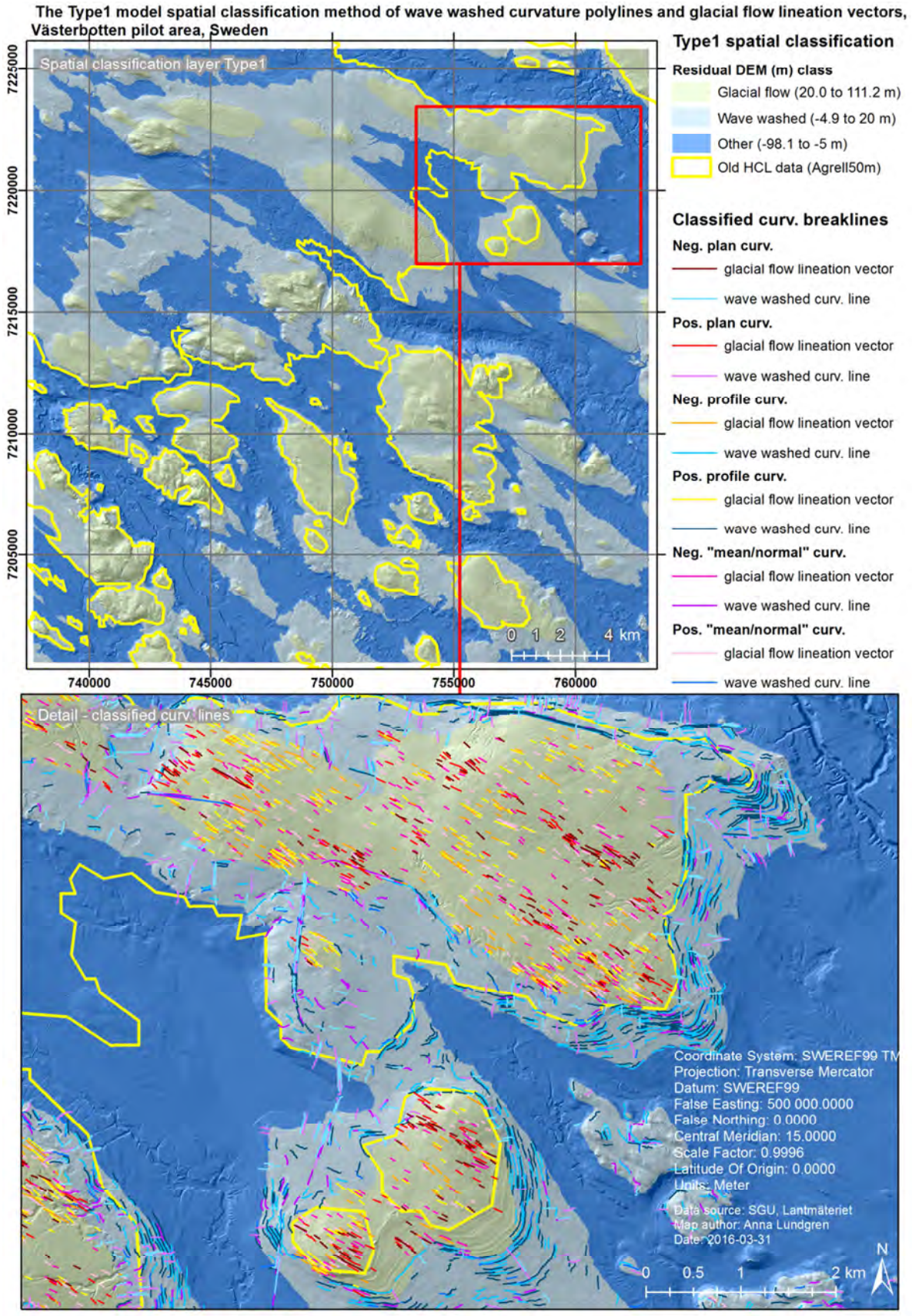

Figure 13 Coarse scale dimensioned (2999x2999 cells) residual DEM LSP raster used for separating land area with wave washed features from land area with glacial flow lineation features in the Type1 model method breakline classification (also see Figure 18).

4.2 Breakline extraction result for 11x11cell window

Figures 14, 15, and 16 present an overview of the breakline extraction result in the Västerbotten pilot area for “normal/mean” curvature, profile curvature, and plan curvature respectively using the 11x11 cell scale dimension.

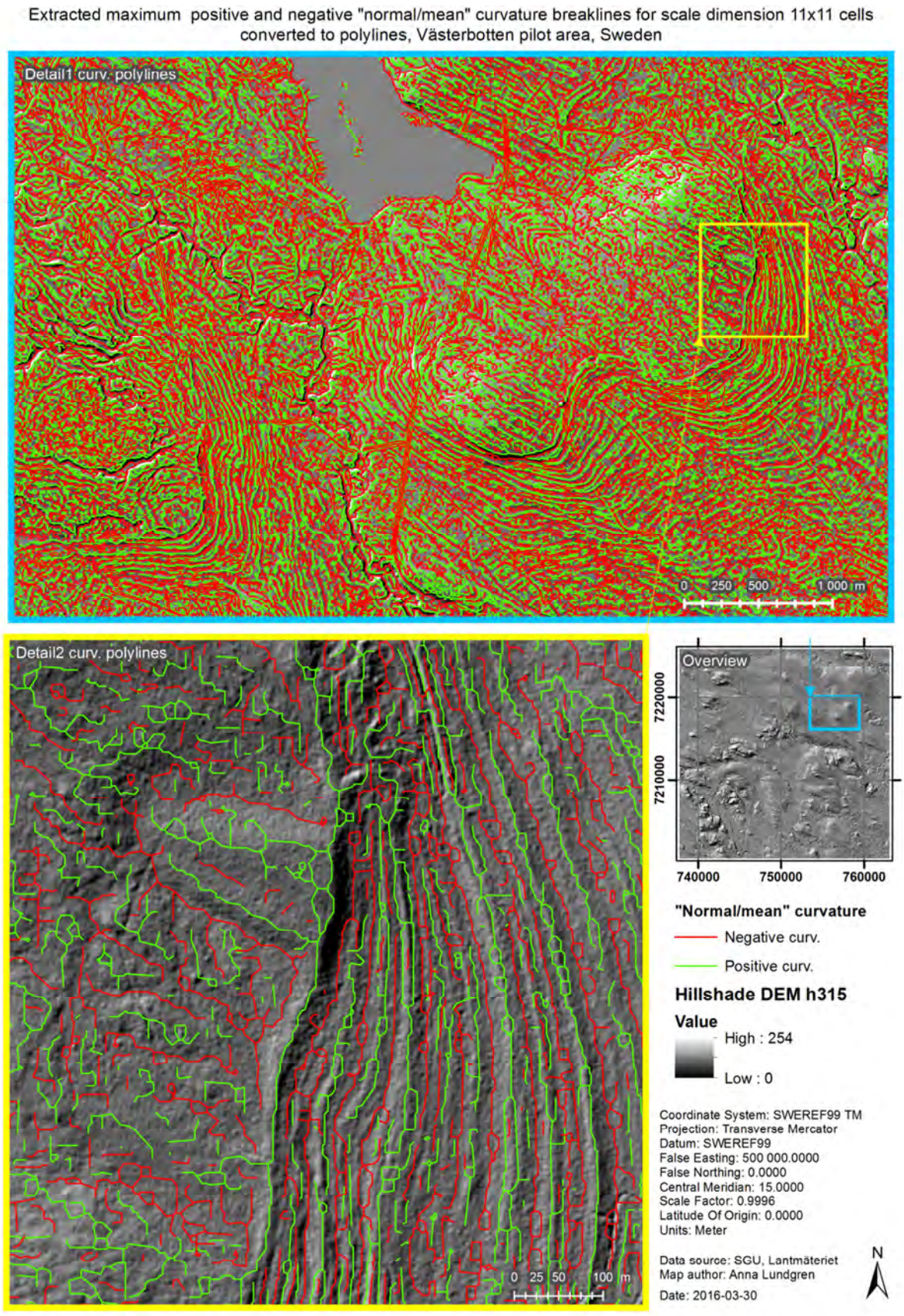

Figure 14 Resulting breaklines extracted from an 11x11 scale dimensioned "normal/mean" curvature LSP raster for the Västerbotten pilot area.

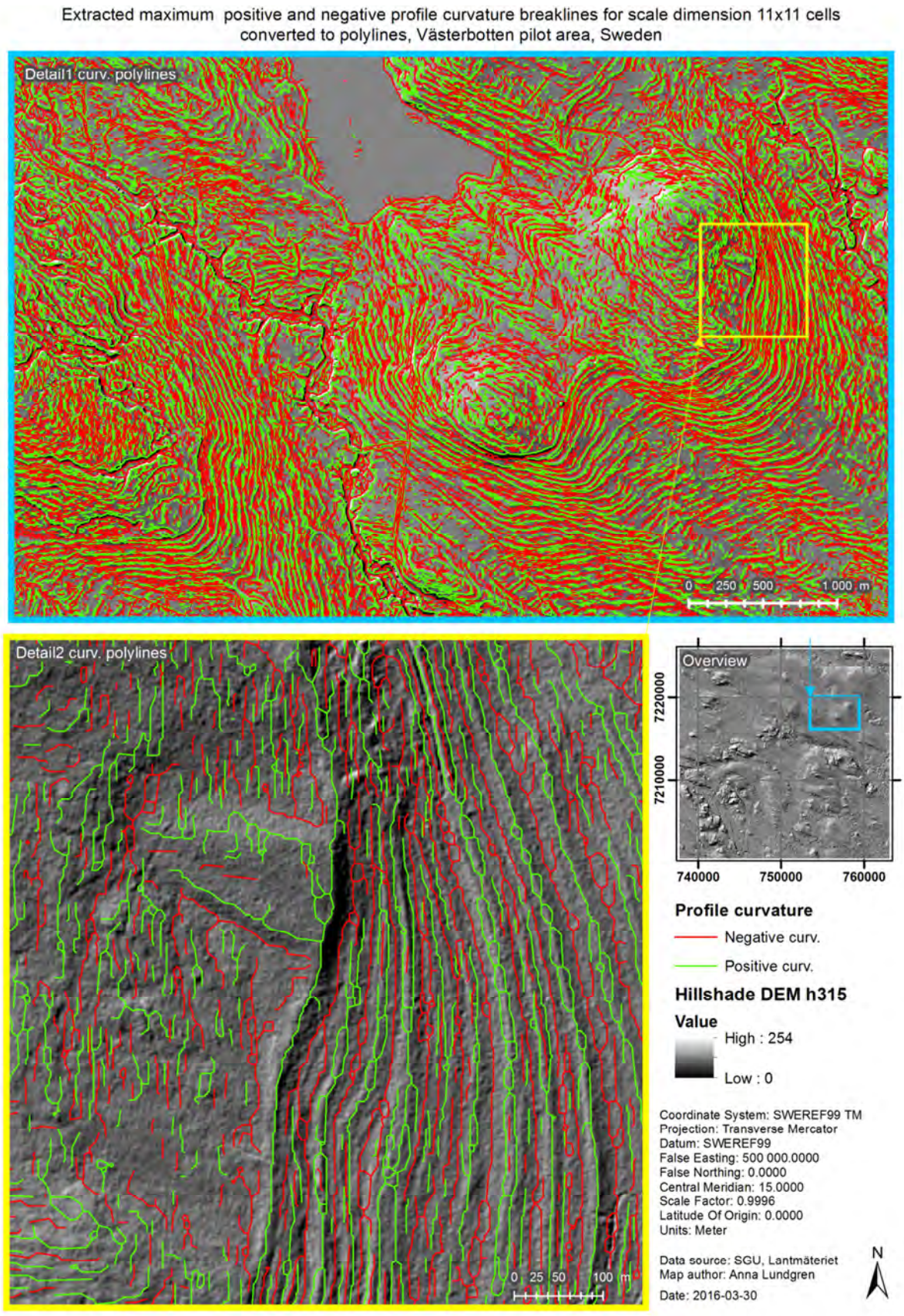

Figure 15 Resulting breaklines extracted from an 11x11 scale dimensioned profile curvature LSP raster for the Västerbotten pilot area.

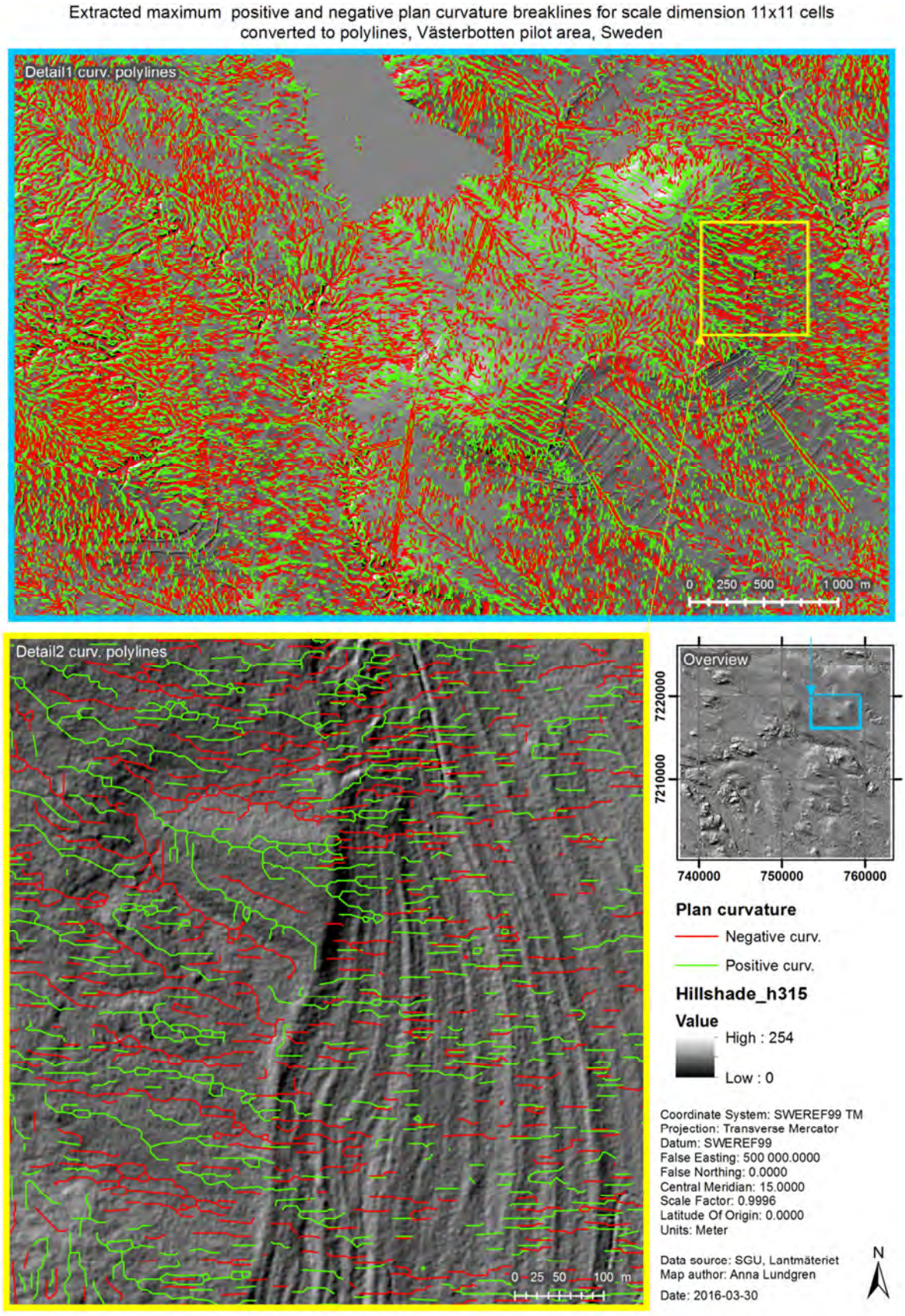

Figure 16 Resulting breaklines extracted from an 11x11 scale dimensioned plan curvature LSP raster for the Västerbotten pilot area.

The visual inspection of the positive and negative curvature polyline data sets (Figures 14-16) shows that “normal/mean” curvature breaklines enhance both wave washed features and glacial flow lineation features, profile curvature breaklines enhance both wave washed features and glacial flow lineation features, and plan curvature breaklines do not enhance wave washed features but they enhance the glacial flow lineation features. Thus “normal/mean” and profile curvature polylines were used as input data sets for the classification of wave washed feature breaklines; and “normal/mean”, profile, and plan curvature polylines were used as input data sets for the classification of glacial flow lineation feature breaklines (see Figure D3 in Appendix D).

Figure 17 presents a detailed example of the extracted breaklines from 11x11 cell scale dimensioned “normal/mean”, profile, and plan curvature LSP rasters within the Västerbotten pilot area. More detail examples of the resulting breakline extraction can be found in Appendix B Figures B4-B14.

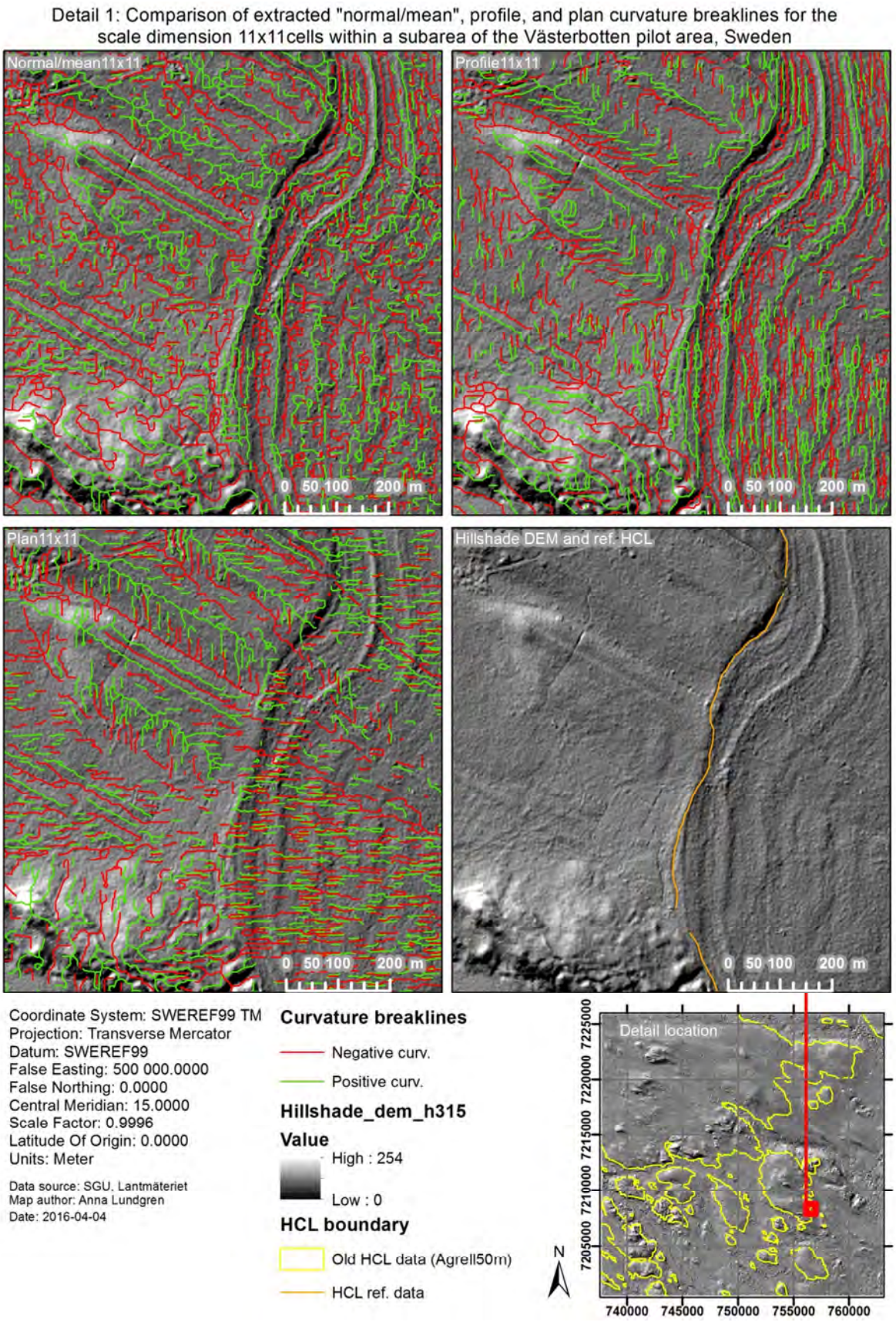

Figure 17 Detail of extracted negative and positive "normal/mean", profile, and plan curvature breaklines for the Västerbotten pilot area. The middle right image shows the hillshade map and the manual digitized HCL boundary reference for the same area.

4.3 Model method classification of breaklines and resulting HCL point generation

The total number of extracted breaklines using the 11x11cell dimensioned “normal/mean”, profile, and plan curvature LSP rasters are presented in Table 3. The number of breaklines classified as glacial flow lineation and as wave washed breaklines by the different model methods are also presented in Table 3.

Table 3 Total number of extracted breaklines and number of breaklines classified as glacial flow lineation and as wave washed feature breaklines by the Type1, Type3, Type4, and Type4top model methods for the Västerbotten pilot area. Results are presented for negative and positive “normal/mean”, profile, and plan curvature.

	Breakline polyline layer – number of curvature polylines						
	positive "normal/mean" curv.	*negative "normal/mean" curv.*	*positive profile curv.*	*negative profile curv.*	*positive plan curv.*	*negative plan curv.*	*sum*
Total no. extracted	729694	838146	536047	619223	592987	561769	3877866
Classification result							
Type1 glacial flow lineation	3823	3496	3480	3282	1897	1699	17677
Type1 wave washed	2848	3056	3919	4160	--	--	13983
Type3 glacial flow lineation	688	533	407	346	329	223	2526
Type3 wave washed	577	533	972	1015	--	--	3097
Type4 wave washed	141	118	188	158	--	--	605
Type4top wave washed	118	32	153	39	--	--	342

Below the resulting breakline classification and HCL point generation for each model method are presented.

4.3.1 Type1 model method

The sinuosity, length, and orientation criteria used in the Type1 model method *Select By Attribute* step to classify breaklines into wave washed features and into glacial flow lineation features are presented in Table 4.

Table 4 Sinuosity, length, and orientation criteria used in the Select By Attribute step and the residual DEM value range criteria used in the Select By Location step of the Type1 model method.

Classification criteria Type 1 model method		
Curv. polyline	wave washed features	glacial flow lineation
Select By Attribute criteria		
sinuosity	1-1.3	1-1.3
length	≥ 100 m	≥ 50 m
orientation	0°-109° or 136°-360°	110-135°
Select By Location criteria		
residual DEM 2999x2999cells	-4.9 m to 20 m	> 20m

The *Select By Attribute* criteria values are based on samples of the extracted curvature polylines manually classified into wave washed feature breaklines and glacial flow lineation breaklines (section 3.2.6.1).

The criteria used in the Type1 model method *Select By Location* classification-step for separating land area with glacial flow lineation from land area with wave washed features are presented in Table 4 and Figure 18.

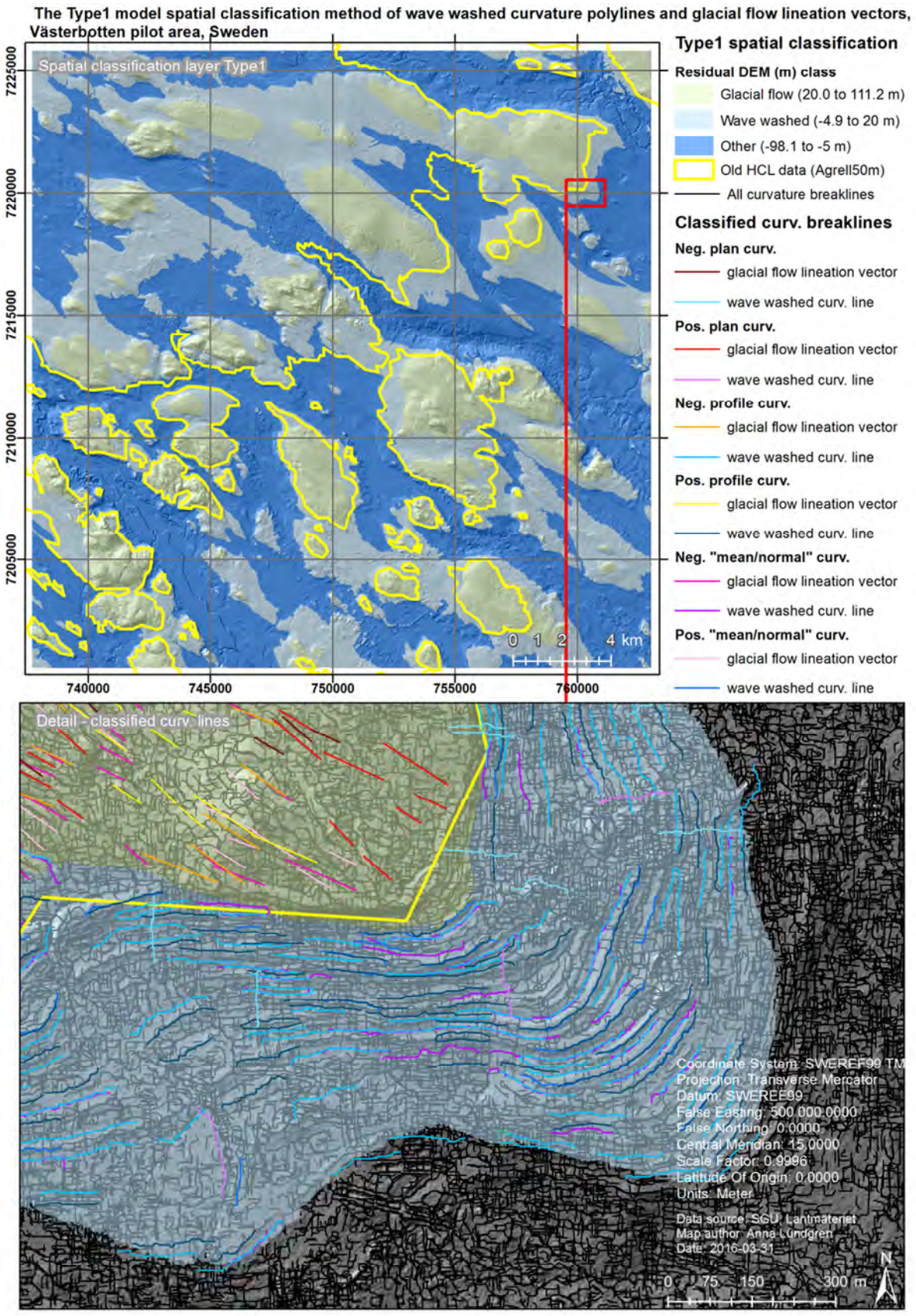

Figure 18 Select By Location-step in the Type1 model method where a 2999x2999 cell dimensioned residual DEM LSP raster is applied for the separation of land area with wave washed features and land area with glacial flow lineation features.

The *Select By Location* criteria was set by a coarse scaled (2999x2999 cells) residual DEM LSP raster reclassified into 3 classes: Wave washed class = residual DEM values -4.9 m to 20 m, Glacial flow class = residual DEM values > 20m, and Other class = residual DEM values < -4.9 m (Figures 18 and 13). See Figure D3 in Appendix D for details on the Type1 model method workflow used in ArcGIS 10.2.

Of the total number of extracted breaklines (3877866) within the Västerbotten pilot area 17677 were classified as breaklines related to glacial flow lineation features and 13983 were classified as breaklines related to wave washed features by the Type1 model method (Table 3 and Figure 19).

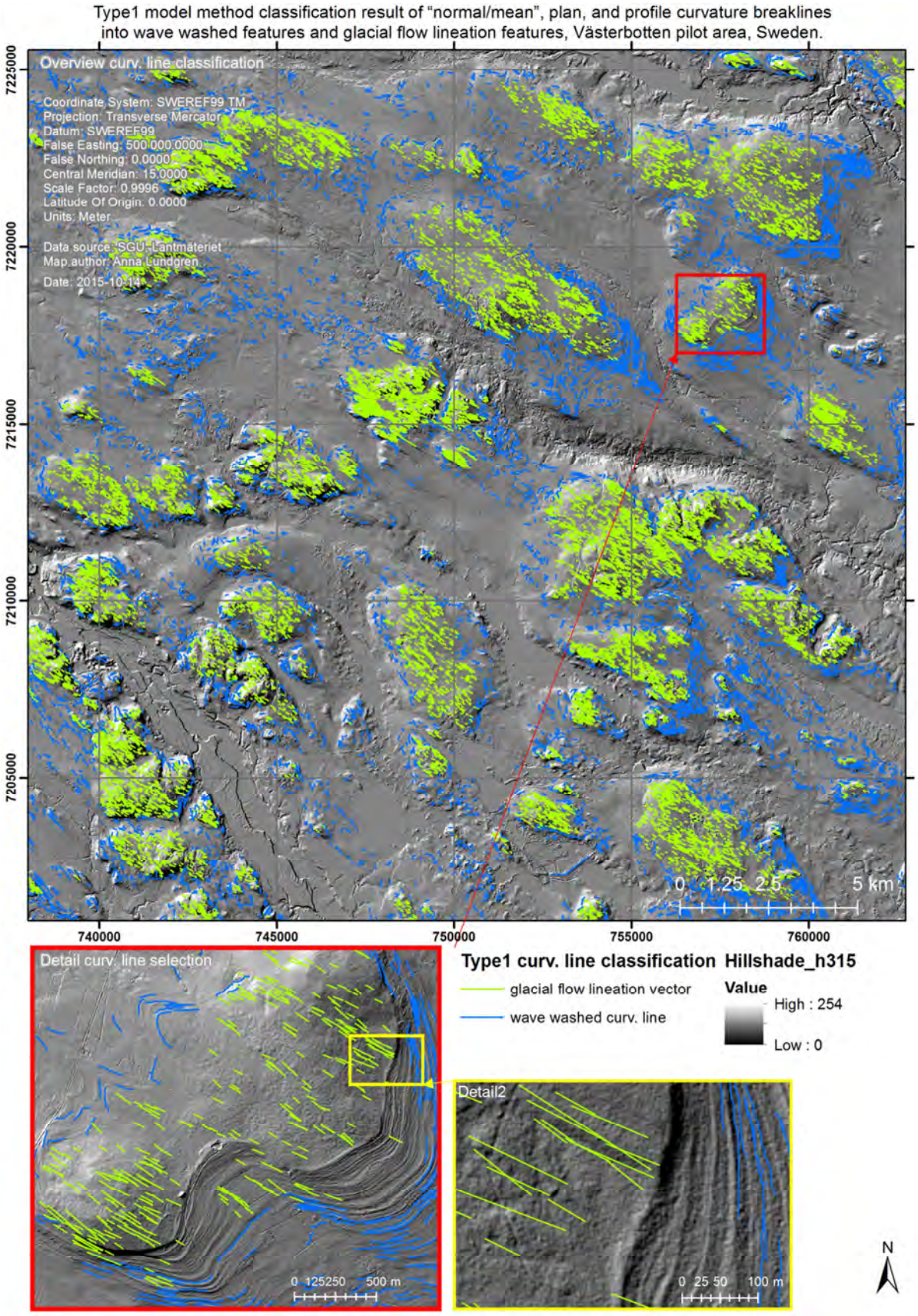

Figure 19 Type1 model method breakline classification result within the Västerbotten pilot area.

All 17677 glacial flow lineation breakline vectors were elongated in the Type1 model method (see Figure D3 in Appendix D). The intersection between the elongated glacial flow lineation breakline vectors and the wave washed feature breaklines in the Type1 model method generated 23827 HCL points in the Västerbotten pilot area (Table 5 and Figure 20).

Table 5 Number of HCL-points generated within the Västerbotten pilot area by the model methods: Type1, Type3, Type4, Type4top, Manual, Agrell50m, and Agrell2m; point type, and interpolation method used for the HCL surface generation. The figure given in barracks for the Manual, Agrell50m, and Agrell2m model method is the number of HCL points available for the whole of Sweden.

Model method	No. HCL points	Point type	Interpolation method
Type1	23827	intersection point	IDW
Type3	1739	intersection point	IDW
Type4	6680	breakline vertex	IDW
Type4top	3736	breakline vertex	IDW
Manual	18 (735)	manual digitized	IDW
Agrell50m	3(937)	manual digitized	IDW
Agrell2m	3(937)	manual digitized	IDW

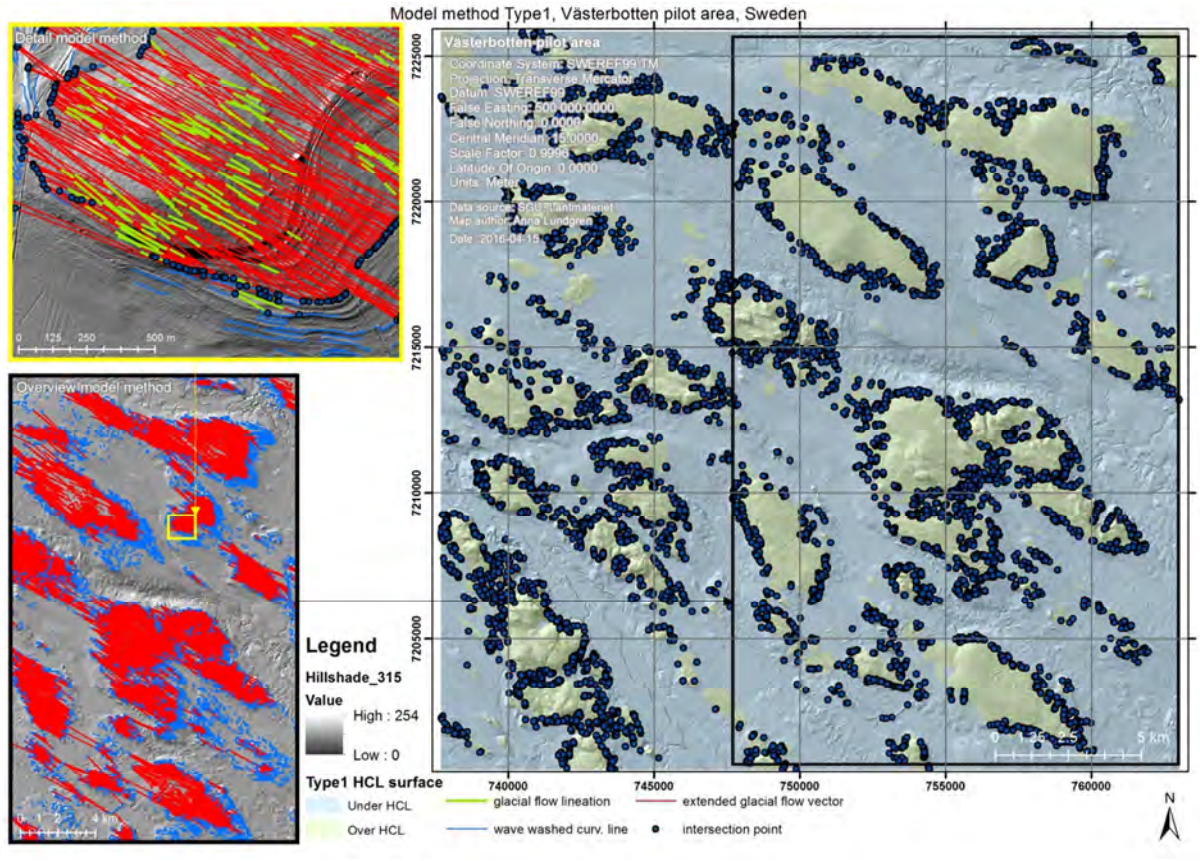

Figure 20 Overview of the elongation and intersection result generated by the Type1 model method within the Västerbotten pilot area.

4.3.2 Type3 model method

Within the Västerbotten pilot area 2526 of 3877866 extracted breaklines were classified as breaklines related to glacial flow lineation features and 3097 were classified as breaklines related to wave washed features by the Type3 model method (Table 3 and Figure 21).

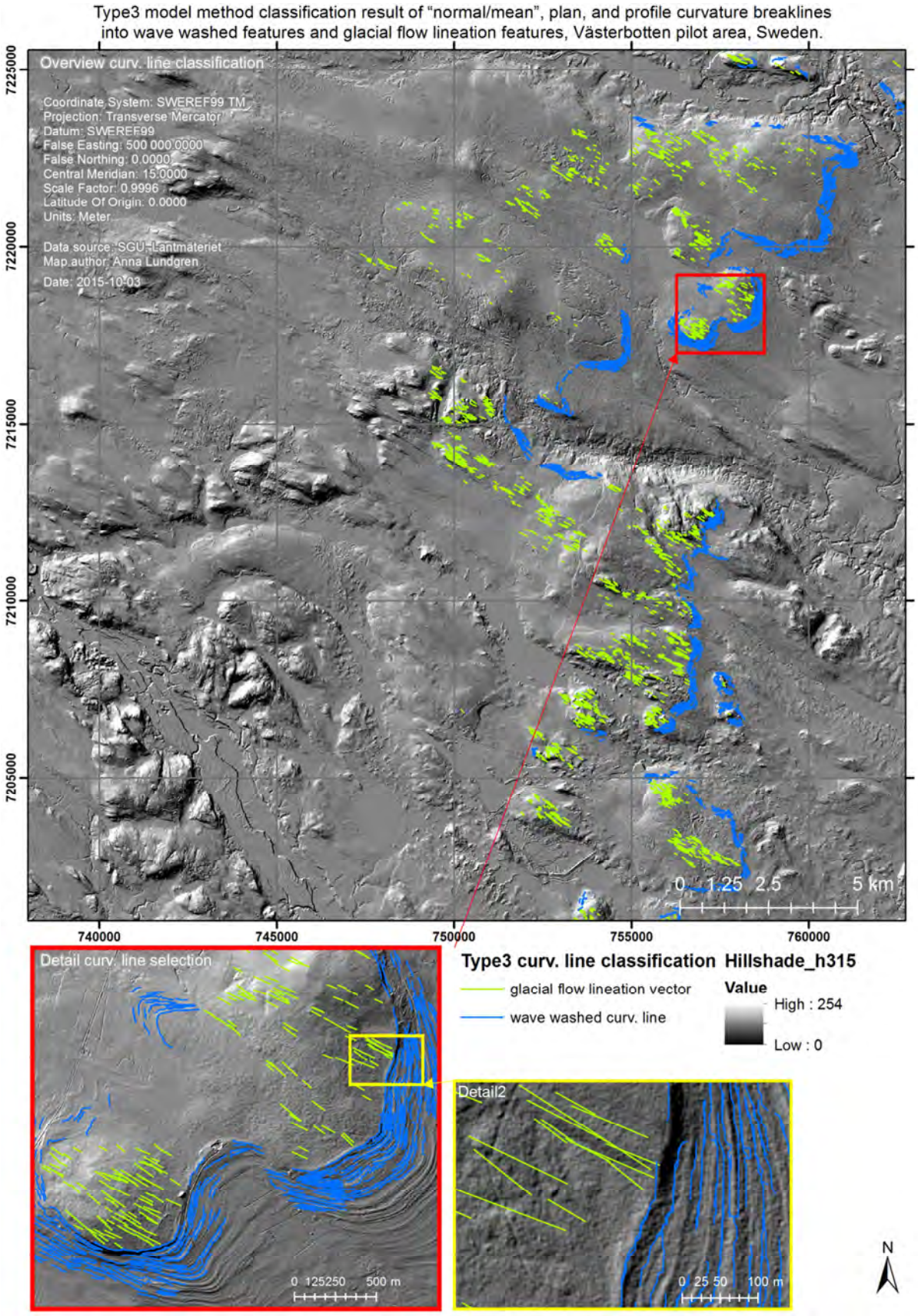

Figure 21 Type3 model method breakline classification result within the Västerbotten pilot area.

1511 of the 2526 breaklines classified as glacial flow lineation breakline vectors in the Type3 model method were elongated (Figure 22). The intersection between the elongated glacial flow lineation breakline vectors and the wave washed feature breaklines in the Type3 model method generated 1739 HCL points in the Västerbotten pilot area (Table 5 and Figure 22).

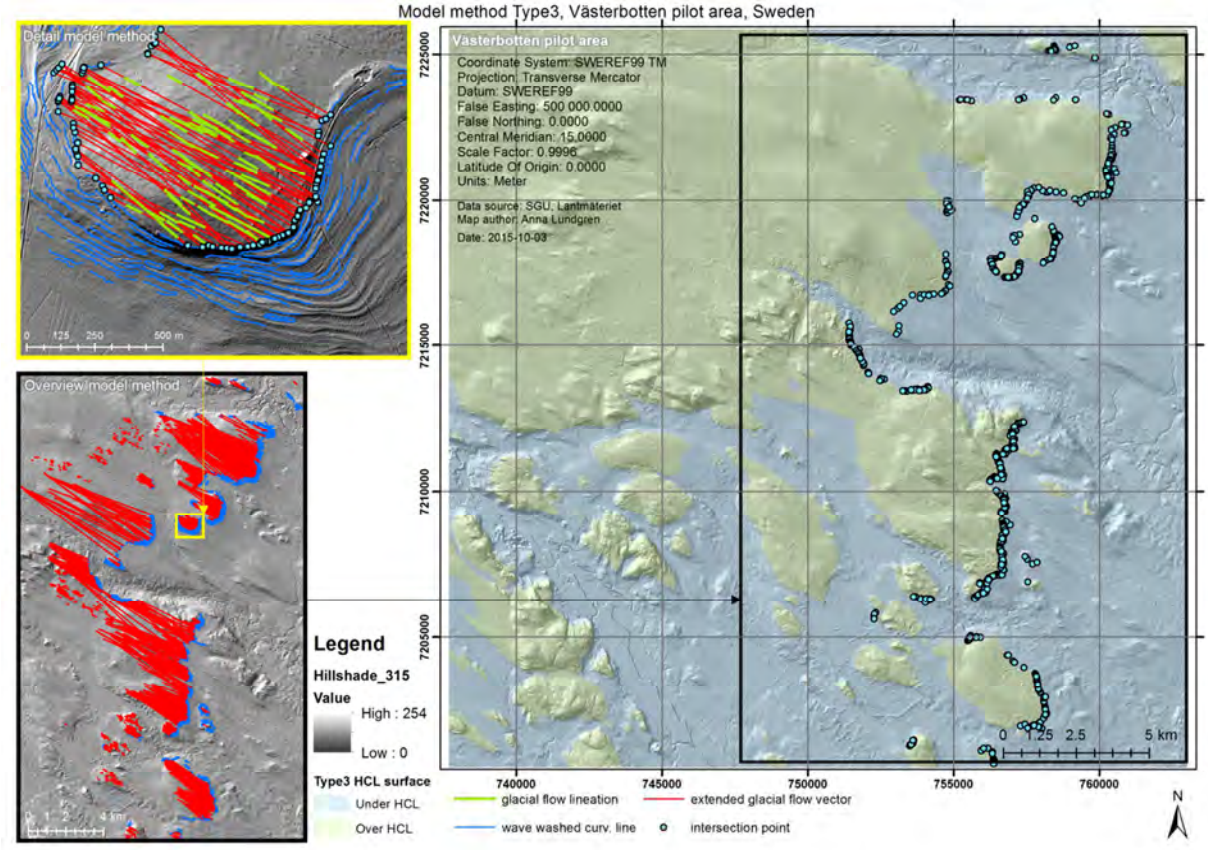

Figure 22 Overview of the elongation and intersection result generated by the Type3 model method within the Västerbotten pilot area.

4.3.3 Type4 model method

Within the Västerbotten pilot area, 605 of 3877866 extracted breaklines were classified as breaklines related to the two uppermost wave washed features by the Type4 model method (Table 3 and Figure 23). No glacial flow lineation feature breaklines were used by the Type4 model method.

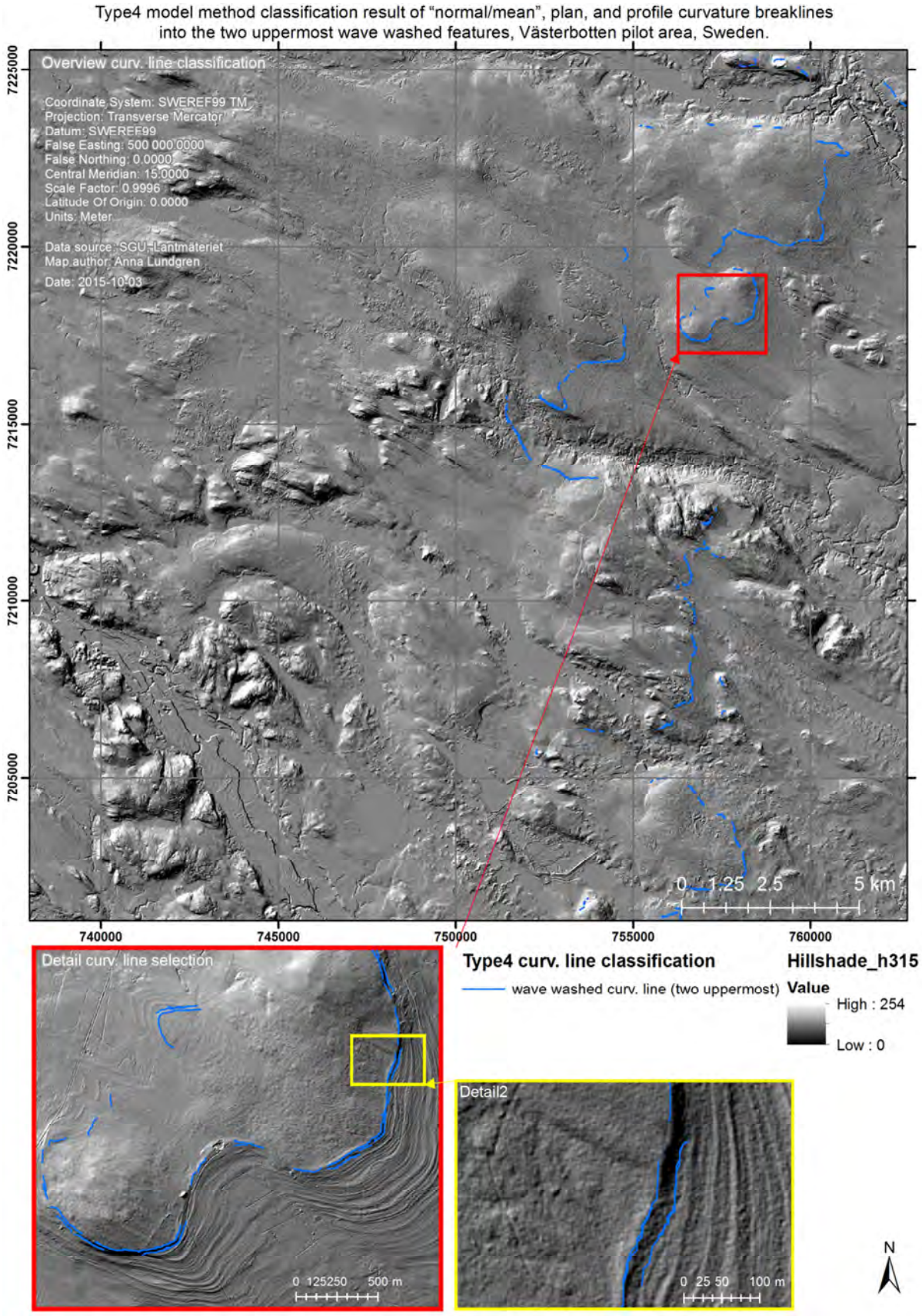

Figure 23 Type4 model method breakline classification result within the Västerbotten pilot area. The breaklines related to the two uppermost wave washed features adjacent to the HCL were used in the Type4 model method.

6680 HCL points were generated by the Type4 model method (Table 5 and Figure 24).

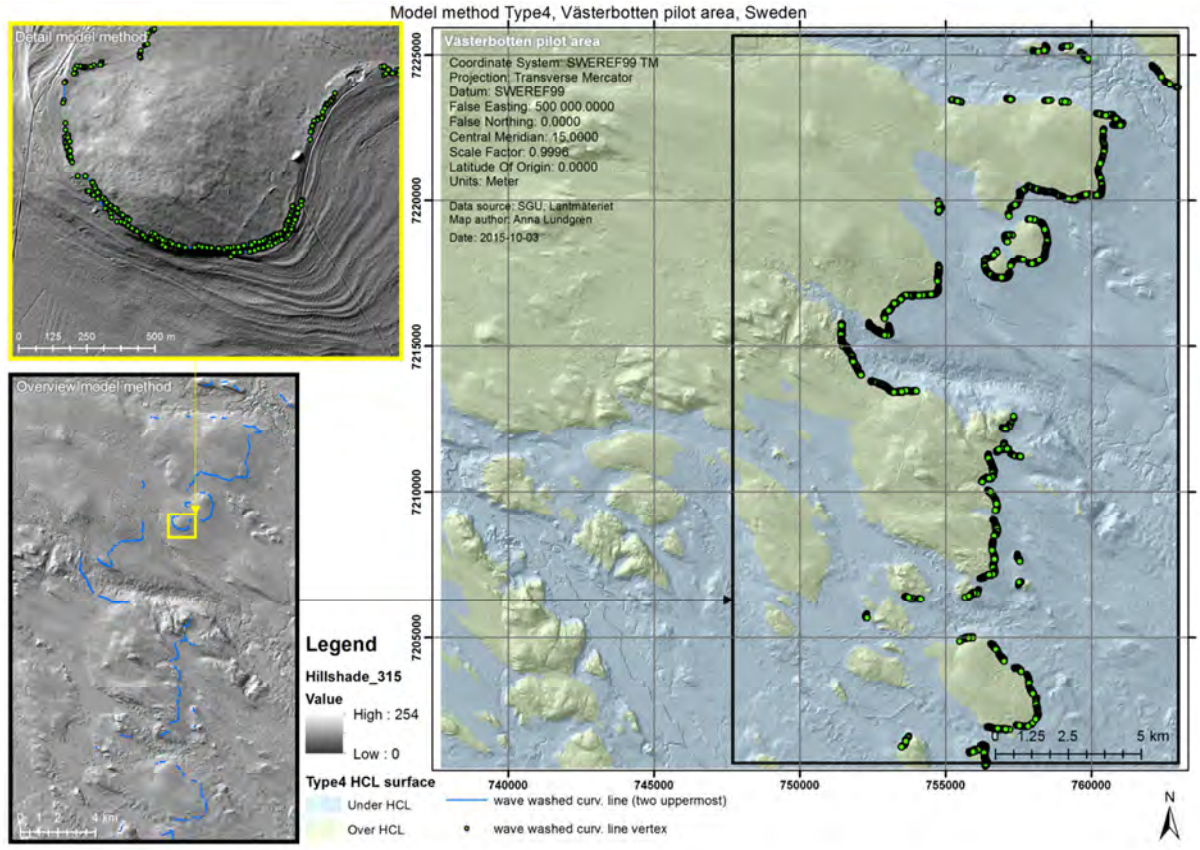

Figure 24 Overview of the HCL-points generated by the Type4 model method within the Västerbotten pilot area.

4.3.4 Type4top model method

Within the Västerbotten pilot area, 342 of 3877866 extracted breaklines were classified as breaklines related to the uppermost wave washed features by the Type4top model method (Table 3 and Figure 25). No glacial flow lineation feature breaklines were used by the Type4top model method.

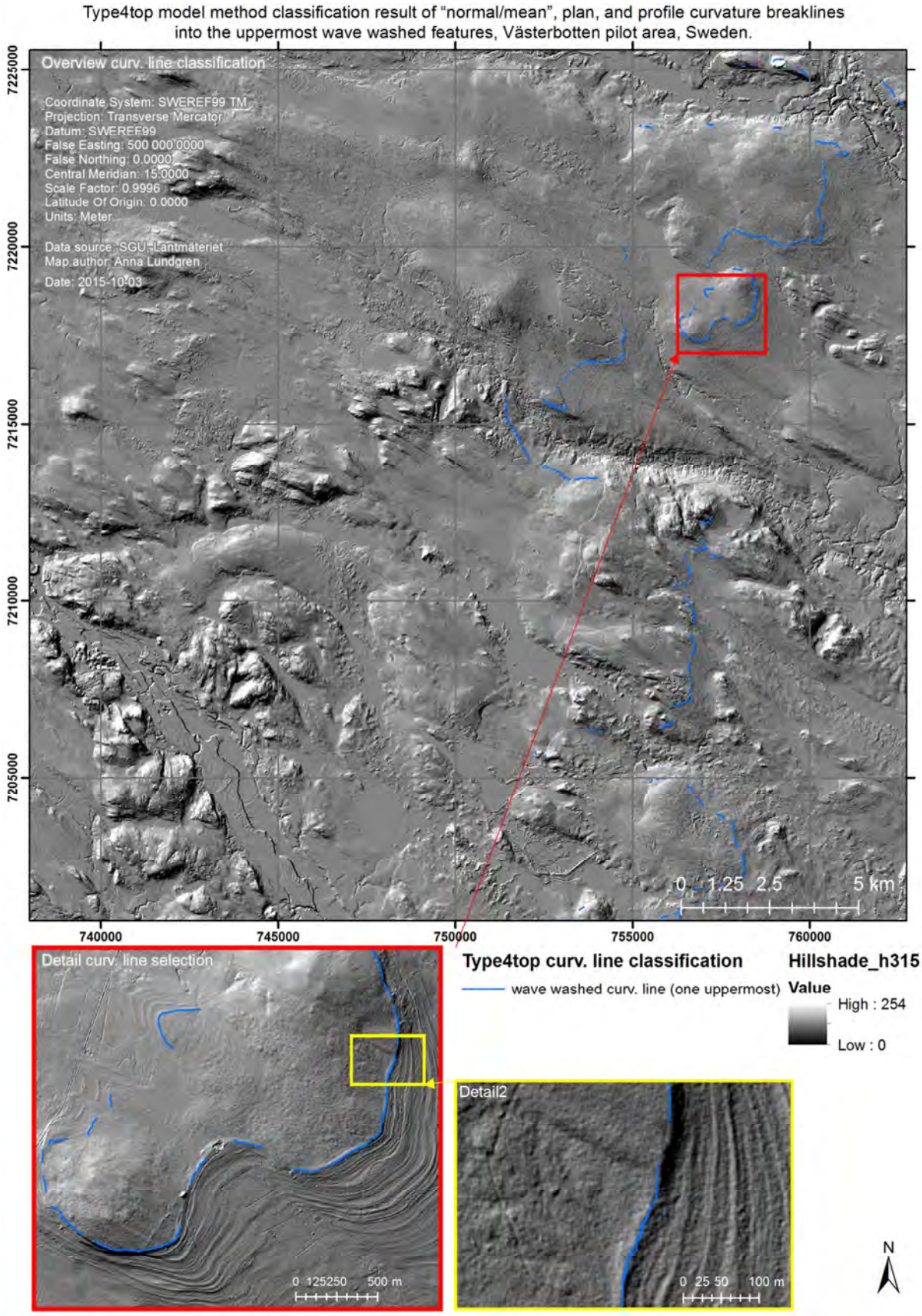

Figure 25 Type4top model method breakline classification result within the Västerbotten pilot area. The breaklines related to the uppermost wave washed features adjacent to the HCL were used in the Type4top model method.

3736 HCL points were generated by the Type4top model method (Table 5 and Figure 26).

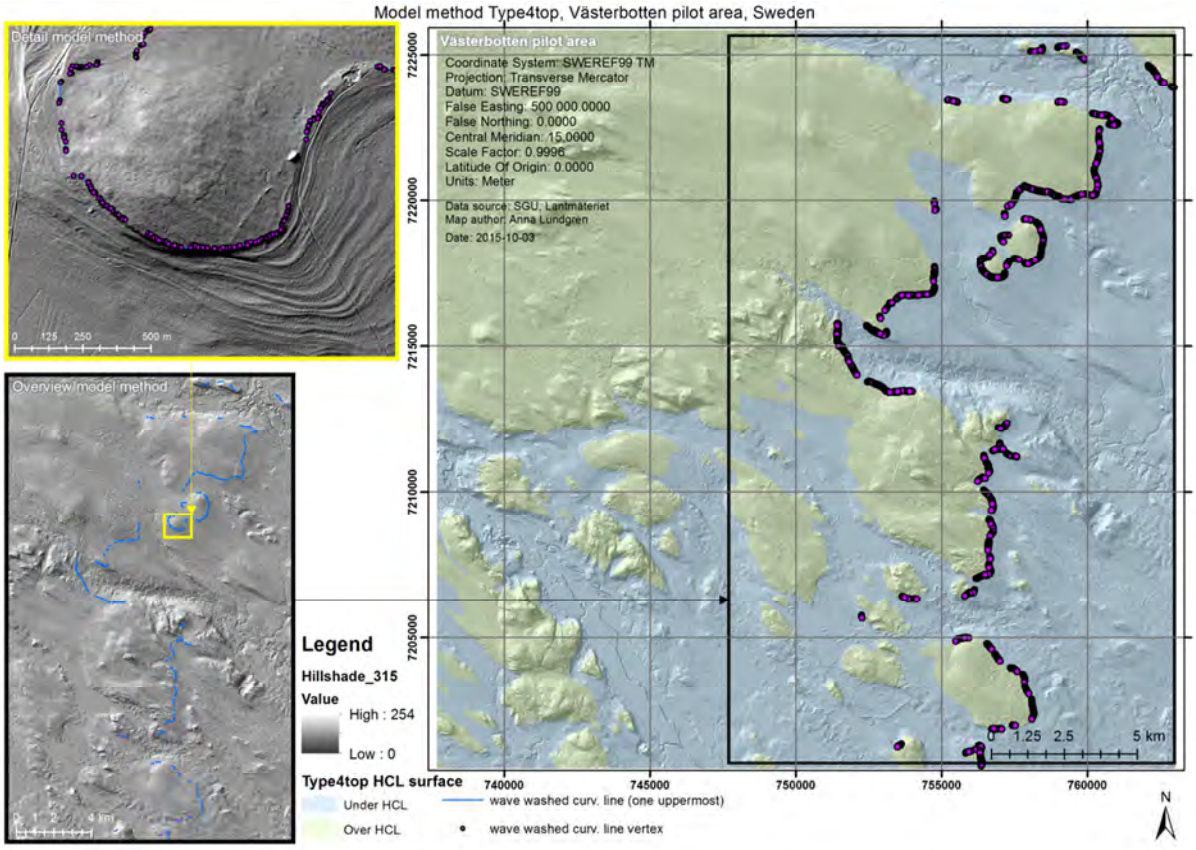

Figure 26 Overview of the HCL-points generated by the Type4top model method within the Västerbotten pilot area.

4.3.5 Manual model method HCL points

In the pre-study, 18 HCL point locations of wave washed type were manually digitized within the Västerbotten pilot area (Table 5 and Figure 27).

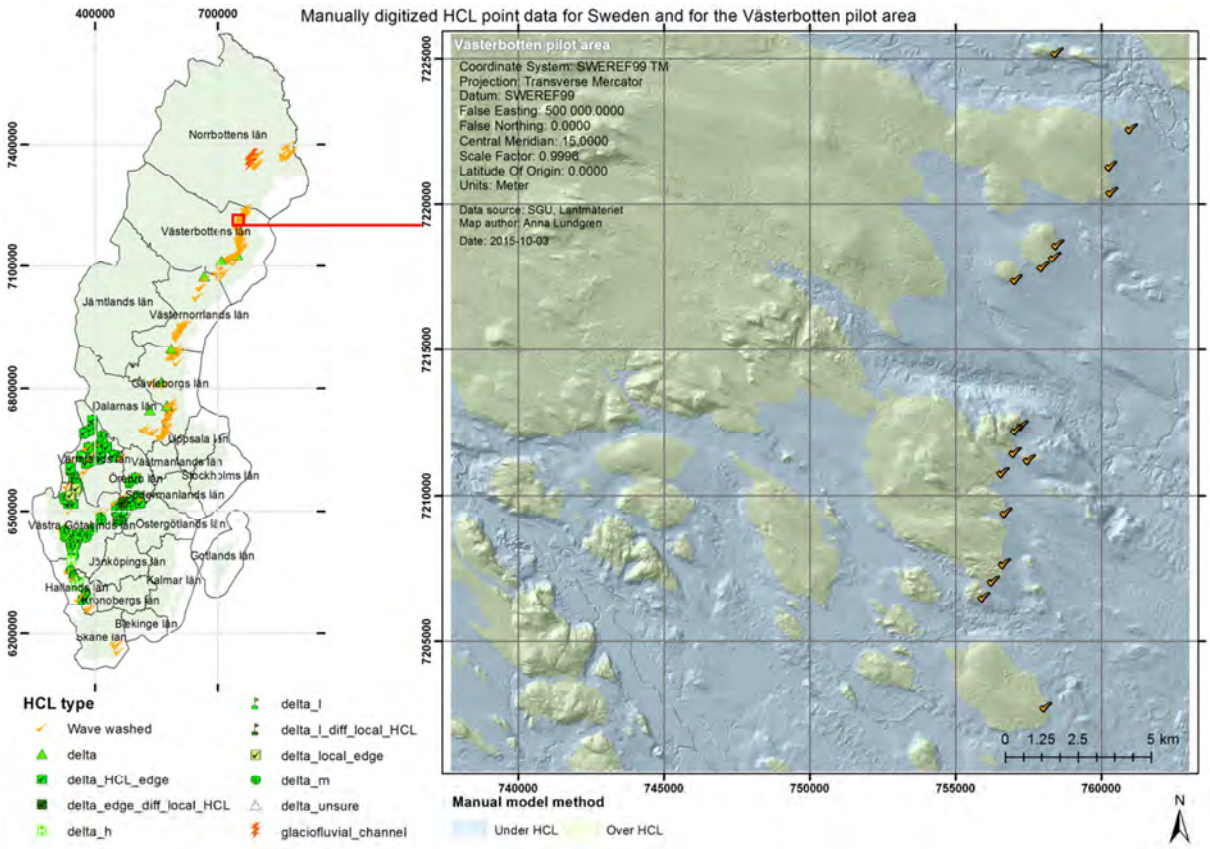

Figure 27 HCL point locations of wave washed type manually digitized in the pre-study within the Västerbotten pilot area. Other HCL point locations manually digitized during the pre-study of this project is presented in the overview map to the left and in Figure 3.

4.3.6 Agrell model method HCL points

The old HCL data set compiled by Agrell (2001) has 3 HCL point locations within the Västerbotten pilot area (Table 5 and Figure 28).

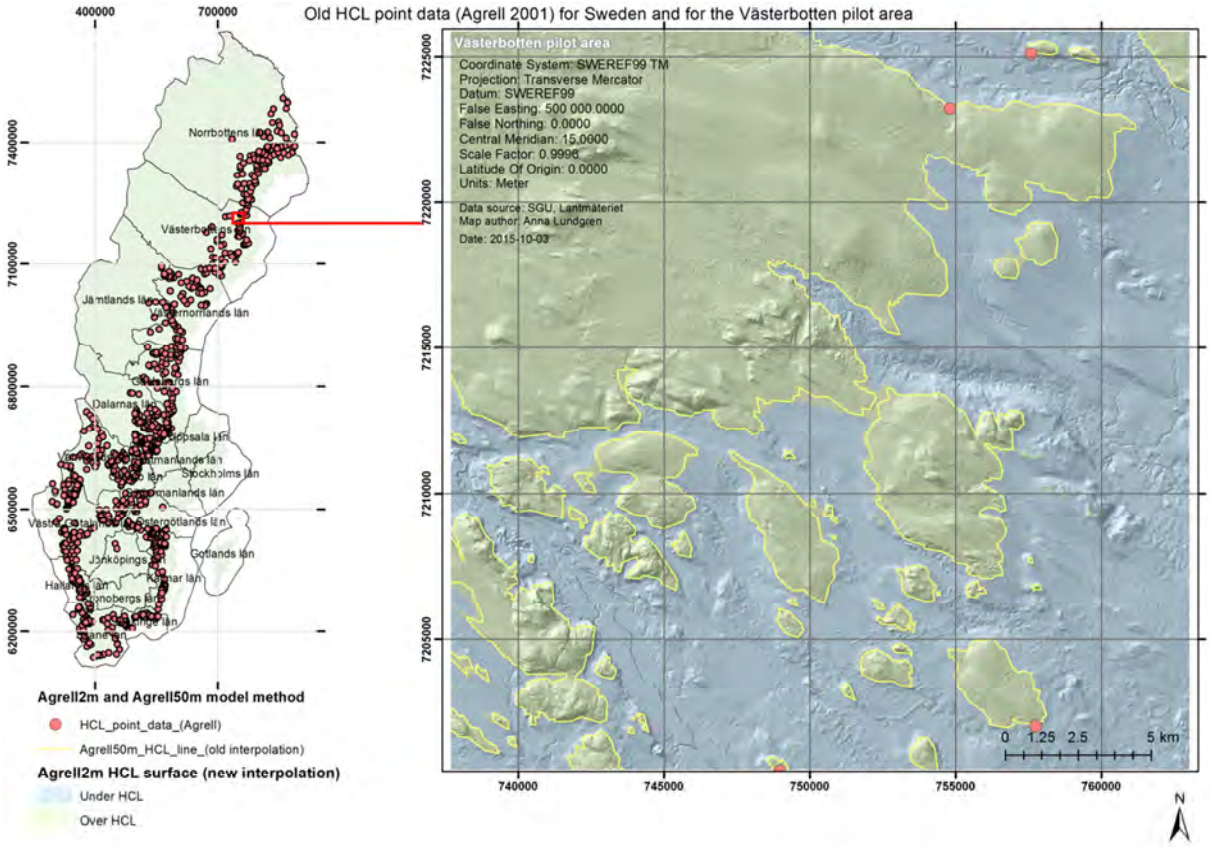

Figure 28 Old HCL data points (Agrell 2001) present in the Västerbotten pilot area. All available HCL point locations in the old HCL data are presented in the overview map to the left.

4.4 Resulting HCL maps – surfaces and boundaries

HCL boundaries resulting from the Type1, Type3, Type4, Type4top, Manual, Agrell50m, and Agrell2m model methods are presented in Figures 29 and 30.

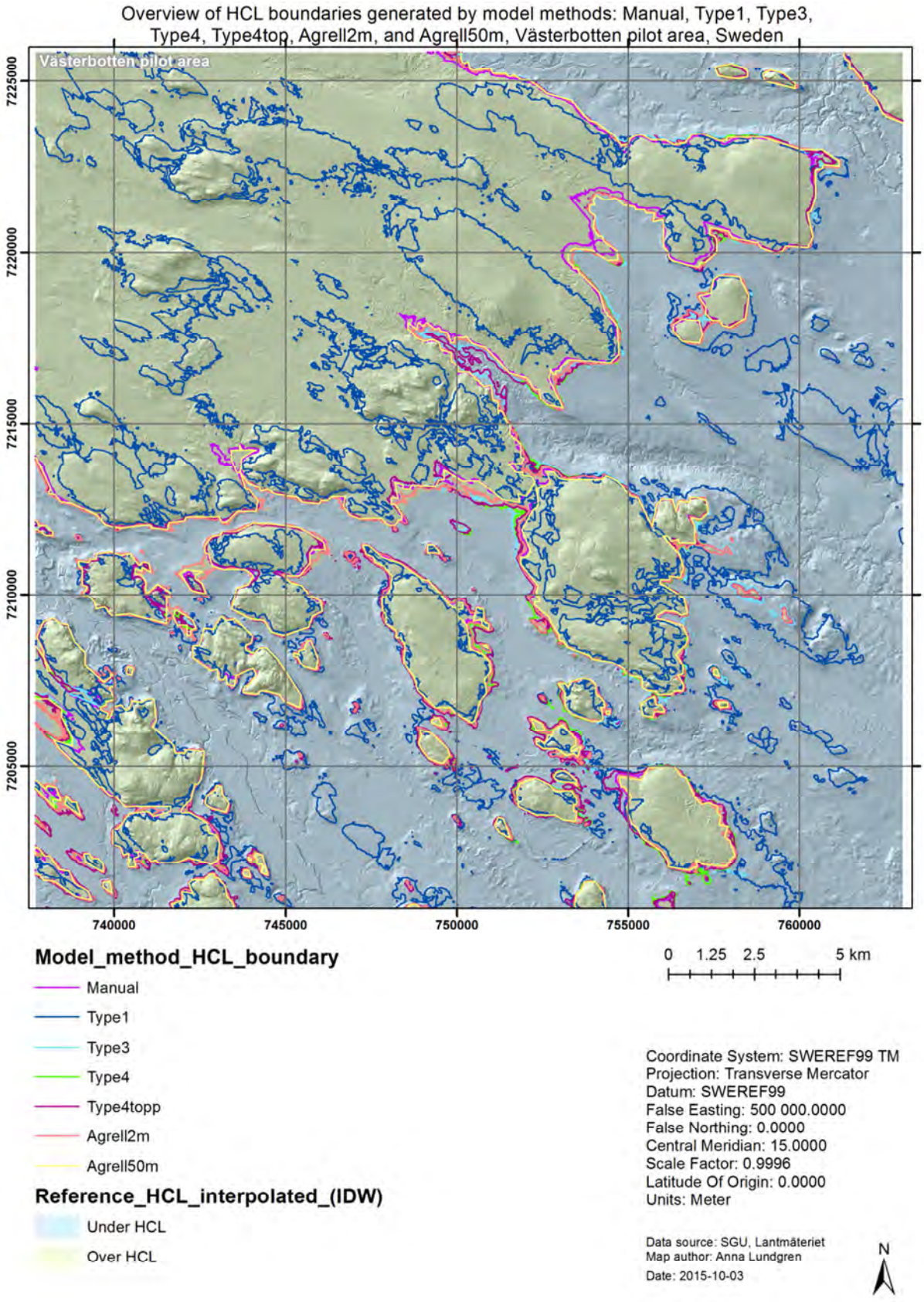

Figure 29 Overview map of the HCL boundaries resulting from the Type1, Type3, Type4, Type4top, Manual, Agrell50m, and Agrell2m model methods. The HCL surface reference interpolated from the manual digitized reference data is displayed in the background.

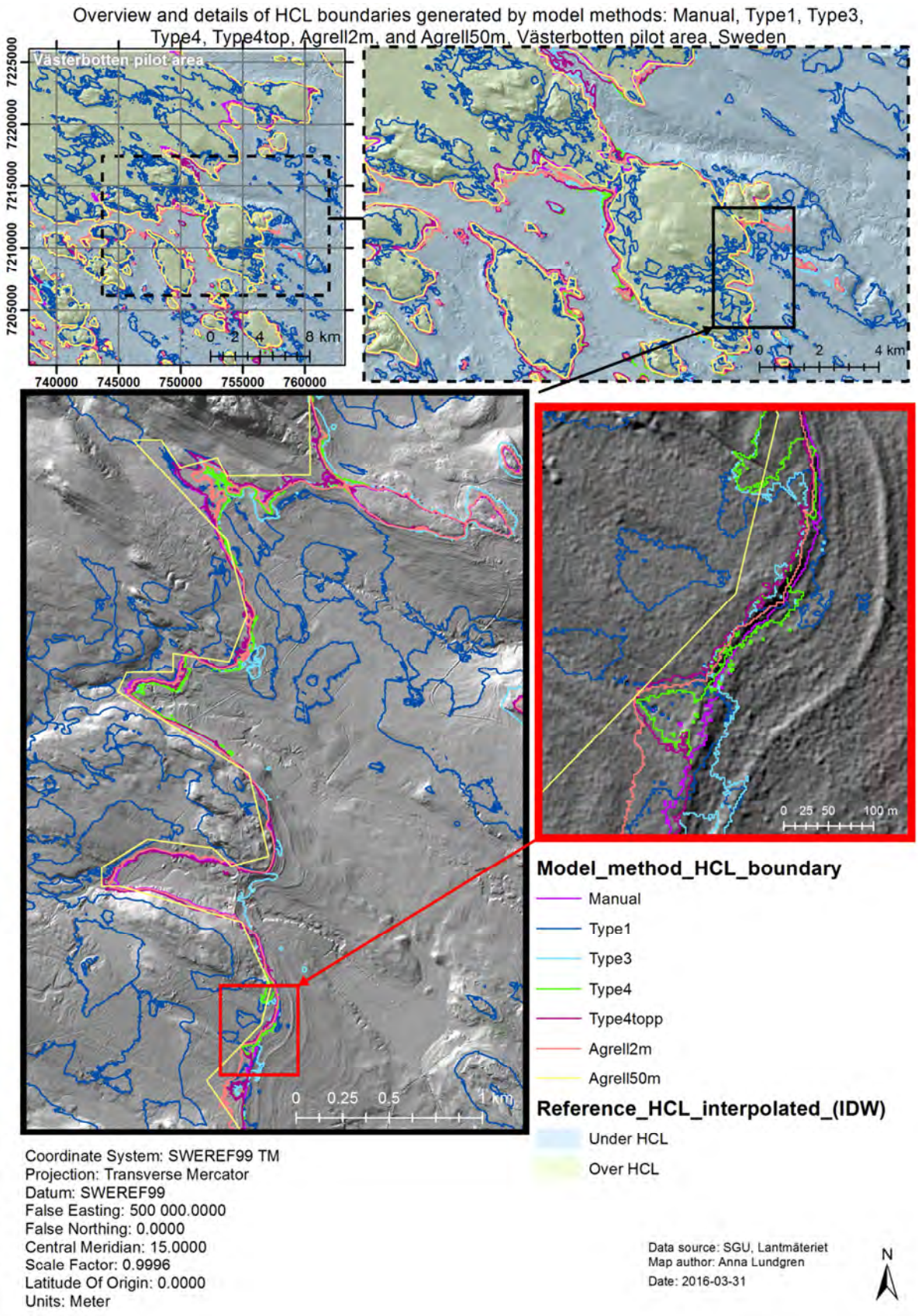

Figure 30 Overview and detail of the HCL boundaries resulting from the Type1, Type3, Type4, Type4top, Manual, Agrell50m, and Agrell2m model methods.

4.5 Map evaluation results – accuracy estimations

In this section, accuracy measures for the model methods performance in the Västerbotten pilot area estimated by the error matrix, "buffer method", and elevation error approaches are presented. Maps over the reference data used for the evaluation of the model methods in the Västerbotten pilot area can be found in Appendix E Figures E1-E2.

4.5.1 Error matrix result for interpolated HCL-surface

The overall Kappa, individual Kappa, and areal difference measures computed from the error matrices are presented in this section and can be used as estimates of the classification accuracy of land area below (class 1) and above (class 2) the HCL generated by the model methods. Different sized evaluation areas around the reference data estimates the accuracy at different scales (see Figure 6 in section 3.3.1). For further discussion of the results see section 5.1.

4.5.1.1 Overall Kappa estimation

The overall Kappa estimation for each model method and evaluation area for the classification of land area over and under the HCL is presented in Figures 31 and 34 and in Table F1 in Appendix F.

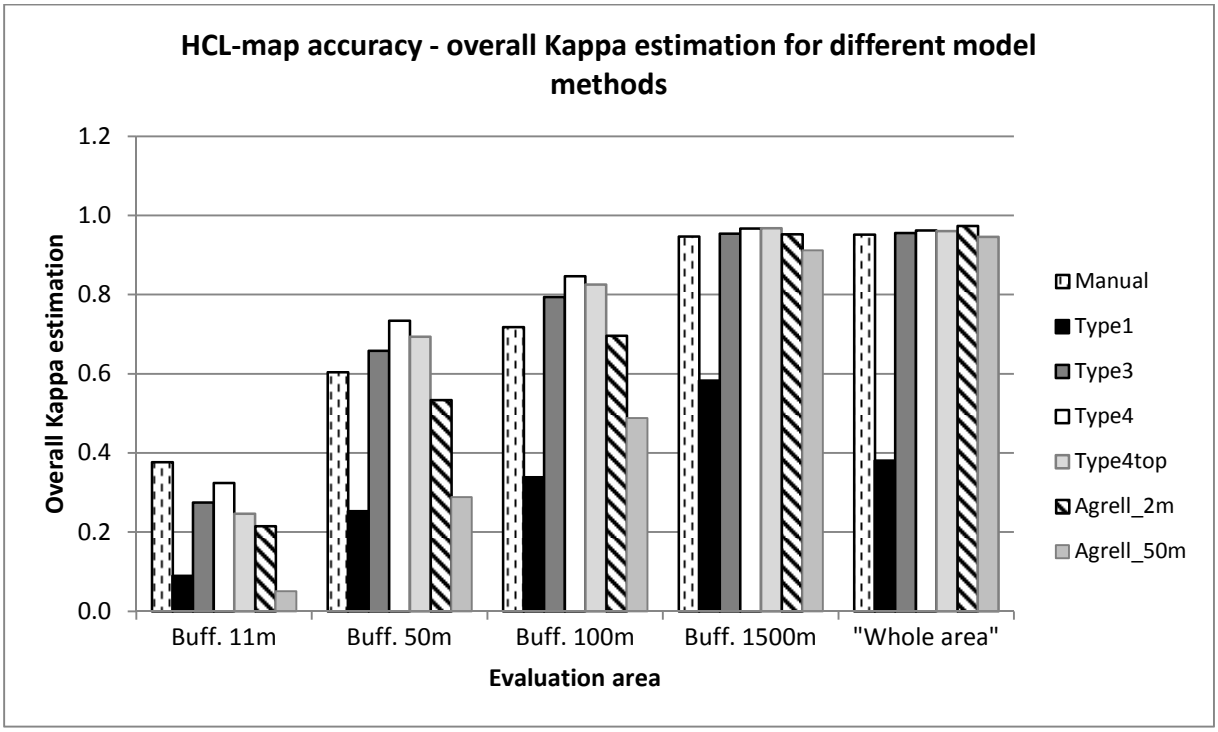

Figure 31 The overall Kappa estimation generated by the model methods within each evaluation area; buff 11m, 50m, 100m, 1500m, and 'whole area' (Figure 6).

The overall Kappa estimation increases with increased area of evaluation i.e. increased buffer size around the manual digitized reference data. The Type4 model method generates the highest overall Kappa estimation value (0.73-0.97) in 3/5 of the evaluated areas (buff. 50m, 100m, and 1500m) and second highest overall Kappa estimation value (0.32 and 0.96) in 2/5 of the evaluated areas (buff. 11m and the 'whole area') compared to the other model methods. Of all investigated model methods the Type1 model method generates the lowest overall Kappa estimation values (0.25-0.58) throughout all evaluated area sizes except for the 11 m buffer were the Agrell50m model method generates a slightly lower overall Kappa estimation value (0.05).

4.5.1.2 Kappa estimation for individual classes

The individual Kappa estimation for class 1 (land area under the HCL) and class 2 (land area over the HCL) are presented in Figures 32, 33, and 34 and in Table F2 in Appendix F.

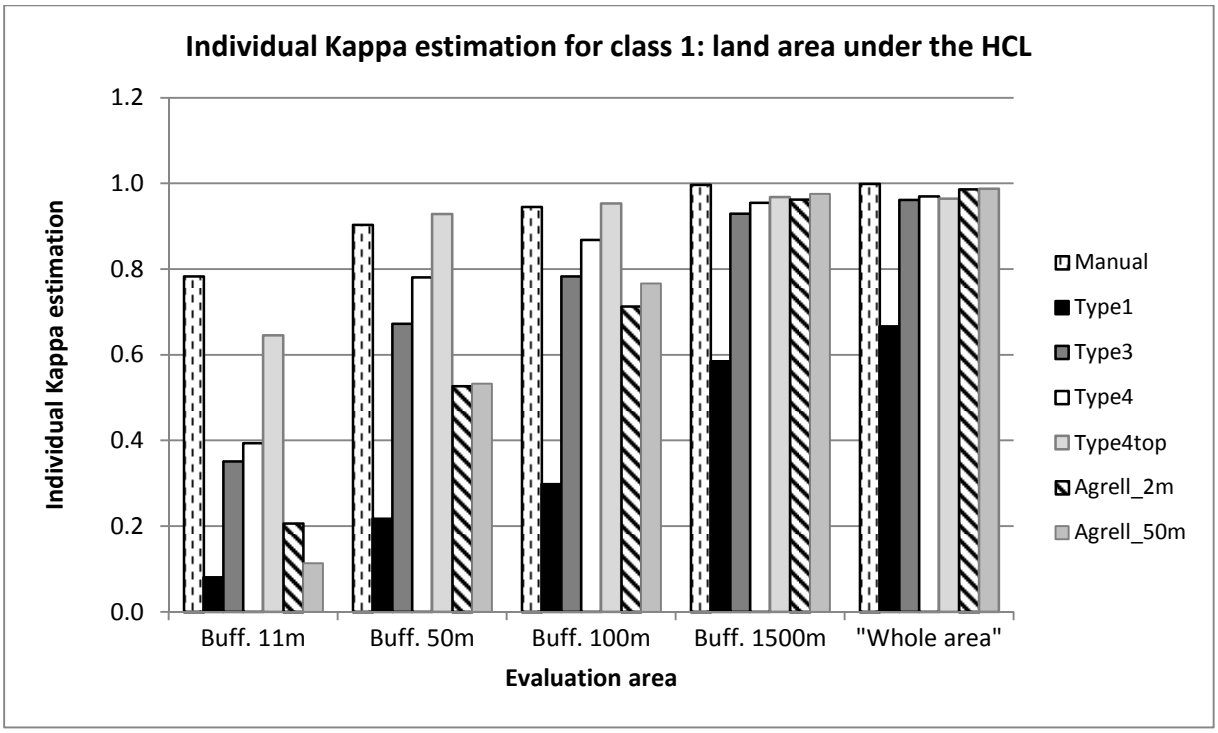

Figure 32 Individual Kappa estimation for class 1 generated by the model methods within each evaluation area; buff 11m, 50m, 100m, 1500m, and 'whole area' (Figure 6).

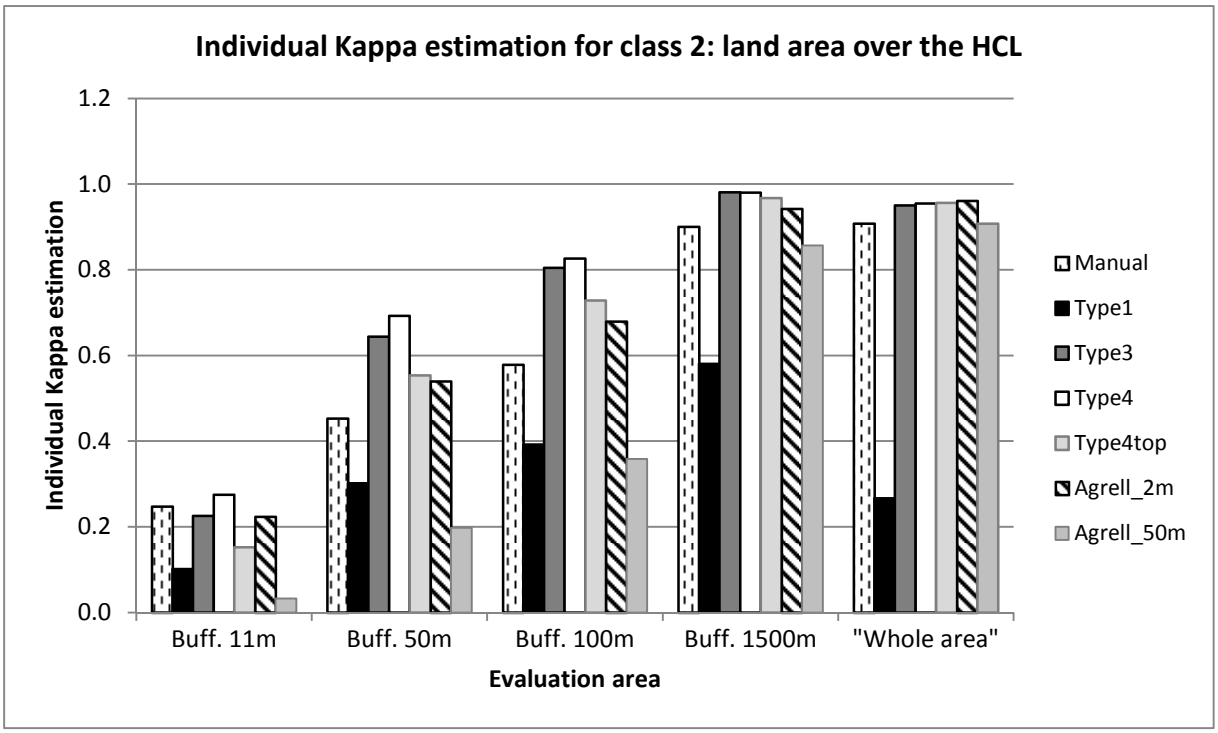

Figure 33 Individual Kappa estimation for class 2 generated by the model methods within each evaluation area; buff 11m, 50m, 100m, 1500m, and 'whole area' (Figure 6).

The estimated individual Kappa values increase with increased evaluation area (buffer size). In general the individual Kappa estimation values are greater for class 1 than for class 2.

Class 1 – land area under the HCL

The Manual model method and the Type4top model method generate the greatest individual Kappa estimation values (0.65-0.95) for class 1 within the evaluation areas: buff. 11m, buff. 50m, and buff 100m. The class 1 individual Kappa estimation values for the two largest evaluation areas (buff. 1500m and 'whole area') are above 0.95 for all model methods except the Type1 model method which generates the lowest individual Kappa values within all evaluation areas (Figures 32 and 34 and Table F2 in Appendix F).

Class 2 – land area over the HCL

The Type4 model method generates the greatest individual Kappa estimation values (0.27-0.83) for class 2 within the evaluation areas: buff. 11m, buff. 50m, and buff. 100m. The Agrell50m model method generates the lowest individual Kappa estimation values (0.03-0.36) for class 2 within the evaluation areas: buff. 11m, buff. 50m, and buff. 100m. The individual Kappa estimation values are greater than 0.85 within the two largest evaluation areas (buff. 1500m and 'whole area') for all model methods except the Type1 model method (Figures 33 and 34 and Table F2 in Appendix F).

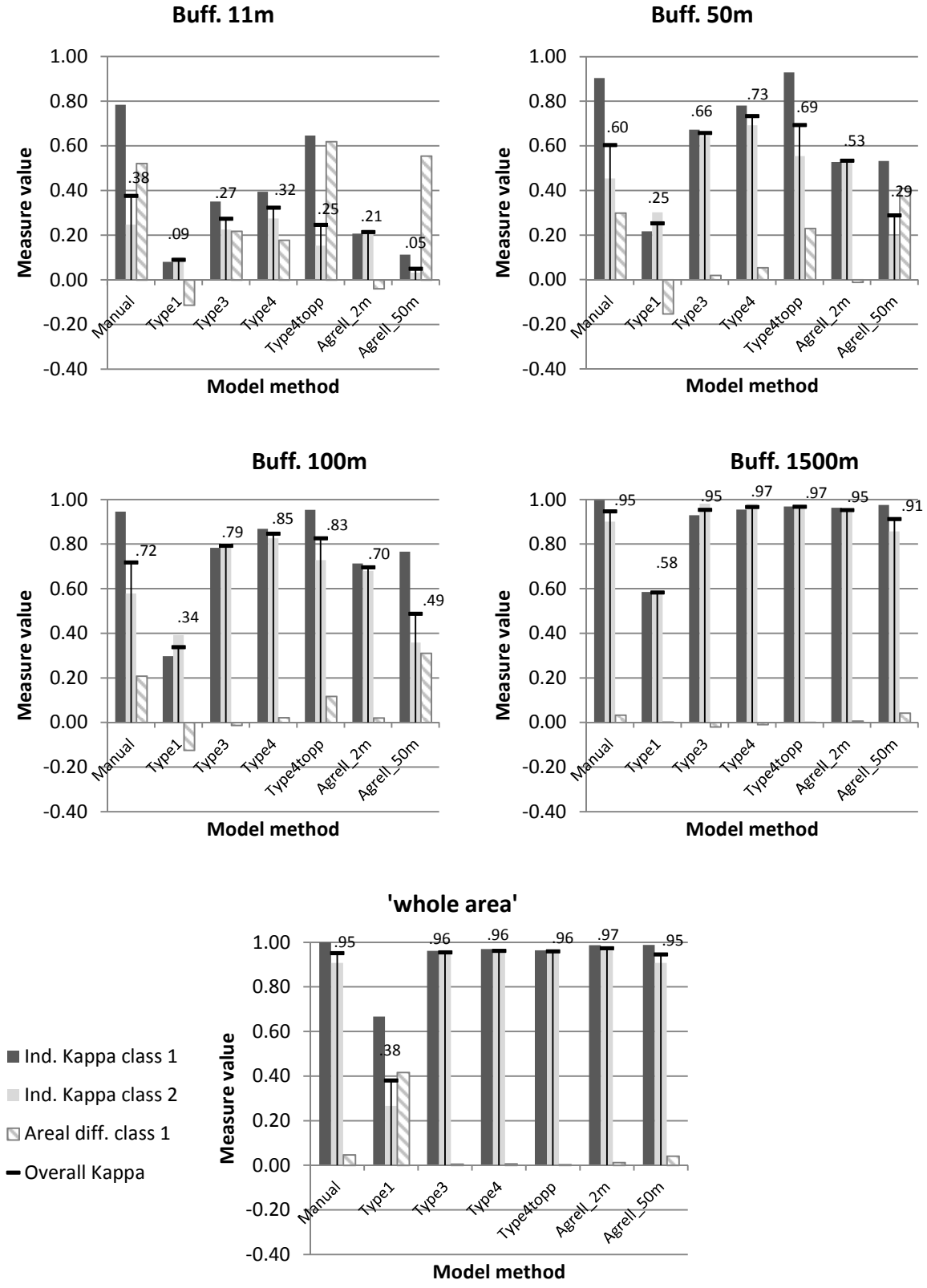

Figure 34 Comparison of overall Kappa and individual Kappa estimations for the model methods within the different sized evaluation areas; buff 11m, 50m, 100m, 1500m, and 'whole area' (Figure 6). The areal difference for class 1 is included to illustrate its linkage to the Kappa values. A greater areal difference value generates increased difference between the individual Kappa values for class 1 and class 2. Numbers for the estimated overall Kappa values for each model method are inserted in the figure.

4.5.1.3 Areal difference

The areal difference of class 1 (land area under the HCL) and class 2 (land area over the HCL) for the model methods compared to the interpolated reference data within evaluation areas: buff. 11m, buff. 50m, buff. 100m, buff. 1500m, and 'whole area' are presented in Figures 35 and 36 and in Table F3 in Appendix F.

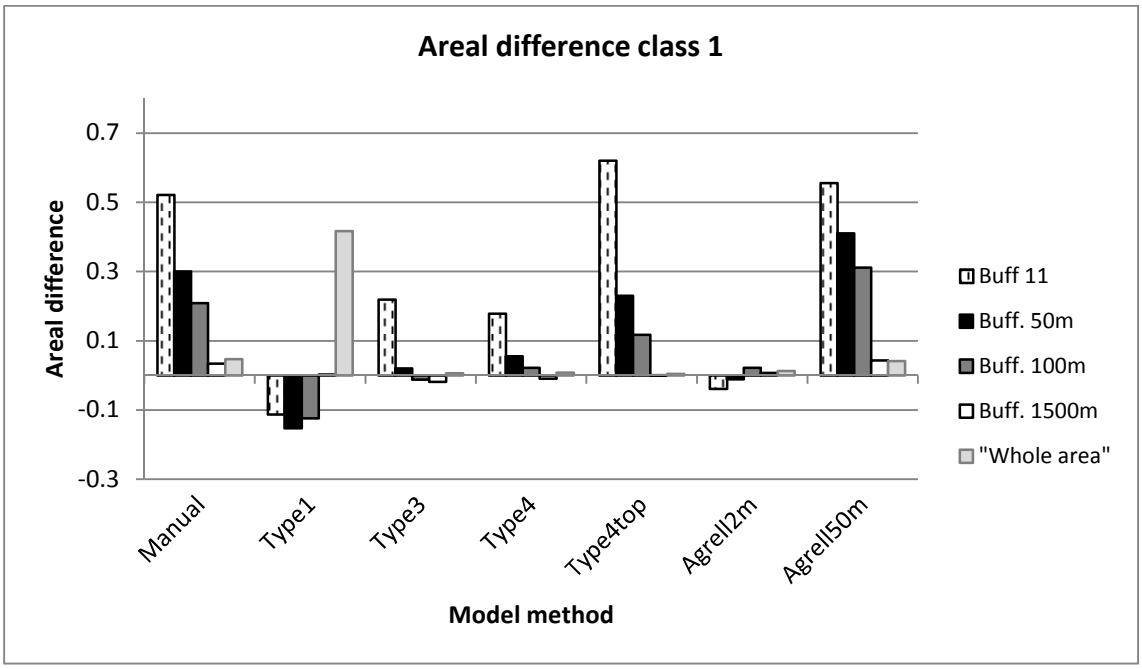

Figure 35 Class 1 areal difference values for model methods: Manual, Type1, Type3, Type4, Type4top, Agrell2m, and Agrell 50m within the evaluation areas: buff. 11m, buff. 50m, buff. 100m, buff. 1500m, and 'whole area'.

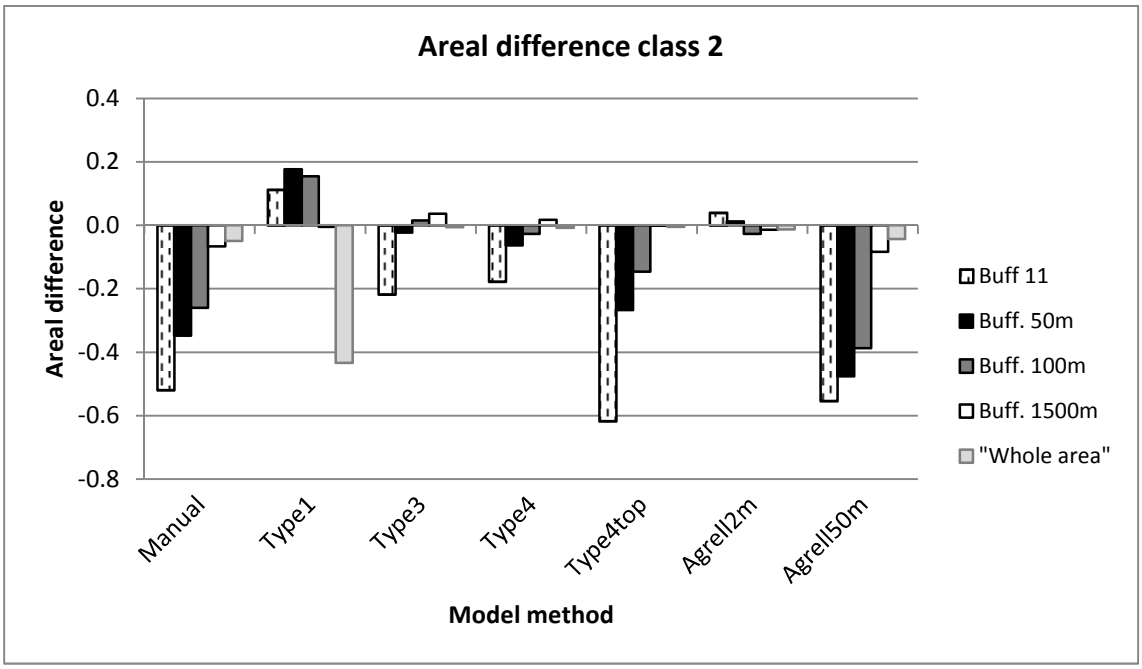

Figure 36 Class 2 areal difference values for model methods: Manual, Type1, Type3, Type4, Type4top, Agrell2m, and Agrell 50m within the evaluation areas: buff. 11m, buff. 50m, buff. 100m, buff. 1500m, and 'whole area'.

The areal differences decreases with increased evaluation area size for all model methods except for the Agrell2m model method which withholds more constant areal difference (below ±0.04) throughout the evaluation areas. The Type1 model method differs from this trend in the largest evaluation area (‘whole area’) generating its maximum areal difference value of around ±0.4. The significant areal difference values are in general positive for class 1 and negative for class 2 for all model methods except for Type1 model method. The areal difference values are greatest for model methods: Manual (from ±0.03 up to ±0.52), Type4top (from ±0.0004 up to ±0.62), and Agrell50m (±0.04 up to ±0.56). The areal difference values are intermediate for model methods: Type3 (±0.006 up to ±0.21) and Type4 (±0.0004 up to ±0.18). The Type1 model method areal difference varies from ±0.002 to ±0.18 excluding the largest evaluation (‘whole area’, explained above).

The number of cells included in the computations of the Kappa and areal difference estimations for each evaluation area in the Västerbotten pilot area is presented in Table 6.

Table 6 Number of cells included in the computations of the Kappa and areal difference estimations for each evaluation area within the Västerbotten pilot area.

Evaluation area	No. of cells
11m buffer	120159
50m buffer	593372
100m buffer	1277537
1500m buffer	28569234
'whole area'	160199649

4.5.2 HCL boundary classification accuracy – “buffer method”

In this section, the resulting completeness, correctness, quality, and redundancy measures for the model methods computed using the “buffer method” are presented. The completeness, correctness, quality, and redundancy are used to measure the classification accuracy of the HCL boundary lines generated by the model methods in relation to a HCL boundary line interpolated from the reference data. For further discussion of the results see section 5.1.

4.5.2.1 Completeness

The percentage of the HCL boundary interpolated from the reference data for the whole of the Västerbotten pilot area which is explained by the modeled HCL boundaries is according to the completeness measure 30.2%, 9%, 16.7%, 26.3%, 23.7%, 26.0%, and 7.7% for the model methods Manual, Type1, Type3, Type4, Type4top, Agrell2m, and Agrell50m respectively (Figure 37 and Table F4 in Appendix F).

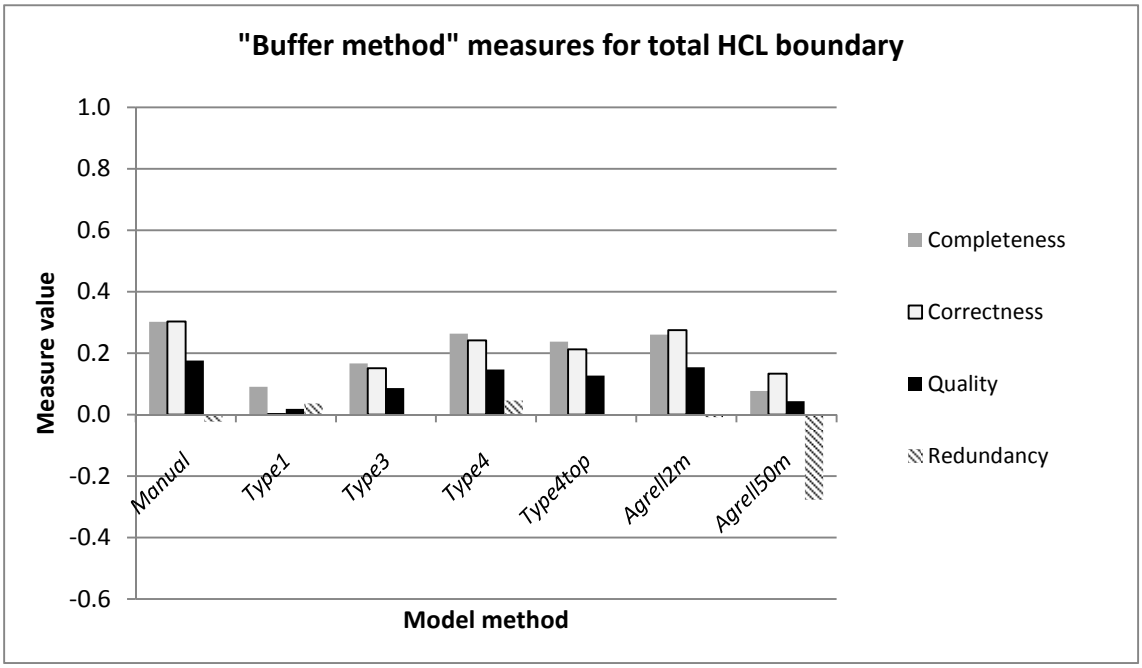

Figure 37 Completeness, correctness, quality and redundancy measures for the evaluation of the classification accuracy of the total HCL boundary within the Västerbotten pilot area. Percentage numbers for the quality measures are inserted in the figure.

The percentage of the HCL boundary interpolated from the reference data for the area within the 200 m flat buffer which is explained by the modeled HCL boundaries is according to the completeness measure is 41.9%, 15.6%, 43.5%, 66.0%, 42.9%, 21.2%, and 6.3% for the model methods Manual, Type1, Type3, Type4, Type4top, Agrell2m, and Agrell50m respectively (Figure 38 and Table F4 in Appendix F).

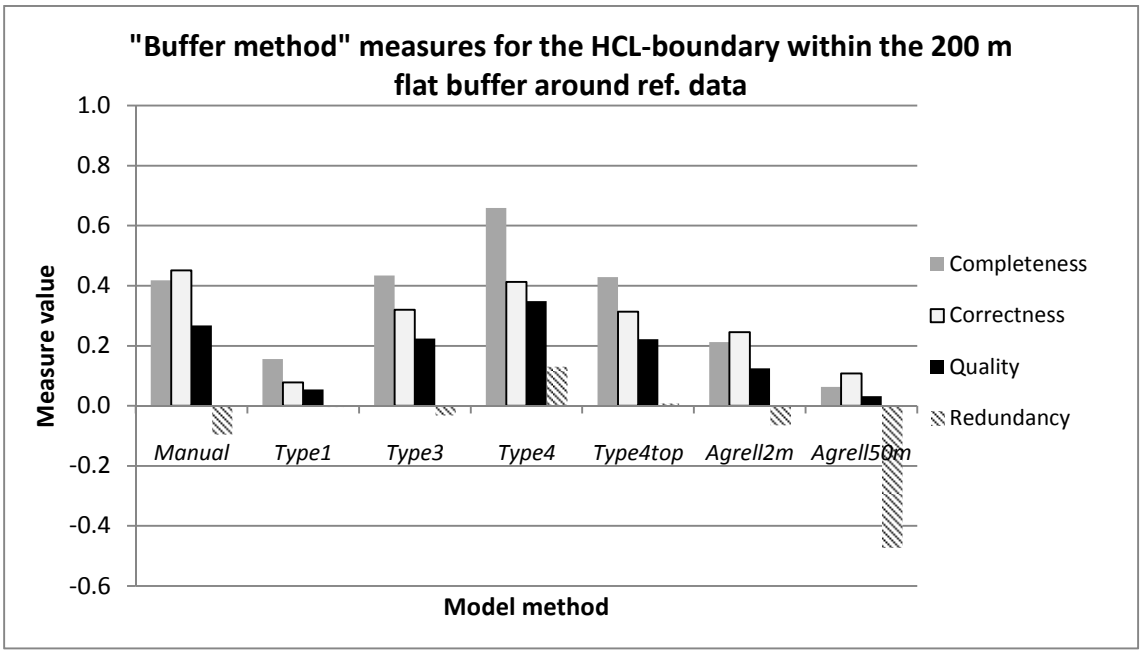

Figure 38 Completeness, correctness, quality and redundancy measures for the evaluation of the classification accuracy of the HCL boundary within the 200 m flat buffer around the reference data for the Västerbotten pilot area. Percentage numbers for the quality measures are inserted in the figure.

The lowest completeness measure values are generated by the Type1 model method (9%) and the Agrell50m model method (7.7%) and the highest completeness measure values are generated by the Manual model method (30.2%), the Type4 model method (26.3%), and the Agrell2m Model method (26.0%) if total HCL boundaries within the Västerbotten pilot area are included in the computations. If only HCL boundaries adjacent (within the 200 m flat buffer) to the reference data (digitized using hillshade relief maps) are included the lowest completeness measure values are generated by the Agrell50m model method (6.3%) and the Type1 model method (15.6%) and the highest completeness measure values are generated by the Type4 model method (66%), the Type3 model method (43.5%), and the Type4top model method (42.9%).

4.5.2.2 Correctness

The percentage of correctly modeled HCL boundary i.e. the percentage of modeled HCL boundary which lie within the 6.25 m buffer around the reference data for the whole of the Västerbotten pilot area is 30.2%, 0.1%, 15.1%, 24.1%, 21.3%, 27.5%, and 13.3% for the model methods Manual, Type1, Type3, Type4, Type4top, Agrell2m, and Agrell50m respectively (Figure 37 and Table F4 in Appendix F). The percentage of correctly modeled HCL for the area within the 200 m flat buffer is 45.1%, 7.8%, 32.0%, 41.3%, 31.4%, 24.5%, and 3.2% for the model methods Manual, Type1, Type3, Type4, Type4top, Agrell2m, and Agrell50m respectively (Figure 38 and Table F4 in Appendix F).

4.5.2.3 Quality

The quality measure values i.e. the percentage of matched modeled HCL boundary (TP) to the sum of the length TP, FP, and FN for the whole of the Västerbotten pilot area is 17.6%, 1.8%, 14.7%, 12.6%, 15.4%, and 4.4% for the model methods Manual, Type1, Type3, Type4, Type4top, Agrell2m, and Agrell50m respectively (Figure 37 and Table F4 in Appendix F). The quality measure values for the area within the 200 m flat buffer around the reference data is 26.7%, 5.5%, 22.4%, 34.8%, 22.2%, 12.5%, and 3.2% for the model methods Manual, Type1, Type3, Type4, Type4top, Agrell2m, and Agrell50m respectively (Figure 38 and Table F4 in Appendix F).

4.5.2.4 Redundancy

The percentage to which the matched modeled HCL boundary lengths (TP) are redundant i.e. overlaps itself compared to the matched reference data ("TP") for the whole of the Västerbotten pilot area is with -2.2%, 3.8%, -0.3%, 4.6%, 0.3%, -0.7%, and – 27.6% for the model methods Manual, Type1, Type3, Type4, Type4top, Agrell2m, and Agrell50m respectively (Figure 37 and Table F4 in Appendix F). The percentage to which the matched modeled HCL boundary lengths (TP) are redundant for the area within the 200 m flat buffer is -9.6%, -0.4%, -3.2%, 13.0%, 0.7%, -6.4%, and -47.3 % for the model methods Manual, Type1, Type3, Type4, Type4top, Agrell2m, and Agrell50m respectively (Figure 38 and Table F4 in Appendix F).

4.5.3 Elevation error for model methods

The elevation errors for the model methods based on the 100 random sample points (section 3.3.3) are presented in this section. For further discussion of the results, see section 5.1.6. Normal Quantile plots of the signed elevation error for the 100 random samples indicate non-normal error distributions for all model methods (see Figures C1-C7 in Appendix C).

The elevation error for the model methods measured at the 100 random samples are described by the median (for both signed and absolute elevation errors), the normalized median absolute deviation (NMAD), the 68.3% quantile (for absolute elevation errors), and the 95% quantile (for absolute elevation errors) values in Table 7 and Figure 39. The standard deviation (Std.) values for the model

methods signed elevation errors are included for comparison with the NMAD values (Hasan et al. 2012, Höhle and Höhle 2009).

Table 7 The median, NMAD, 68.3% quantile, and 95% quantile of the elevation error for the different model methods. The largest error values are highlighted in red, the second largest error values are highlighted in orange, the second smallest error values are highlighted in yellow, and the smallest error values are highlighted in green.

Measure (input data = |Δh| or Δh)	**Elevation error measures (m) for the model methods**						
	Manual	*Type 1*	*Type 3*	*Type 4*	*Type 4top*	*Agrell2m*	*Agrell50m*
68.3% Q |Δh|	2.70	11.47	1.52	1.15	1.51	2.38	4.35
95% Q |Δh|	4.95	27.70	5.97	2.98	3.47	3.56	10.73
median|Δh|	1.16	6.01	0.96	0.79	1.10	1.83	2.92
median Δh	+1.16	-0.04	+0.79	+0.25	+1.01	-0.42	+2.49
NMAD Δh	1.59	8.97	1.17	0.92	0.82	2.91	3.51
Std. Δh	1.66	12.06	2.13	1.33	1.34	3.41	6.34

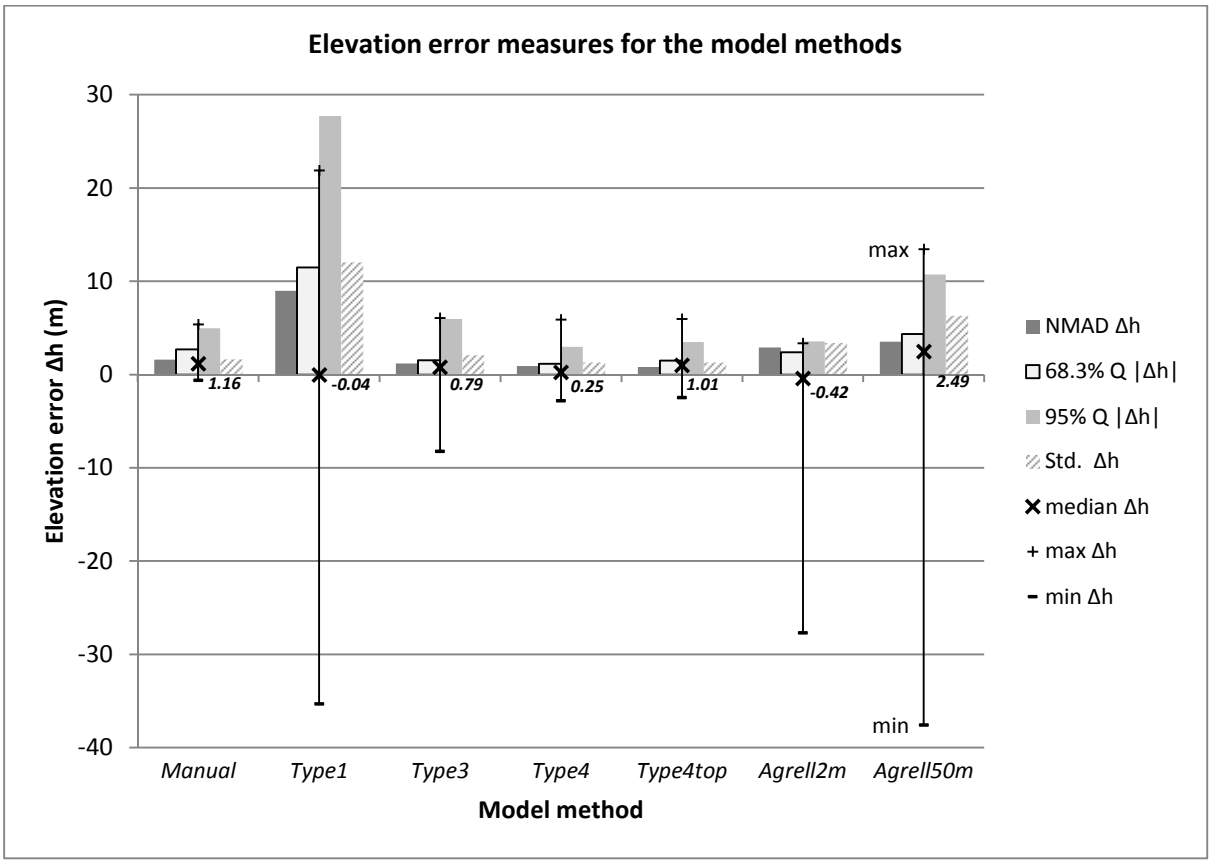

Figure 39 Maximum (max), minimum (min), median (50% quantile), Normalized Median Absolute Difference (NMAD), and standard deviation (Std.) computed using signed elevation error Δh and 68.3% quantile (68.3%Q) and 95% quantile (95%Q) computed using absolute elevation error |Δh| for the model methods Manual, Type1, Type3, Type4, Type4top, Agrell2m, and Agrell50m. Horizontal aligned numbers shown in bold are the median values. The standard deviation (Std.) values for the signed elevation errors Δh are shown for comparison with the NMAD values.

4.5.3.1 Median

The signed median (50% quantile) elevation error (median Δh) is greatest for the Agrell50m model method (+2.49 m) and the Manual model method (+1.16 m). The lowest signed median elevation error is generated by the Type1 model method (-0.04 m) and the Type4 model method (+0.25 m). The absolute median (50% quantile) elevation error (median|Δh|) is greatest for the Type1 model method (6.01 m) and the Agrell50m model method (2.92m). The lowest absolute median elevation error is generated by the Type4 model method (0.79 m) and the Type3 model method (0.96 m) (Table 7 and Figure 39).

4.5.3.2 NMAD

The NMAD measure (NMAD Δh) is greatest for the Type1 model method (8.97 m) and lowest for the Type4top and Type4 model methods (0.82 m and 0.92 m respectively, Table 7 and Figure 39).

4.5.3.3 68.3% quantile and 95% quantile

68.3% quantile:

68.3 % of the absolute elevation errors (68.3% Q |Δh|) have a magnitude within the range 0-11.47 m for the Type1 model method, 0-4.35 m for the Agrell50m model method, 0-2.70 m for the Manual model method, 0-2.38 m for the Agrell2m model method, 0-1.52m for the Type3 model method, 0-1.51 m for the Type4top model method, and 0-1.15 m for the Type4 model method (Table 7 and Figure 39).

95% quantile:

95 % of the absolute elevation errors (95% Q |Δh|) have a magnitude within the range 0-27.7 m for the Type1 model method, 0-10.37m for the Agrell50m model method, 0-5.97m for the Type3 model method, 0-4.95 m for the Manual model method, 0-3.56 m for the Agrell2m model method, 0-3.47 m for the Type4top model method, and 0-2.98 m for the Type4 model method (Table 7 and Figure 39).

The 68.3% Quantile, 95% Quantile, median, and NMAD values for the 100 random evaluation sample points indicate overall greater elevation errors for the Type1 model method and the Agrell50m model method and overall lower elevation errors for the Type4 model method.

5 Discussion

5.1 Result

The evaluation methods (error matrix, “buffer method” and elevation error assessment) applied to compare the model methods indicate that the Type4 model method generates results nearest the manually digitized reference data. In this section the results from the evaluation of the HCL data generated by the model methods within the Västerbotten pilot area are discussed.

5.1.1 Error matrix

The estimated overall Kappa and individual Kappa values computed from the error matrices increase with increased size of the evaluation area due to the HCL being a boundary line and the error matrix designed for evaluating classification of area. Thus, adding area on either side of the HCL boundary increases the ratio of successful classified cells compared to the ratio of unsuccessful classified cells as well as decreases the areal difference measure (see Figures 31 and 36 in the Results chapter). This fact makes the error matrix evaluation method (Lillesand et al. 2008, Mårtensson and Pilesjö 2004) not ideal for evaluating boundary classifications, but the result gives an indication of the general performance of the model methods. The smaller evaluation areas are applied to approach Kappa estimations for the actual HCL boundaries instead of Kappa estimations for the two HCL surface classes: land area under the HCL (class 1) and land area over the HCL (class 2). Within the Västerbotten pilot area the estimated overall Kappa values are highest for the Manual, Type3, Type4, and Type4top model methods at smaller evaluation scales (11m to 100m buffer) and similar for all model methods except the Type1 model method at larger evaluation scales (1500m buffer and ‘whole area’). The Type4 model method generates HCL maps that are 32.4%, 73.4%, and 84.6% better than a HCL-map made by chance (Mårtensson and Pilesjö 2004) for the evaluation areas buff. 11m, buff. 50m, and buff. 100m respectively (see Figure 31 and Table F1 in Appendix F). For the same evaluation areas the Agrell50m model method (the current HCL surface data available at SGU) generates HCL maps that are 5.0%, 28.9%, and 48.8% better than a HCL-map made by chance.

A greater areal difference value generates increased difference between the individual Kappa values for class 1 and class 2 (Figure 36 in the Results chapter). This illustrates that the HCL boundary generated by a model method possesses a systematic shift towards land area under the HCL or land area over the HCL. E.g. a positive areal difference for class 1 means the area under the HCL is overestimated and a negative areal difference for class 1 means the area under the HCL is underestimated. The areal difference of class 1 and class 2 is confirmed by the median values of the signed elevation error samples for the model methods (see Figure 39 in the Results chapter).

5.1.2 Completeness

Generally the lowest completeness measure values (see Figures 37-38 in the Results chapter) are found in the evaluation of the total HCL boundary for the Västerbotten pilot area and the highest completeness measure values are found in the evaluation of the HCL boundaries adjacent (within a 200 m flat buffer) to the reference data. This can be interpreted as that there is a greater difference between the modeled HCL boundaries and the interpolated reference data in areas lacking the actual manually digitized reference data (thus lacking apparent wave washed features to base the digitizing on). A conclusion drawn from this observation is that uncertainty of the completeness measure increases with distance from the actual manually digitized reference data. For both the total accuracy evaluation and the accuracy evaluation including only data adjacent to the HCL reference data (within 200 m flat buffer) the lowest completeness measure values are generated by the model methods Agrell50m (7.7% and 6.3% respectively) and the Type1 (9% and 15.6% respectively). The Type4 model method generates the highest completeness measure value for the evaluation adjacent to the

digitized HCL-boundaries with 66% i.e. Type4 explains 66% of the reference data. The Type4 model method is also among the three model methods generating the highest completeness measure values for the accuracy evaluation of the total HCL boundary (26.3%) (Figures 37 and 38).

5.1.3 Correctness

The correctness measure values (see Figures 37-38 in the Results chapter) are generally higher for the evaluation of modeled HCL boundaries adjacent (within a 200 m flat buffer) to the digitized reference data than for the evaluation of correctness for the whole Västerbotten pilot area. The highest correctness measure values are found for the model methods Manual (45.5%) and Type4 (41.3%) within the 200 m flat buffer and for the model methods Manual (30.2%) and Agrell2m (27.5%) for the evaluation of the total HCL boundaries. Lowest correctness values are generated by the Type1 (0.1% and 7.8%) model method and the Agrell50m (13.3% and 3.2%) model method for the whole area and the 200 m flat buffer area evaluations respectively. I conclude that according to the correctness measures, the Manual model method and the Type4 model method models the interpolated reference HCL boundary most accurately in areas adjacent to the actual manually digitized reference data, and the Manual model method and the Agrell2m model method models the interpolated reference HCL boundary most accurately in average for the entire area (Figures 37 and 38).

5.1.4 Quality

The quality measure takes into account both the completeness and the correctness measure values (Heipke et al. 1997). In general the quality measures (see Figures 37-38 in the Results chapter) are lowest for the accuracy evaluation of the total HCL boundaries within the Västerbotten pilot area. Quality measures range from 1.8% (Type1) to 17.6% (Manual) for the classification accuracy assessment of the total boundaries generated by the model methods for the Västerbotten pilot area. The Quality measures for HCL boundary within the 200 m flat buffer around the manually digitized reference data range from 3.2% (Agrell50m) to 34.8% (Type4). The highest quality measure values are generated by the Type4 (34.8%) model method and the Manual (26.7%) model method for the accuracy evaluation of HCL boundaries adjacent to the manually digitized reference data (within the 200 m flat buffer). The lowest quality measure values are generated by the Type1 model method and the Agrell50m model method confirming the visual inspection of the resulting HCL maps (see Figures 29-30 in the Results chapter). A quality value of 1 represents a 100% match between a modeled HCL boundary and the reference HCL boundary data meaning that the length of modeled HCL boundary falling within the 6.25 m buffer around the reference HCL boundary (TP) is the same as the summed length of extracted data (TP+FP) and unmatched reference data (FN) i.e. FP and FN are 0 (see Eq. 7 in the Methods chapter). The resulting quality measures support the conclusion that the Type4 model method is in summary the model method that produces a HCL boundary with closest match to the reference HCL data (Figures 37 and 38). The classification accuracy results are generated using a 6.25 m buffer radius corresponding to approximately half the width of the extracted feature i.e. wave washed ridges within the Västerbotten pilot area (Heipke et al. 1997). The HCL boundary line is assumed to be modeled correctly if it falls within the width of the crest or trough of an average sized wave washed ridge within the Västerbotten pilot area. Choosing a too large radius risks the inclusion of HCL sections belonging to other parts resulting in an overestimation of the classification accuracy (Rutzinger et. Al 2012). Choosing a buffer smaller than the internal accuracy of the extracted feature i.e. a wave washed ridge would risk underestimating the classification accuracy (Heipke et al. 1997).

5.1.5 Redundancy

The redundancy for the model methods are in general low and even negative (from -27.6% to 4.6% for the total HCL and from -47.3% to 13.0% for the HCL within the 200m buffer, see Figures 37-38 in the Results chapter) indicating that the interpolated reference HCL boundary falling within the 6.25

buffers around the modeled HCL boundaries has a greater length than the modeled HCL boundary. A negative redundancy can be interpreted as that the interpolated reference data is more complex than the modeled HCL data (thus has a greater length) or that the percentage of the reference data that is explained by the model method ("TP") is greater than the percentage of extracted data that lies within the 6.25 m reference buffer (TP) (see Eq. 8 in the Methods chapter).

5.1.6 Elevation error

The average vertical elevation error for the input datasets used in the model methods is 0.5 m for the high resolution DEM (Lantmäteriet 2015) and 2 m for the HCL data based on the old 50 m resolution DEM (SGU 2015d) (Table 1). The accuracy of the manually digitized HCL boundary reference data based on the high resolution DEM can be expected to be around 0.5m, ignoring errors introduced by the digitizing process and by interpreter bias. According to Smith et al. (2006) geomorphological features manually digitized from LiDAR generated high resolution DEM are near ground truth accuracy. The accuracy of the model methods based on the old HCL data i.e. the Agrell50m and the Agrell2m model methods, depends on the accuracies of the original methods used to determine the HCL locations which are varying for this dataset (compiled by Agrell 2001 from different HCL studies), the digitizing process of the compiled HCL location data and the accuracy of elevation data extracted to the HCL locations (determined by the original leveling method or extracted from DEMs). According to the metadata linked to the old HCL data provided by SGU (SGU 2015d) the average elevation error is about 2m.

The absolute elevation error measures (median, NMAD, 68.3 % quantile, and 95 % quantile) are used to determine the magnitude of the elevation error produced by the model methods in relation to the reference data (see Figure 39 in the Results chapter). NMAD can be used as an estimate of the standard deviation of error datasets not normally distributed and is not sensitive to outliers (Höhle and Höhle 2009). NMAD approaches the standard deviation for normally distributed datasets if the sample size is sufficient (Höhle and Höhle 2009). Sample quantiles of the absolute elevation error distribution can be used to illustrate the magnitude of the errors for non-parametric distributions. 68.3 % of the absolute elevation errors ($|\Delta h|$) have a magnitude within the range 0 – 68.3% quantile, and 95% of the absolute elevation errors ($|\Delta h|$) have a magnitude within the range 0 – 95% quantile (Figure 39).

The model methods with smallest elevation error according to the elevation error evaluation of the 100 random samples are Type4, Type4top, and Agrell2m with 95 % of the absolute elevation error having magnitudes within the ranges 0-2.98 m, 0-3.47 m, and 0-3.56 m respectively. 68.3% of the elevation errors for model methods Type4, Type4top, and Agrell2m have a magnitude of 0-1.15 m, 0-1.51 m, and 0-2.38 m respectively. Note the high elevation error of the minimum value for the Agrell2m model method (about -27 m) which most likely represents an outlier. Also 68.3% of the elevation errors for Type3 model method (0-1.52 m) have a magnitude lower than for the Agrell2m model method although 95% of the Type3 model methods elevation errors have a magnitude range (0-5.97 m) greater than the Agrell2m model method. The Type1 model method and the Agrell50m model method have the greatest elevation errors with 95% of the errors having magnitudes within the ranges 0-27.70 m and 0-10.73 m respectively and 68.3% of the errors having magnitudes within 0-11.47 m and 0-4.35 m respectively (Figure 39 in the Results chapter).

The signed median (50 % quantile) for the elevation error data sets can be used to determine around what value the errors are distributed. The signed median can thus be used as an indicator of if the HCL boundary line generated by the model method possesses a positive or negative systematic elevation error distribution or random elevation error distribution (Figure 39 in the Results chapter). The estimated areal differences measures resulting from the error matrix for the 11 m buffer evaluation

area (Figure 34 in the Results chapter) are confirmed by the median values of the signed elevation errors. Notable is that the median of the signed elevation errors for the model methods Manual, Type4, and Type4top are between +0.25-1.16 m and the maximum elevation error values (about 5-6 m) are slightly larger than the minimum elevation errors (about 0.65-3 m), thus by shifting the median towards 0 m by adjusting the model methods would produce overall lower absolute values of the elevation error.

5.2 Method

In this section different aspects of the methods involved in the development of the model methods are discussed.

5.2.1 Method choice

A method based on only the high resolution DEM data was chosen over a multivariate method using different data sources available to this study e.g. quaternary data supplied by SGU (SGU 2015e-g) mainly due to the difference in spatial resolution between these datasets (Table 1). One aim of this project is to develop an automated method which can be used to update the HCL database to fit the resolution of the national high resolution DEM, which cannot be achieved by introducing data with lower spatial resolution. Quaternary information is, however, advantageously used for manually digitizing the HCL using hillshade maps generated from the high resolution DEM. A multivariate cell-classification approach utilizing other datasets and/or LSP rasters generated from the DEM data could be used to automate the identification of areas of interest with HCL characteristics. This is not necessary for areas were the HCL location is well documented, but can be useful for areas were the elevation of the HCL is unknown. A method that enhances the specific patterns of landforms used for identifying the HCL in high resolution hillshade maps at wave wash dominated areas was of interest. Both wave washed features and glacial flow lineation features often appear in parallel ridges why the choice (supported by a literature study) fell on linear extraction methods. Breakline extraction methods are aimed for mapping boundaries more so than classification on cell level.

5.2.2 Choice of LSP for HCL landform extraction

The choice of using curvature LSP to extract linear features related to wave washed features and glacial flow lineation was based on literature study and visual evaluation. An alternative can be to use roughness index LSP at certain scale dimension(s) to distinguish wave washed land areas consisting of several parallel ridges from other land area similar to the methods used by McKean and Roering (2004) and Berti et al. (2013) to map units within landslides. Roughness index LSP was however used for the breakline classification step in the Test run 1 area within the Gästrikland pilot area with limited success (see Figure 12 in the Results chapter). The visual evaluation of the LSP rasters showed that the residual DEM LSP enhances local linear features related to wave washing and glacial flow as well and may thus be an alternative to using curvature LSP for the extraction of breaklines. However the literature study conducted for this project more frequently suggest curvature LSP than residual DEM LSP to be used for extraction of breaklines.

5.2.3 Scale dimension

By applying a similar method as Rutzinger et al. (2012) the visual scale dimension evaluation step can be made more automatic and thus more objective. Rutzinger et al. (2012) process several LSP rasters with a range of scale dimensions and compare the resulting completeness, correctness, and quality measures to select the optimal moving window size for the application. By applying the model methods on all the suggested LSP rasters (residual DEM, roughness index, “normal/mean” curvature, profile curvature, and plan curvature) for every scale dimension investigated in this project (around 20) would make the model methods more objective but also more time demanding.

5.2.4 Breakline classification using coarse scale LSP and object attributes

Of the investigated LSPs (residual DEM, roughness index, curvature, and relative topographic position) no ideal LSP is found to separate land area with wave washed features from land area with glacial flow lineation features satisfactory. Coarse scale dimensioned (99x99 cells) roughness index LSP works to some degree in the Test run 1 area within the Gästrikland pilot area (see Figure 12 in the Results chapter) but not in the Västerbotten pilot area. The reasoning behind using de-trended LSP rasters (Lillesand et al. 2008) is that it will result in an acceptable separation of wave washed features and glacial flow lineation features for larger study areas since the elevation trend is removed. Even though a change of roughness often is present close to the HCL boundary, a simple de-trended roughness index LSP is not enough to distinguish the characteristics of areas with wave washed ridges from other areas with similar roughness index. Also, the roughness index for areas with wave washed features can differ between regions depending on e.g. the type and amount of sediment present at the location. Coarse scale dimensioned (2999x2999 cells) residual DEM (high-pass filter image) looks promising when visually evaluated within the Västerbotten pilot area (see Figure 13 in the Results chapter) and was used in the Type1 model method. However the resulting HCL boundary generated by the Type1 model method (see Figure 18 in the Results chapter) appears to depict the LSP raster used for the separation of wave washed features and glacial lineation features to a greater extent than the actual HCL alone (Figure 40).

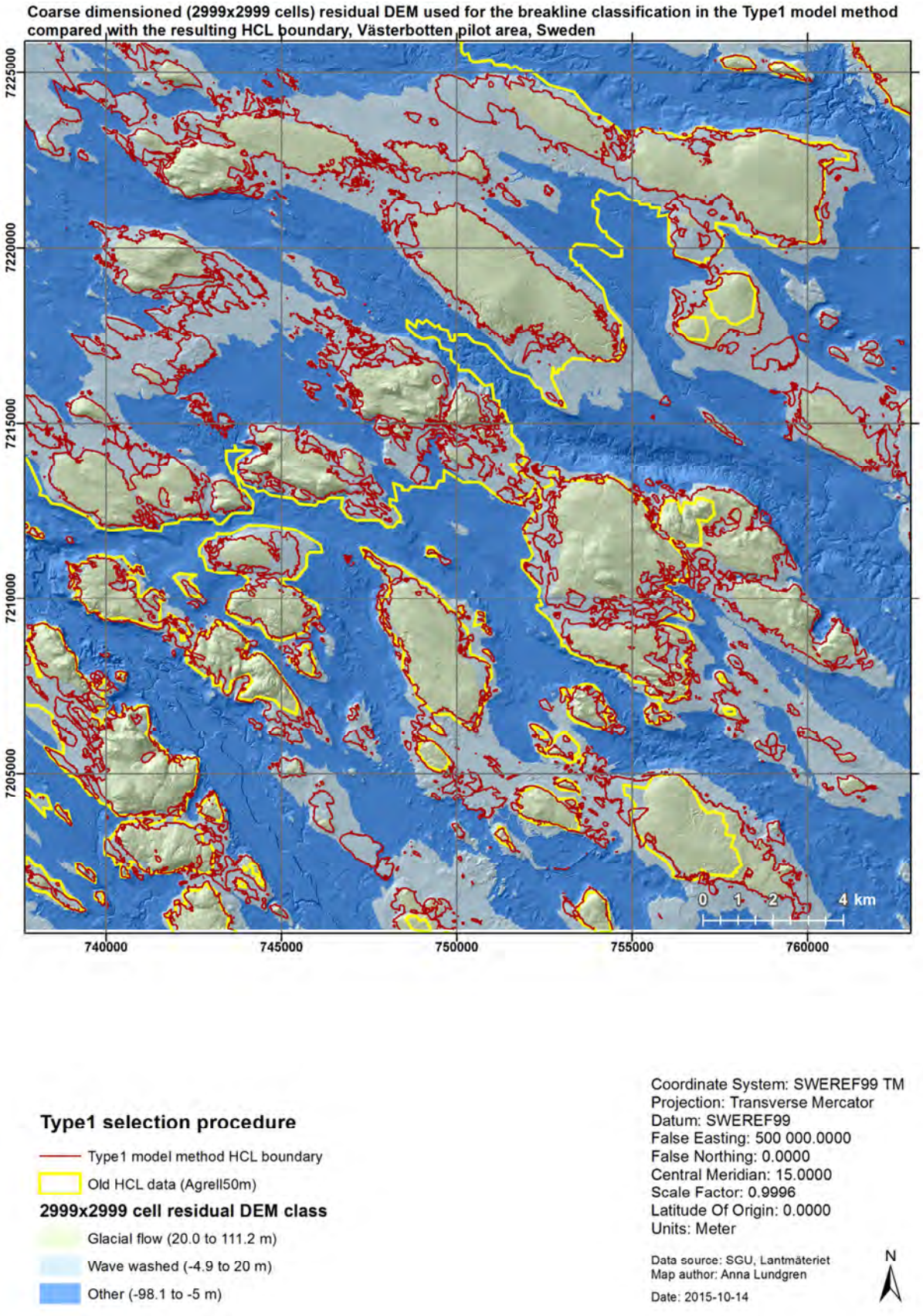

Figure 40 Coarse scale dimensioned (2999x2999 cells) residual DEM used for the classification of land area with wave washed features and land area with glacial flow lineation features within the Västerbotten pilot area compared with the resulting HCL boundary generated by the Type1 model method.

A method to separate extracted wave washed breaklines from glacial flow lineation breaklines is an essential classification step in the Type1 model method to succeed with the intersection procedure that generates the final potential HCL points. However the spatial classification step seems to require a result near a model of the HCL to succeed with a separation of the breaklines which may be hard to achieve using only one LSP or even a combination of LSPs at certain scale dimension. The question one may ask is what the breaklines would add to a model already describing the HCL at a level able to separate land area with wave washed features from landarea with glacial flow lineation features? The answer must be that the resulting intersection between glacial flow lineation vectors and breaklines related to wave washed features adds precision and thus increases the models resolution to fit information present in the high resolution DEM. To keep the spatial classification step objective consideration of what data to use (old HCL data, elevation ranges customized to local HCL mean, coarse scale roughness index data (used in test run 1), coarse scale curvature data, coarse scale slope or aspect data, etc.) and how the choice will affect the result must be taken. Using, for instance, the old HCL data to classify land area with wave washed features and land area with glacial flow lineation features may limit new findings of the HCL. The attribute classification step used in theType1 model method is in its current version too coarse e.g. breaklines with mean orientation, sinuosity, and length attributes corresponding to the criteria set for glacial flow lineation breakline attributes are misclassified as glacial flow lineation breaklines. A successful Type1 model method could be assumed to produce accuracies near the Type3 model method which is based on the same method but uses a manual breakline classification. The Type1 model method results concludes that further work is needed to develop an automated classification method using LSP classes and breakline attributes to separate wave washed features and glacial lineation features by e.g. adding more steps to refine the separation and classification of the extracted breaklines to filter away unwanted breaklines.

5.2.5 Interpolation method

The IDW interpolation method (ESRI 2015k) was chosen for the interpolation of the HCL surfaces because it is a commonly used interpolation method, it has been used by SGU to produce the current HCL surface (SGU 2015d), and the IDW methods process time is faster than the alternative Kriging interpolation methods (ESRI 2015l) which, is an important point when working with large datasets. The elevation of the HCL can be described to change gradually from one location to the neighboring locations with a general picture of minimum elevation in the south of Sweden and maximum elevation in the northern parts of Sweden. The IDW interpolation method takes into account the distance to input values when interpolating a value which would capture the main elevation changes of the HCL well. Disadvantages mentioned for the IDW interpolation at the ArcGIS 10.2 desktop help webpage (ESRI 2015k) is its decreased performance to generate a desired surface if input data is sparse and unevenly distributed. All input data points lie along lines (the HCL boundary) and are not spread over the surface to be interpolated i.e. a model of the old sea surface at the time when it reached its maximum extent of the transgression and thus greatest sea level elevation (not synchronic for the whole of Sweden and thus not resembling a natural water surface). Although located along the HCL boundary the input data is dense for the Type1 (23827 points), Type3 (1739 points), Type4 (6680 points), and Type4top (3736 points) model methods but sparse for the Manual (18 points), Agrell2m (3 points), and Agrell50m (3 points) model methods within the Västerbotten pilot area (see Table 5 in the Results chapter). The interpolated HCL surface would obviously decrease in accuracy with distance from the HCL boundary and thus the input data however it is the accuracy of actual boundary which is of interest in this study. The total number of input data points varies with model method and generally an increased number of input data points results in an interpolation surface with higher accuracy nevertheless dependent on the accuracy of the input data.

A variable search radius was used for the IDW interpolation of the HCL surfaces instead of a fixed search radius to base each interpolated point on equal number of points (here 12) and to produce a complete surface without holes/gaps. This parameter setting was used due to varying density of input HCL data points generated by the model methods. This is a larger source of error for the model methods having very few HCL points within the pilot area i.e. the Manual model method, the Agrell2m model method, and the Agrell50m model method. The other model methods generate denser HCL points and thus will use a similar search radius. The HCL surface used as reference interpolated from points along the manually digitized HCL boundary (reference data for the pilot area) have densely spaced HCL-points corresponding to the resolution of the high resolution DEM to minimize error (see section 3.2.11).

5.2.6 Processing time

The automated elongation step of glacial flow lineation vectors used in the Type1 model method had the longest processing time of all process steps used in the model methods mainly explained by lacking functionality of the ArcGIS 10.2 tools available (see Appendix A). This problem can presumably be solved by designing a more suitable tool for the elongation step using e.g. Python.

Processing time for the Type4 and Type4top model methods is estimated to be lower than for manually digitizing using the argument that the operator does not need to digitize objects manually only classify breaklines which have been automatically digitized using the curvature breakline extraction method. The Type4 and Type4top model methods do not include the elongation and intersection method (included in the Type1 and the Type3 model methods) which eliminates classification of breaklines related to glacial flow lineation and the time demanding elongation step.

Estimated length of HCL sections with delta dominating (10753 km) and wave washed dominated (6719 km) landform types of the HCL areas mapped during the pre-study is approximately 17472 km (Figure 41). Approximately 236 km of the wave washed dominated HCL boundary line lies within the Västerbotten pilot area which corresponds to about 3.5% of the total wave washed dominated HCL boundary mapped during the pre-study. The length estimations are based on the current HCL data provided by SGU (SGU 2015d, referred to as the Agrell50m model method in this study) in combination with the manually digitized HCL locations generated during the pre-study (see Figure 3 in the Methods chapter).

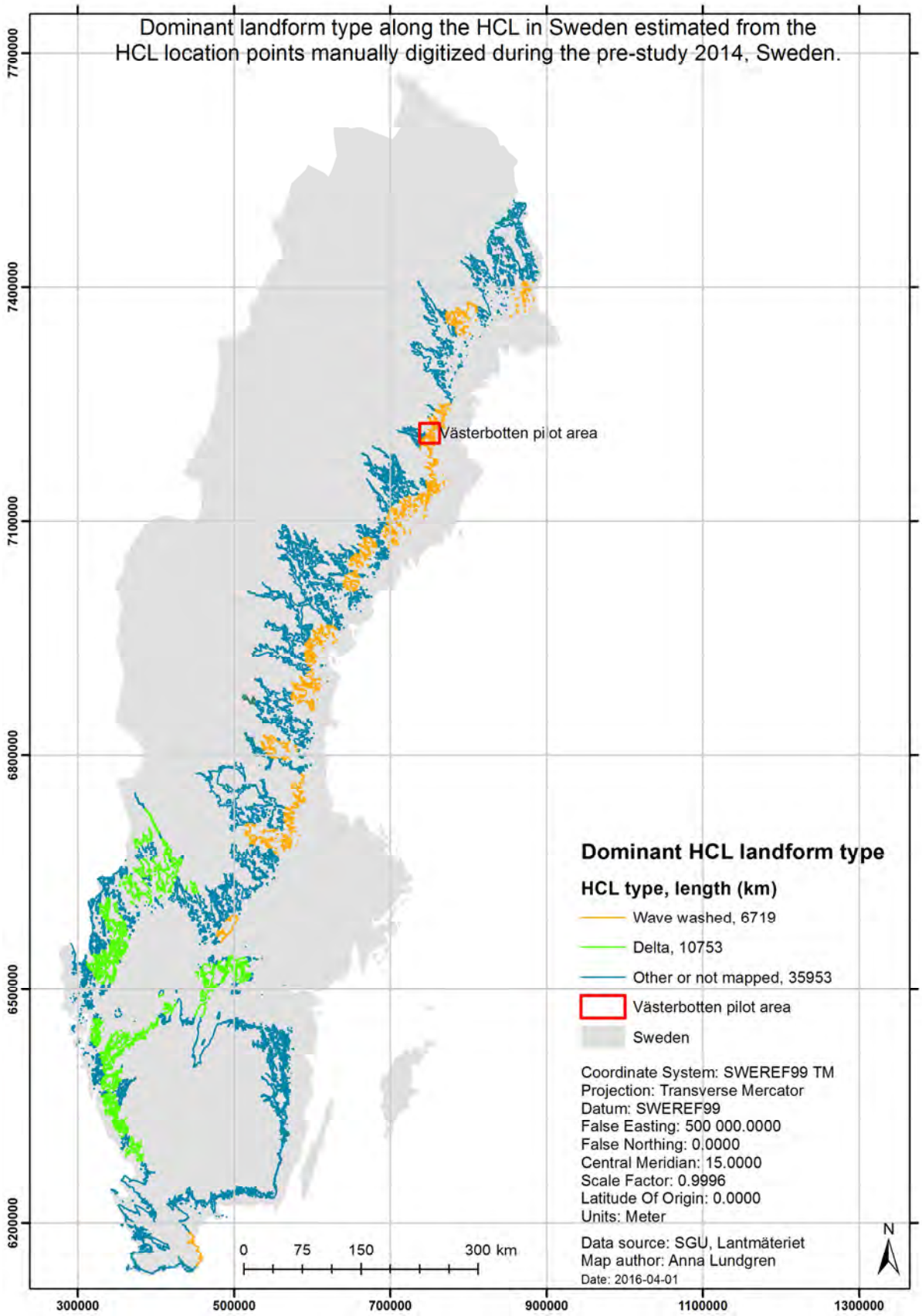

Figure 41 Estimation of dominating landform along the HCL in Sweden based on manually digitized HCL location data points generated in the pre-study 2014 to this study (see Figure 3). The current HCL surface data supplied by SGU (SGU 2015d) is used for the visualization of the HCL boundary. The HCL boundary is linked to dominating HCL landform type: delta or wave washed.

5.3 Sources of error

Main sources of errors include input data accuracy, interpreter bias during manual mapping and parameter settings of GIS-tools, uncertainty in method development path due to the experimental nature of the project using an iterative trial and error approach, and limits of ArcGIS 10.2 tools used in the model methods e.g. interpolation algorithms.

5.3.1 Input data

The accuracies of the input data (original DEM, old HCL data, Quaternary data) and the refined data (extracted breaklines for certain scale dimension) are a contributing source of error.

The objectivity of using related data as 'starting point' for generating new or updated data should be discussed. The HCL data compiled by Agrell (2001) has been used as 'starting point' for the manually digitized HCL location data generated in the pre-study and for narrowing the search area when manually classifying the extracted breaklines in Type4 and Type4top model methods in the present study. 'Starting point' data is important ancillary information to make the mapping process efficient. The supporting HCL data used in this project is validated at least once by SGU through the compiling work of Agrell (2001) which makes it a reliable source of data. Attention should however be paid on not letting the ancillary data completely control the mapping process (e.g. manually digitizing or breakline classification) to increase the chances of finding new information.

5.3.2 Interpreter bias

As for all manual mapping, interpreter bias is a source of error and therefore present in the manually digitized reference data and the HCL data points digitized during the pre-study used in the Manual model method. The interpreter bias can be assumed to be greater for the HCL points digitized for the whole of Sweden during the pre-study (Figure 3) than for the reference data digitized for the Västerbotten pilot area (see Appendix E) due to the difference in study area size and operator learning phase. The time limit of the project, the study area size, and the varying HCL environments present throughout Sweden with differentiating difficulty level of identifying the HCL are factors contributing to errors introduced in the manually digitizing of HCL points during the pre-study.

Where to actually draw the boundary of the HCL is open to interpretation and thus can be a source of error when manually mapping the HCL if not standardized e.g. should the HCL boundary be drawn above, on or below the highest positioned beach ridge in wave washed HCL locations? At HCL locations identified by glaciofluvial delta plains, the positioning of the HCL boundary is even more unclear due to lack of guidelines and therefor the operator is left to decide if the HCL should be positioned e.g. at the outer delta edge (sometimes eroded by later events), at a point representing the mid-elevation of the delta plain, or at the relict glacial river mouth? A discussion of the HCL position in relation to beach ridges and beach ridge complexes in wave washed areas can be found in Påsse (1983). Berglund (2012) discusses the mean sea level in relation to the HCL position determined using wave washed features or glaciofluvial delta plains. The automated digitizing of breaklines and finally the HCL boundary line is the strength of the developed model methods in this project since it minimizes some of the decisions open to interpretation and therefore structures the mapping process making it standardized and reproducible independent on operator.

A source of uncertainty is the experimental nature of this project with a constant development of method throughout the project including the pre-study and the project presented in this report. The initial methods are taken from methods used in studies with similar applications (Cracknell et al. 2013, Rutzinger et al. 2012; 2011; 2007, Lillesand et al. 2008, Cavalli and Marchi 2008) and then adapted to this projects application with consideration of knowledge base, data, and software available to this

project. The methods used in the present project are based on knowledge gained in the pre-study as well as knowledge gained throughout the development phase of the present study.

5.3.3 Parameter settings and tool functionality

Parameter settings for ArcGIS 10.2 tools (ESRI 2015m) used in the model methods e.g. scale dimension on moving window, curvature thresholds, and raster to polyline conversion settings are only visually evaluated in this project. If all parameter settings used in the model methods (see the Methods chapter for more details) were systematically optimized using e.g. a similar approach as Rutzinger et al. (2012) used for optimizing moving window size, curvature thresholds, and buffer radius for the classification accuracy assessment a clearer picture of what parameters affect the accuracies of the model methods would be available. Applying this kind of optimization assessment would increase the data quality of the output for the successful model methods in this project but may be a time demanding task.

The moving window scale dimension was set by generating low-pass filtered (smoothed) images of the DEM at a certain scale dimension instead of directly in the curvature tool settings due to the ArcGIS 10.2 *Curvature* tool lacking this functionality (ESRI 2015f). The ArcGIS 10.2 *Curvature* tool uses a fixed moving window size of 3x3 cells which may alter the results of the applied curvature breakline extraction method. However the visual evaluation show that curvature LSP using different scale dimensions set by the smoothed DEM input enhance the sought features to different degree (see Appendix B Figures B1-B3).

5.4 Future work

Possible future development steps for this project are:

- to apply the Type4 model method on all wave washed dominated areas along the HCL in Sweden (Figure 41),
- to optimize parameter settings for the successful model methods to reach the highest accuracy possible i.e. model methods producing results closer to manual methods,
- to study the possibilities to improve the classification step used in Type1 model method to reach a more automated and objective model method with the same accuracies as the Type3 model method,
- to find existing or design a new program (using e.g. Python) more suitable for the elongation step used in the Type1 model method,
- to investigate if number of input data points significantly affect the model methods accuracies,
- to investigate if there is advantages of applying Kriging interpolation which is a more advanced interpolation method (however processer intensive) taking advantage of geostatistics of the phenomena to be modeled and is often used within geology and soil science (ArcGIS 10.2 2015m),
- to develop a similar mapping method for HCL areas dominated by HCL-deltas (Figures 41 and 3). Generating HCL surfaces extracted from HCL-deltas and from HCL locations dominated by wave washed features gives the opportunity to e.g. estimate the difference in local formation elevation level.

6 Conclusions

The Type4 model method and Manual model method generate HCL maps closest to the reference data (i.e. manually digitized HCL data based on high resolution DEMs) according to the classification accuracy assessment measures resulting from the error matrix and 'buffer' method. The Manual model method performs slightly better for the HCL boundary as a whole (see completeness, correctness, and quality measures for total HCL boundary Figure 37) but the Type4 model method performs better for HCL boundary adjacent to the actual digitized reference data (see completeness, correctness, and quality measures for HCL boundary within 200 m flat buffer Figure 38). The higher accuracy measures for the Manual model method are most likely explained by the fact that the input data points are part of the manually digitized HCL boundary reference data. The Type1 model method and the Agrell50m model method produces HCL maps that deviates the most both in classification accuracy and elevation accuracy from the reference data.

The Manual model method uses manually digitized HCL points as input which is more time consuming than the automated methods used in the Type4 and Type4top model methods. The result of a fully manual method is not reproducible to the same degree as an automated method. The Type4 or Type4top model methods are more efficient and reproducible mapping methods to use than a fully manual mapping method. The Type4 and Type4top model methods generate linear segments (polylines) which can be used to extract elevation data points at desired density further used to interpolate a HCL surface.

To fully automate the manual mapping method used to map the HCL in wave wash dominated HCL areas (see Figure 2) requires further investigation. The main challenge is to succeed with an acceptable separation of breaklines related to wave washed features and breaklines related to glacial flow lineation features in the classification step. The results from the Type1 model method concludes that coarse scaled residual DEM LSP rasters combined with length, mean orientation, and sinuosity breakline attributes is an insufficient method to reach the desired classification. The results from Type3 model method indicates that even a successful Type1 model method will reach accuracies (in relation to the manually digitized reference data) below the Type4 and Type4top models.

Objectivity, reproducibility, time efficiency and spatial accuracy are desirable characteristics of a mapping methodology. In summary the Type4 model method of the methods developed for mapping the HCL presented in this report comes closest to these objectives.

7 Acknowledgements

I would like to thank my supervisor Tore Påsse (SGU) for his support and patience throughout this project. Without your knowledge, guidance and input this project would not have moved forward. Thank you.

I would also like to thank SGU for providing the material resources and data resources used in this project. Many thanks to the staff at the SGU Gothenburg office for sharing your knowledge and letting me be part of your group.

I would like to thank my supervisor Harry Lankreijer (LU) for reviewing my thesis and giving valuable comments and for being my connection point to Lund University and the LUMA-GIS staff during this project.

Thank you Petter Pilesjö (LU) for discussing my work midterm and for reviewing the final GIS applications of my master thesis.

I would like to thank Micael Runnström (LU) and David Tenenbaum (LU) for critically examining my thesis and giving valuable comments. I would also like to thank David Tenenbaum (LU) for reviewing my thesis for language improvements.

To my family and friends (you know who you are). Thank you for always supporting and believing in me. Without you I would not have reached this day.

Marcus, thank you for being by my side.

8 References

Agrell H. 1976 . The highest coastline in south-eastern Sweden. *Boreas 5*: 143-154.

Agrell H. 2001. List of all HCL locations in Sweden. [In Swedish: Förteckning över alla HK-lokaler i Sverige.] Geological Survey of Sweden (SGU) Gothenburg office 2014.

Berti M., Corsini A., and Daehne A. 2013. Comparative analysis of surface roughness algorithms for the identification of active landslides. *Geomorphology 182*: 1-18. doi: 10.1016/j.geomorph.2012.10.022.

Berglund M. 2012. The highest postglacial shore levels and glacio-isostatic uplift pattern in northern Sweden. *Geografiska Annaler: Series A, Physical Geography 94*: 321–337. doi: 10.1111/j.1468-0459.2011.00443.x.

Björck S. 1995. A review of the history of the Baltic Sea, 13.0-8.0 ka BP. *Quaternary international 27*: 19-40.

Blaschke T. 2010. Review article: Object based image analysis for remote sensing. *ISPRS Journal of Photogrammetry and Remote Sensing 65(1)*: 2-16. doi: 10.1016/j.isprsjprs.2009.06.004.

Cavalli M. and Marchi L. 2008. Characterisation of surface morphology of an alpine alluvial fan using airborne LiDAR. *Natural Hazards and Earth System Science (NHESS) 8*: 323-333. doi: 10.5194/nhess-8-323-2008.

Cooly S. W. 2015. *Terrain Roughness – 13 Ways*. GIS4Geomorphology. Available online: http://gis4geomorphology.com/roughness-topographic-position/ [2015-01-20].

Cracknell M. J., Roach M., Green D. and Lucieer A. 2013. Estimating Bedding Orientation From High-Resolution Digital Elevation Models. *IEEE Transaction on Geoscience and Remote sensing 51(5)*: 2949-2959. doi: 10.1109/TGRS.2012.2217502.

Dowling T. P. F., Alexanderson H., and Möller P. 2013. The new high-resolution LiDAR digital height model (‘Ny Nationell Höjdmodell’) and its application to Swedish Quarternary geomorphology. *GFF 135(2)*: 145-151. doi: 10.1080/11035897.2012.759269.

Drăguţ L. and Eisank C. 2011. Object representations at multiple scales from digital elevation models, *Geomorphology 129*: 183-189. doi: 10.1016/j.geomorph.2011.03.003.

Eisank C., Smith M. and Hillier J. 2014. Assessment of multiresolution segmentation for delimiting drumlins in digital elevation models. *Geomorphology 214*: 452-464. doi: 10.1016/j.geomorph.2014.02.028.

ESRI 2015a. *How Focal Statistics works*. ArcGIS Help 10.2. ArcGIS 10.2.2 for Desktop, Environmental Systems Research Institute, Redlands. Available online: http://resources.arcgis.com/en/help/main/10.2/index.html#//009z000000r7000000 [2015-07-11].

ESRI 2015b. *Extend Line (Editing).* ArcGIS Help 10.2. ArcGIS 10.2.2 for Desktop, Environmental Systems Research Institute, Redlands. Available online: http://resources.arcgis.com/en/help/main/10.2/index.html#//001v00000004000000 [2015-07-21].

ESRI 2015c. *What is ModelBuilder?*. ArcGIS Help 10.2. ArcGIS 10.2.2 for Desktop, Environmental Systems Research Institute, Redlands. Available online: http://resources.arcgis.com/en/help/main/10.2/index.html#//002w00000001000000 [2015-07-21].

ESRI 2015d. *Focal Statistics (Spatial Analyst)*. ArcGIS Help 10.2. ArcGIS 10.2.2 for Desktop, Environmental Systems Research Institute, Redlands. Available online: http://resources.arcgis.com/en/help/main/10.2/index.html#//009z000000qs000000 [2015-07-21].

ESRI 2015e. *Raster Calculator (Spatial Analyst)*. ArcGIS Help 10.2. ArcGIS 10.2.2 for Desktop, Environmental Systems Research Institute, Redlands. Available online: http://resources.arcgis.com/en/help/main/10.2/index.html#//009z000000z7000000 [2015-07-21].

ESRI 2015f. *Curvature (Spatial Analyst)*. ArcGIS Help 10.2. ArcGIS 10.2.2 for Desktop, Environmental Systems Research Institute, Redlands. Available online: http://resources.arcgis.com/en/help/main/10.2/index.html#//009z000000tw000000 [2015-07-21].

ESRI 2015g. *Majority Filter (Spatial Analyst)*. ArcGIS Help 10.2. ArcGIS 10.2.2 for Desktop, Environmental Systems Research Institute, Redlands. Available online: http://resources.arcgis.com/en/help/main/10.2/index.html#//009z00000037000000 [2015-07-21].

ESRI 2015h. *Thin (Spatial Analyst)*. ArcGIS Help 10.2. ArcGIS 10.2.2 for Desktop, Environmental Systems Research Institute, Redlands. Available online: http://resources.arcgis.com/en/help/main/10.2/index.html#//009z0000003n000000 [2015-07-21].

ESRI 2015i. *Raster to Polyline (Conversion)*. ArcGIS Help 10.2. ArcGIS 10.2.2 for Desktop, Environmental Systems Research Institute, Redlands. Available online: http://resources.arcgis.com/en/help/main/10.2/index.html#//001200000009000000 [2015-07-21].

ESRI 2015j. *Linear Directional Mean (Spatial Statistics)*. ArcGIS Help 10.2. ArcGIS 10.2.2 for Desktop, Environmental Systems Research Institute, Redlands. Available online: http://resources.arcgis.com/en/help/main/10.2/index.html#//005p00000017000000 [2015-07-21].

ESRI 2015k. *IDW (Spatial Analyst)*. ArcGIS Help 10.2. ArcGIS 10.2.2 for Desktop, Environmental Systems Research Institute, Redlands. Available online: http://resources.arcgis.com/en/help/main/10.2/index.html#//009z0000006m000000 [2015-07-22].

ESRI 2015l. *Kriging (Spatial Analyst)*. ArcGIS Help 10.2. ArcGIS 10.2.2 for Desktop, Environmental Systems Research Institute, Redlands. Available online: http://resources.arcgis.com/en/help/main/10.2/index.html#//009z0000006n000000 [2015-08-27].

ESRI 2015m. *A complete listing of the Spatial Analyst tools*. ArcGIS 10.2.2 for Desktop, Environmental Systems Research Institute, Redlands. Available online: http://resources.arcgis.com/en/help/main/10.2/index.html#/A_complete_listing_of_the_Spatial_Analyst_tools/009z000000wv000000/ [2015-09-02].

ESRI 2015o. *Model elements*. ArcGIS 10.2.2 for Desktop, Environmental Systems Research Institute, Redlands. Available online: http://resources.arcgis.com/EN/HELP/MAIN/10.2/index.html#/Model_elements/002w00000003000000/ [2015-09-16].

Fox T. J. USGS 2014. *Split By Attribute Tool*. U.S. Geological Survey, Upper Midwest Environmental Sciences Center, La Crosse, Wisconsin. Available online: http://www.umesc.usgs.gov/management/dss/split_by_attribute_tool.html [2015-03-03].

Fredén C. (Special ed.) 2002. *Rock and soil. The National Atlas of Sweden (SNA)*. [In Swedish: *Berg och jord*: *Sveriges nationalatlas (SNA)*.]Theme manager: Geological Survey of Sweden (SGU). 3rd edition. Vällingby: SNA. 208 p.

Hasan A., Pilesjö P., and Persson A. 2012. On generating digital elevation models from LiDAR data – resolution versus accuracy and topographic wetness index indices in northern peatlands. *Geodesy and cartography 38(2)*: 57-69. doi: 10.3846/20296991.2012.702983.

Heipke C., Mayer H., Wiedemann C., and Jamet O. 1997. Evaluation of automatic road extraction. *"3D Reconstruction and Modeling of Topographic Objects", Stuttgart, September 17-19*. International Archives of the Photogrammetry, Remote Sensing and Spatial Information Sciences *IAPRS 32(3-4W2)*: 151-160. Available online: http://www.ifp.uni-stuttgart.de/publications/wg34/wg34_heipke.pdf [2015-10-17].

Höhle J. and Höhle M. 2009. Accuracy assessment of digital elevation models by means of robust statistical methods. *ISPRS Journal of Photogrammetry and Remote sensing 64(4)*: 398-406. doi: 10.1016/j.isprsjprs.2009.02.003.

Jakobsson M., Björck S., Alm G., Andrén T., Lindeberg G., and Svensson N.-O. 2007. Reconstructing the Younger Dryas ice dammed lake in the Baltic Basin: Bathymetry, area and volume. *Global and Planetary Change 57(3)*: 355-370. doi: 10.1016/j.gloplacha.2007.01.006.

Lang S. 2008. Object-based image analysis for remote sensing applications: modeling reality – dealing with complexity. in *Object-Based Image Analysis Spatial Concepts for Knowledge-Driven Remote Sensing Applications*, Eds. Blaschke T., Lang S., Hay G. J., p. 3-27. Berlin, Heidelberg: Publisher Springer Berlin Heidelberg. doi: 10.1007/978-3-540-77058-9_1.

Lantmäteriet 2015. Product description: GSD-Elevation data, Grid 2+, Document version 2.2 2015-10-01. Available online: http://www.lantmateriet.se/globalassets/kartor-och-geografisk-information/hojddata/produktbeskrivningar/eng/e_grid2_plus.pdf [2015-10-05], or http://www.lantmateriet.se/sv/Kartor-och-geografisk-information/Hojddata/GSD-Hojddata-grid-2/ [2015-10-16].

Lillesand, Keifer and Chipman 2008. 'Chap. 7 Digital Image Interpretation and Analysis' and 'Chap. 8 Microwave and Lidar Sensing'. in *Remote sensing and image interpretation*. 6th edition, p. 482-731. New York: John Wiley & Sons, Inc.

Liu X. 2008. Airborne LiDAR for DEM generation: some critical issues. *Progress in Physical Geography 32(1)*: 31–49. doi: 10.1177/0309133308089496.

Lundqvist G. 1961. Karta över landisens avsmältning och högsta kustlinjen i Sverige. *Sveriges Geologiska Undersökning Ba 18*: 1–148.

Lundqvist J. 2002. Glacial geology of the Råda valley, Värmland, western Sweden. *Norwegian Journal of Geography 56*: 51-55.

McKean J. and Roering J. 2004. Objective landslide and surface morphology mapping using high-resolution airborne laser altimetry. *Geomorphology 57 (2004)*: 331-351. doi:10.1016/S0169-555X(03)00164-8.

Minár and Evans 2008. Elementary forms for land surface segmentation: The theoretical basis of terrain analysis and geomorphological mapping. *Geomorphology (2008) 95(3)*: 236–259. doi: 10.1016/j.geomorph.2007.06.003.

Mårtensson U. and Pilesjö P. 2004. Lecture: *Map accuracy assessment*. GIS402: Advanced Course in Geographical Information Systems (GIS), Master's Programme in GIS (LUMA-GIS), Lund University GIS Centre Lund University, Lund, Sweden.

Nyborg M., Berglund J. and Triumf C-A. 2007. Detection of lineaments using airborne laser scanning technology: Laxemar-Simpevarp, Sweden. *Hydrogeology Journal 15*: 29–32 doi: 10.1007/s10040-006-0134-0.

Ojala A. E.K., Palmu J-P., Åberg A., Åberg S., and Virkki H. 2013. Development of an ancient shoreline database to reconstruct the Litorina Sea maximum extension and the highest shoreline of the Baltic Sea basin in Finland. *Bulletin of the Geological Society of Finland 85*: 127-144.

d'Oleire-Oltmanns S., Eisank C., Drăgut L., and Blaschke T. 2013. An Object-Based Workflow to Extract Landforms at Multiple Scales From Two Distinct Data Types. *IEEE Geoscience and remote sensing letters 10 No. 4*: 947-951.

Peterson G. and Smith C. A. 2013. Description of units in the geomorphic database of Sweden. Geological Survey of Sweden, SGU-report 2013:4, Uppsala, Sweden. 18 p.

Påsse T. 1983. Shore displacement in northern Halland during Holocene time. [In Swedish: Havstrandens nivåförändringar i norra Halland under holocen tid., English summary]. Dissertation Publ. A 45. Gothenburg, Sweden: Institution of geology, Chalmers University of Technology and University of Gothenburg. Lindome: Kompaniet. 174 p.

Påsse T. and Andersson L. 2005. Shore-level displacement in Fennoscandia calculated from empirical data. *GFF 127*: 253-268.

Roering J. J., Mackey B. H., Marshall J. A., Sweeney K. E., Deligne N. I., Booth A. M., Handwerger A. L., and Cerovski-Darriua C. 2013. 'You are HERE': Connecting the dots with airborne lidar for geomorphic fieldwork. *Geomorphology 200*: 172-183. doi: 10.1016/j.geomorph.2013.04.009.

Rutzinger, M., Höfle, B. and Kringer, K., 2012. Accuracy of automatically extracted geomorphological breaklines from airborne LiDAR curvature images. *Geografiska Annaler: Series A, Physical Geography 94*: 33–42. doi: 10.1111/ j.1468-0459.2012.00453.x

Rutzinger M., Höfle B., Vetter M. and Pfeifer N. 2011. Chap. 18: Digital Terrain Models from Airborne Laser Scanning for the Automatic Extraction of Natural and Anthropogenic Linear Structures. In *Geomorphological mapping, Development in Earth Surface Processes 15*: 475-488. doi: 10.1016/B978-0-444-53446-0.00018-5.

Rutzinger M., Maukisch M., Petrini-Monteferri F. and Stötter J. 2007. Development of Algorithms for the Extraction of Linear Patterns (Lineaments) from Airborne Laser Scanning Data. In *Proceedings of the Conference 'Geomorphology for the Future', Obergurgl 2007*, p.161-168. Obergurgl, Austria: Innsbruck University Press.

Sailer R., Rutzinger M., Rieg L., and Wichmann V. 2014. Digital elevation models derived from airborne laser scanning point clouds: appropriate spatial resolutions for multi-temporal characterization and quantification of geomorphological processes, *Earth Surf. Process. Landforms 39*: 272-284. Doi: 10.1002/esp.3490.

Seijmonsbergen A. C., Hengl T, and Anders N. S. 2011, Chap. 10: Semi-automated identification and extraction of geomorphological features using digital elevation data. In *Geomorphological mapping, Developments in Earth Surface Processes 15*: 297-335. doi: 10.1016/B978-0-444-53446-0.00010-0.

SGU 2015a. *From ice age to present day*. [In Swedish: *Från istid till nutid*.] Geological survey of Sweden, Uppsala, Sweden. Available online: http://www.sgu.se/om-geologi/jord/fran-istid-till-nutid/ [2015-07-15].

SGU 2015b. *Land uplift – from seabed to clay plain*. [In Swedish: *Landhöjning – från havsbotten till lerslätt*.] Geological survey of Sweden, Uppsala, Sweden. Available online: http://www.sgu.se/om-geologi/jord/fran-istid-till-nutid/landhojning-fran-havsbotten-till-lerslatt/ [2015-07-15].

SGU 2015c. *Postglacial sand and gravel*. [In Swedish: *Postglacial sand och grus*.] Geological survey of Sweden, Uppsala, Sweden. Available online: http://www.sgu.se/om-geologi/jord/fran-istid-till-nutid/landhojning-fran-havsbotten-till-lerslatt/postglacial-sand-och-grus/ [2015-07-15].

SGU 2015d. *PRODUCT: THE HIGHEST COASTLINE*. [In Swedish: *PRODUKT: HÖGSTA KUSTLINJEN*.], product description version 1 2015-01-16, Geodata/Förvaltning, Geological survey of Sweden, Uppsala, Sweden. Available online: http://resource.sgu.se/dokument/produkter/hogsta-kustlinjen-beskrivning.pdf [2015-07-16].

SGU 2015e. *PRODUCT: Quarternary deposits 1:25 000-1:100 000*. [In Swedish: *PRODUKT: JORDARTER 1:25 000-1:100 000*.], product description version 1 2014-02-05, Geodata/Förvaltning, Geological survey of Sweden, Uppsala, Sweden. Available online: http://resource.sgu.se/dokument/produkter/jordarter-25-100000-beskrivning.pdf [2015-07-20].

SGU 2015f. *PRODUCT: Quarternary deposits 1:200 000, VÄSTERNORRLAND*. [In Swedish: *PRODUKT: JORDARTER 1:200 000, VÄSTERNORRLAND*.], product description version 1 2014-02-05, Geodata/Förvaltning, Geological survey of Sweden, Uppsala, Sweden. Available

online: http://resource.sgu.se/dokument/produkter/jordarter-200000-vasternorrland-beskrivning.pdf [2015-10-05].

SGU 2015g. *PRODUCT: Quarternary deposits 1:250 000, NORDLIGASTE SVERIGE*. [In Swedish: *PRODUKT: JORDARTER 1:250 000, NORDLIGASTE SVERIGE*.], product description version 1 2014-02-05, Geodata/Förvaltning, Geological survey of Sweden, Uppsala, Sweden. Available online: http://resource.sgu.se/dokument/produkter/jordarter-250000-nordligaste-sverige-beskrivning.pdf [2015-10-05].

SGU 2015h. Geological Survey of Sweden, Uppsala, Sweden. SGU homepage: http://www.sgu.se/en/ [2015-10-04].

Slatton K. C., Carter W. E., Shrestha R. L., and Dietrich W. 2007. Airborne Laser Swath Mapping: Achieving the resolution and accuracy required for geosurficial research. *Geophysical Research Letters 34*: L23S10. 5p. doi: 10.1029/2007GL031939.

Smith M.J., Rose J., and Booth S. 2006. Geomorphological mapping of glacial landforms from remotely sensed data: an evaluation of the principal data sources and an assessment of their quality. *Geomorphology 76*: 148–165. doi: 10.1016/j.geomorph.2005.11.001.

Tarolli P. 2014. Invited review article: High-resolution topography for understanding earth surface processes: Opportunities and challenges. *Geomorphology 216*: 295-312. doi: 10.1016/j.geomorph.2014.03.008.

9 Appendices

9.1 Appendix A

Modifying the Extend Line tool in Modelbuilder

The *Extend Line* ArcGIS tool (ArcGIS 10.2 2015b) was modified in the *Modelbuilder* environment due to long processing time and a bug which resulted in the FEATURE setting option to fail. The FEATURE setting in the *Extend Line* tool should limit the lines to be extended only to the original features in the input data layer and not to the extensions of the extending lines (which did not work). This resulted in that each curvature vector classified as a glacial flow lineation feature breakline by the Type1 model method had to be processed individually in the elongation step. The following workflow was used:

1. All mean orientation vectors classified as glacial flow lineation breaklines according to the Type1 model method (see Figure D3 in Appendix D) were selected. Then the third party tool *Split By Attribute* (Figure A1, Fox SBA 2015) was applied to separate all glacial flow lineation vector breaklines into separate files to be able to use the *Extend Line* ArcGIS tool as attended by the Type1 model method.

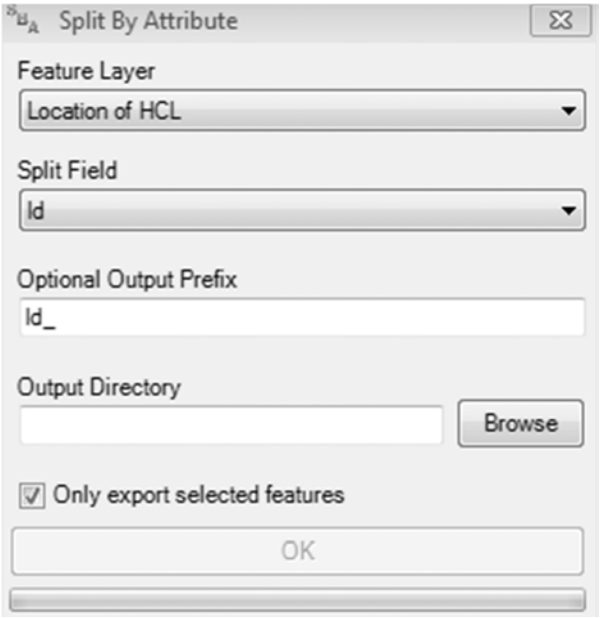

Figure A1. The dialog window for the Split By Attribute tool (Fox SBA 2015) used to separate all glacial flow lineation vector breaklines into separate files.

2. The single glacial flow lineation vectors (separated in step 1.) were merged with the curvature polylines classified as wave washed feature breaklines according to Type1 model method (see Figure D3 in Appendix D) producing a file for each glacial flow lineation breakline included in the analysis (Figure A2).

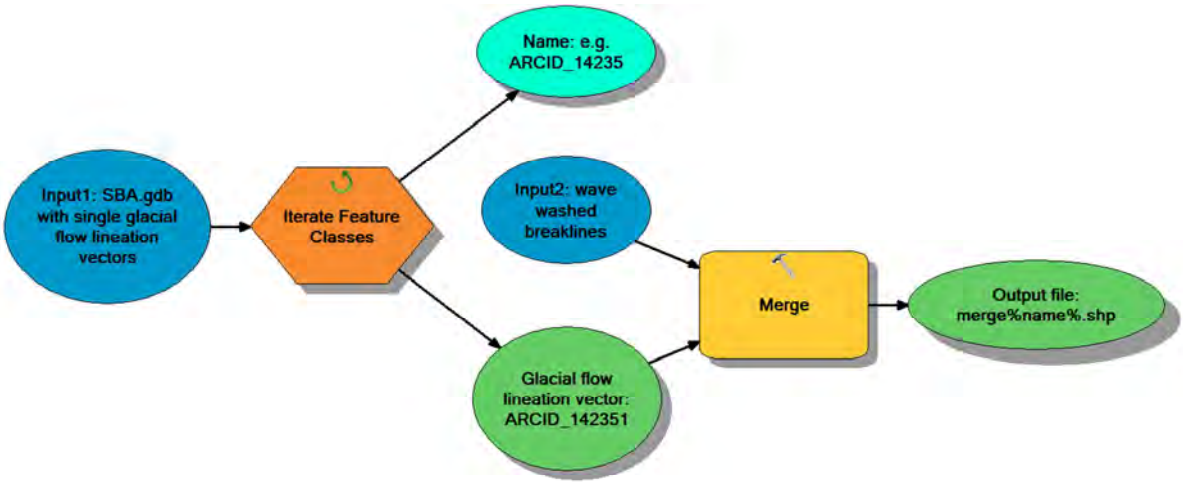

Figure A2. Model used to automate the merging of single curvature vectors classified as glacial flow lineation breaklines by the Type1 model method.

3. Due to the large amount of data (one file for the 17579 glacial flow lineation vectors included in the analysis with 10004 polylines in each file) the files were *Clipped* using a 2050m buffer around the glacial flow lineation vector in process to limit the processing time. The clipping and elongation processes were automatized using *Modelbuilder* (Figure A3 and A4).

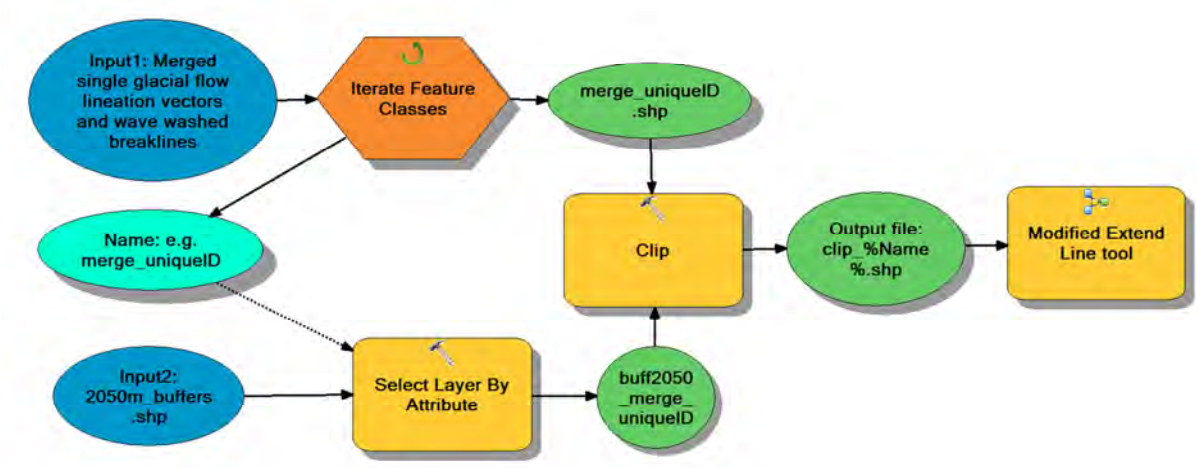

Figure A3. Model for the 2050m buffer clipping process and the elongation process of individual glacial flow lineation vectors.

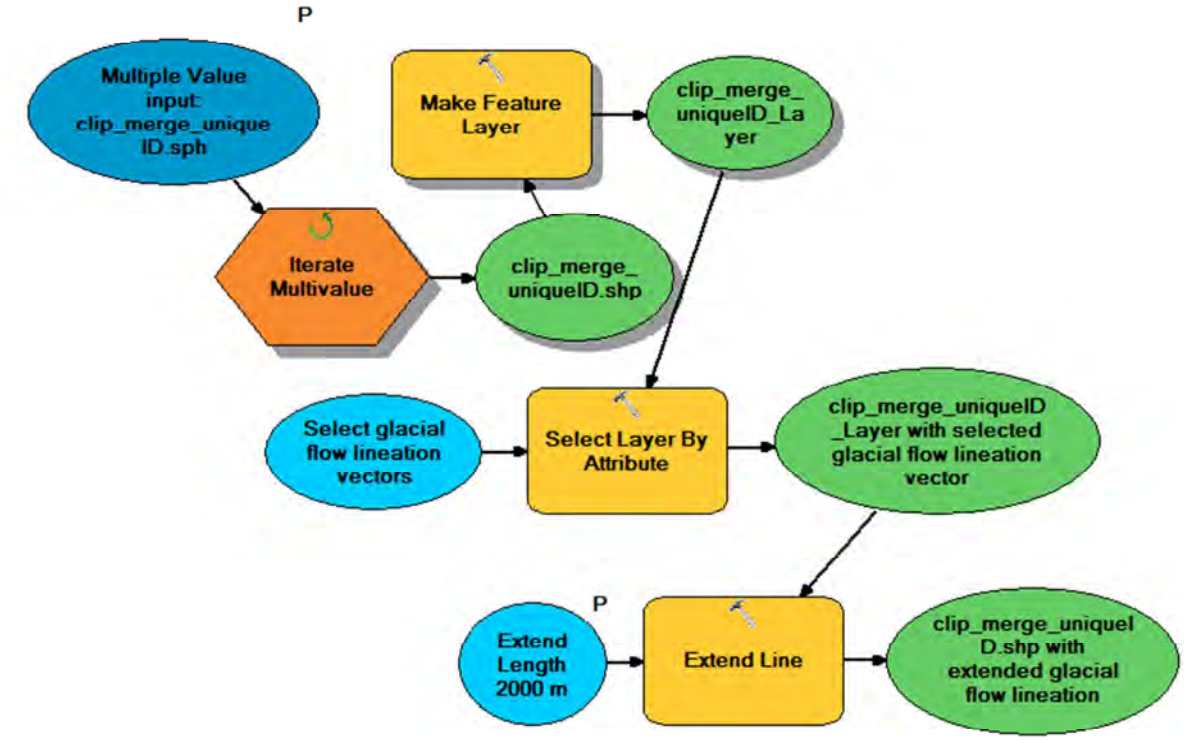

Figure A4. Model of the elongation process (part of the model in Figure A3) used to extend individual glacial flow lineation breakline vectors to the nearest wave washed feature breakline.

9.2 Appendix B

Comparison of scale dimensions: original DEM (2x2 meters) - 19x19cells

Figures B1-B3 presents extracted “normal/mean” curvature polylines for the scale dimensions of the original DEM (2x2 meters) up to 19x19 cells for an area within the Västerbotten pilot area.

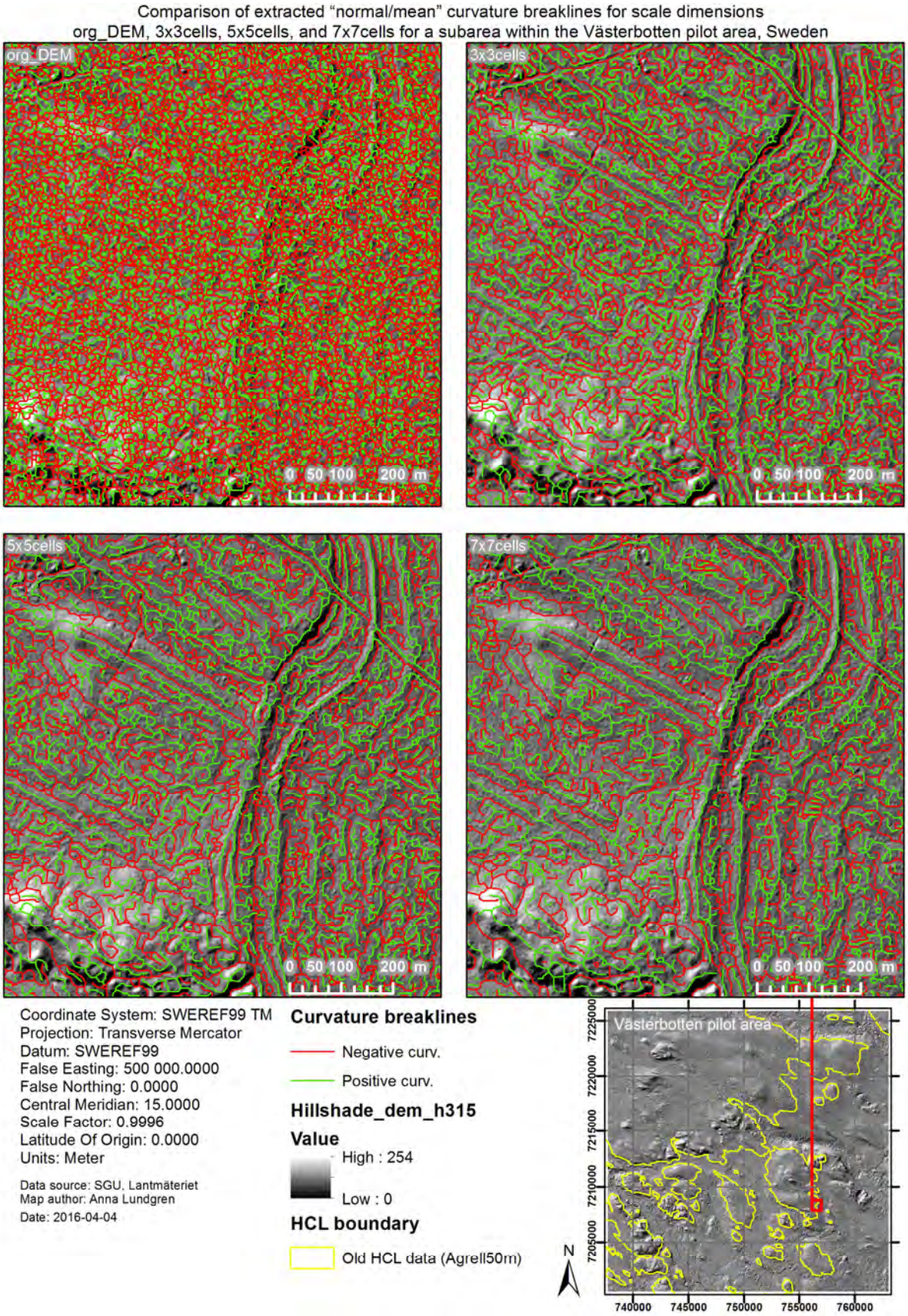

Figure B1 Comparison of breaklines extracted from "normal/mean" curvature LSP rasters with scale dimensions: of the original DEM (2x2 meters), 3x3 cells, 5x5 cells, and 7x7 cells respectively.

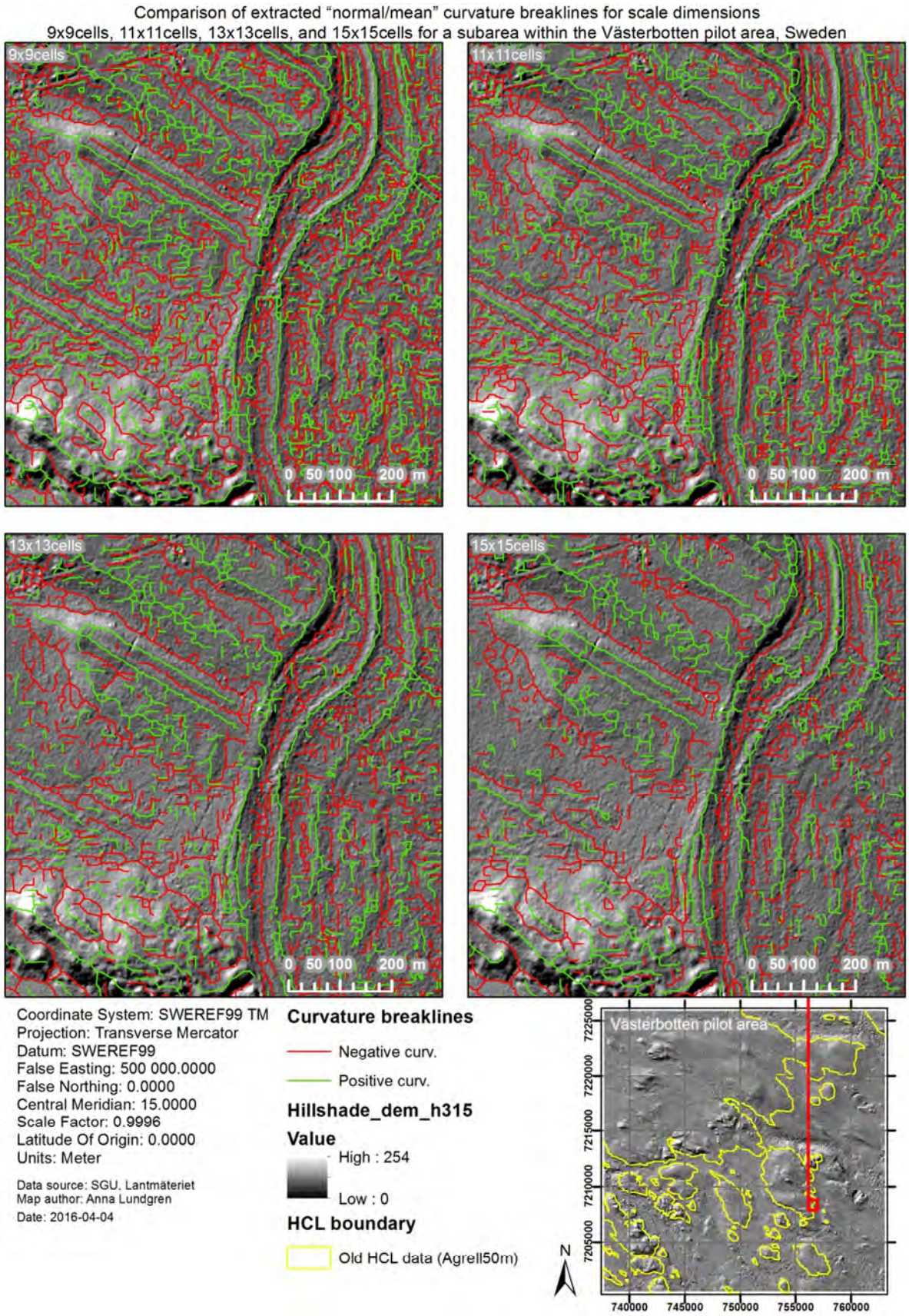

Figure B2 Comparison of breaklines extracted from "normal/mean" curvature LSP rasters with scale dimensions: 9x9 cells, 11x11 cells, 13x13 cells, and 15x15 cells respectively.

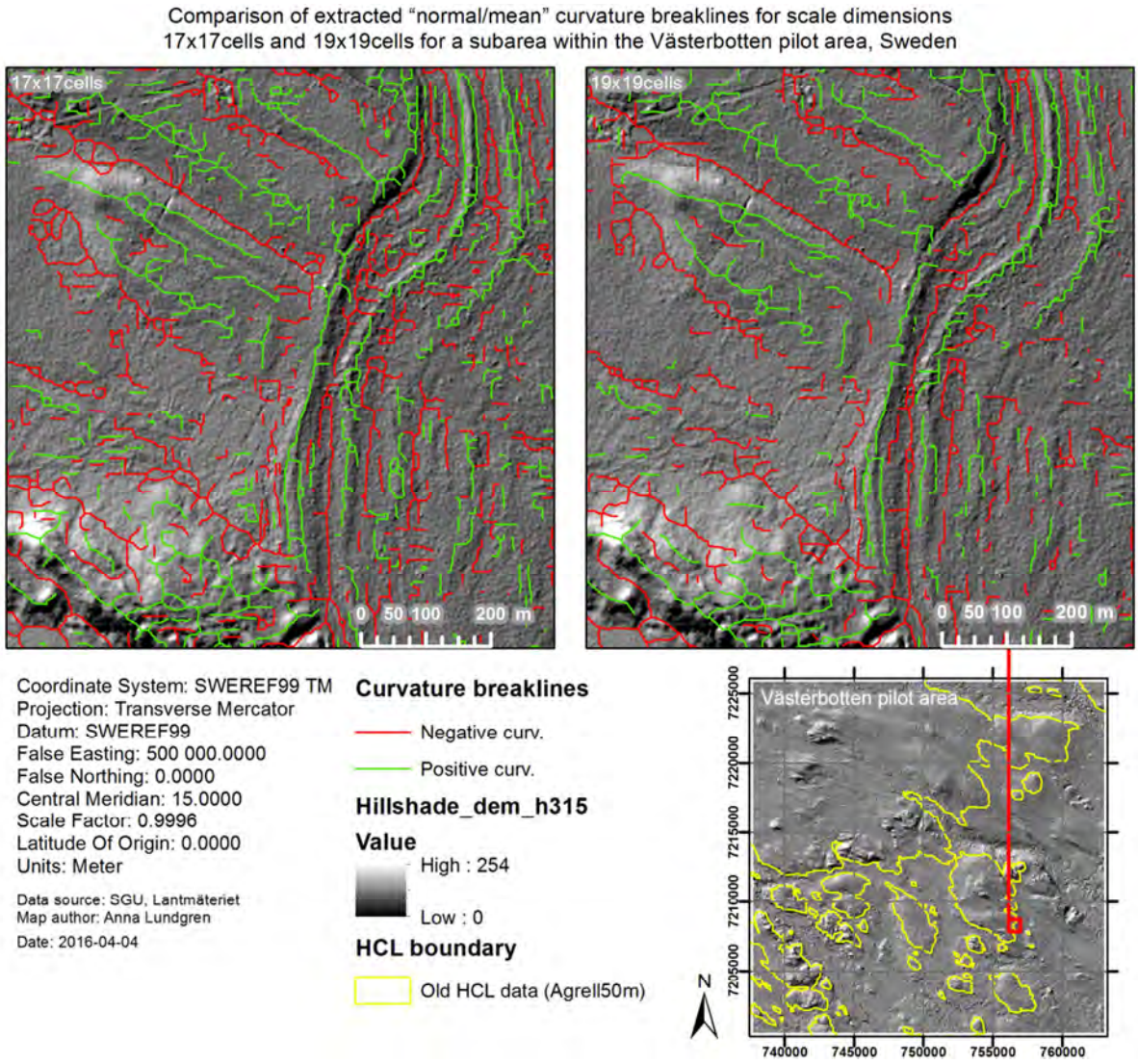

Figure B3 Comparison of breaklines extracted from "normal/mean" curvature LSP rasters with scale dimensions: 17x17 and 19x19 cells respectively.

Detail examples from the breakline extraction in the Västerbotten pilot area

Figures B4-B14 shows detail examples of extracted negative and positive "normal/mean", profile, and plan curvature breaklines for different subareas of the Västerbotten pilot area. The middle right image in the figures shows the hillshade map and the manual digitized HCL boundary reference for the subarea in question.

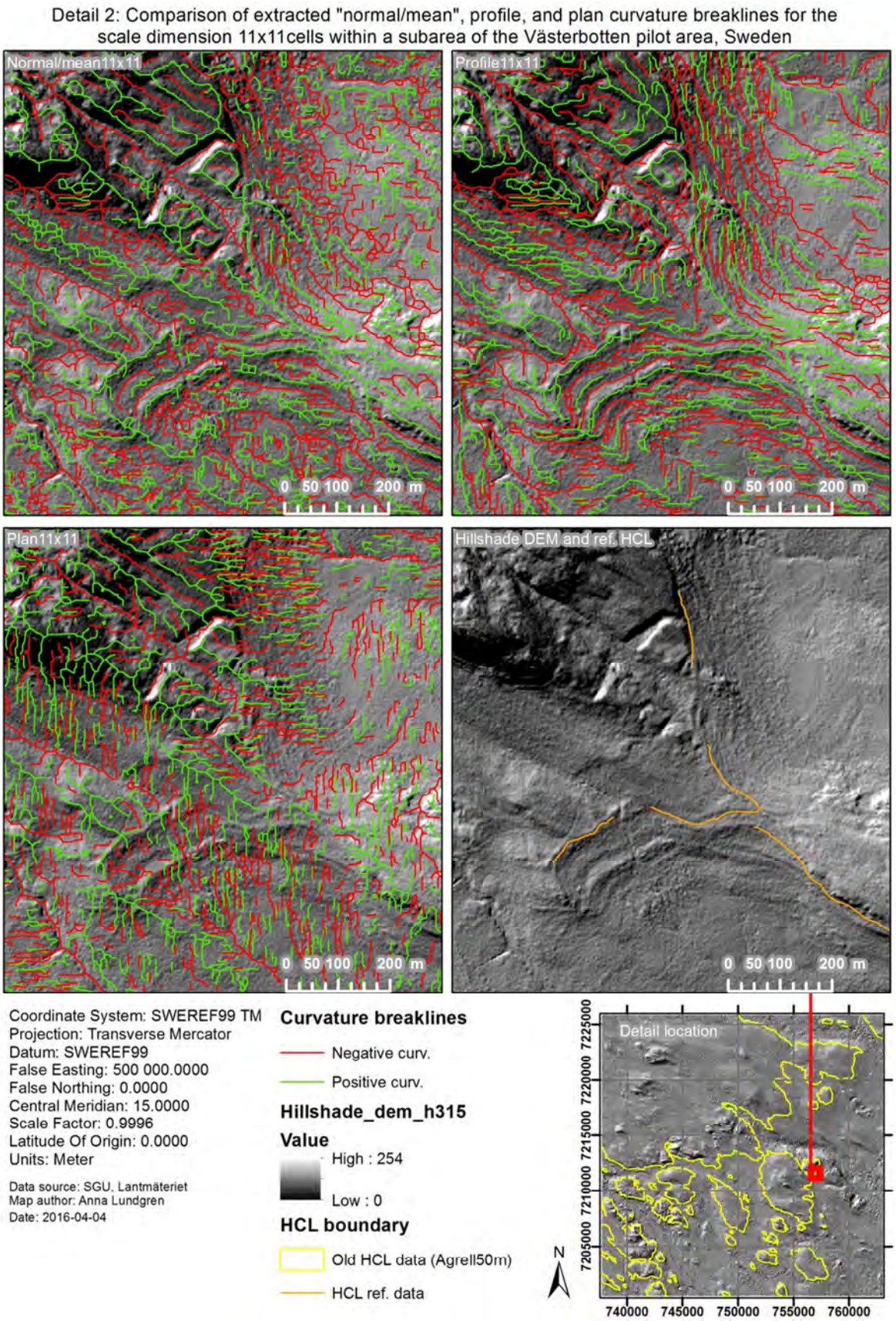

Figure B4. Detail 2 of extracted negative and positive "normal/mean", profile, and plan curvature breaklines for the Västerbotten pilot area.

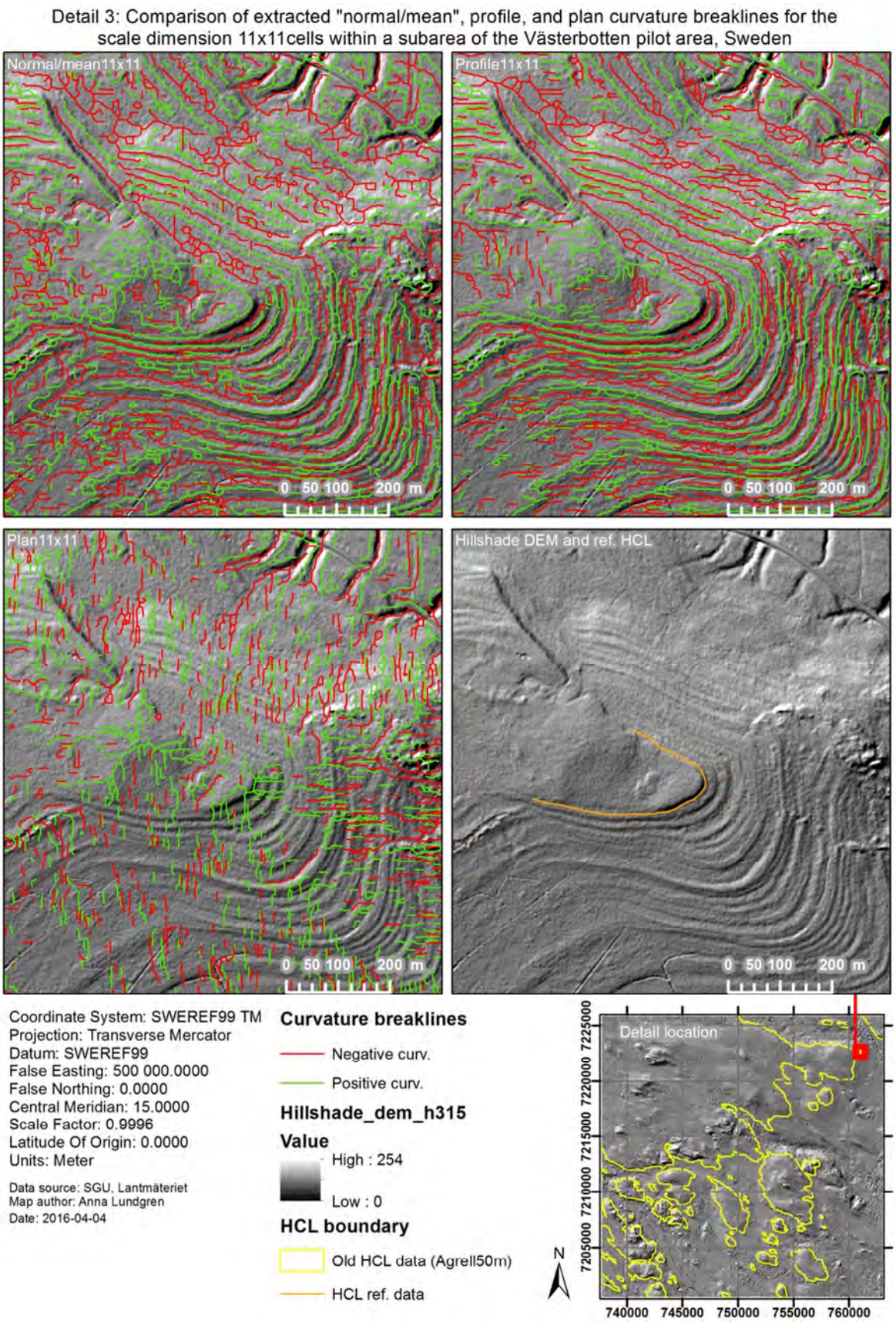

Figure B5. Detail 3 of extracted negative and positive "normal/mean", profile, and plan curvature breaklines for the Västerbotten pilot area.

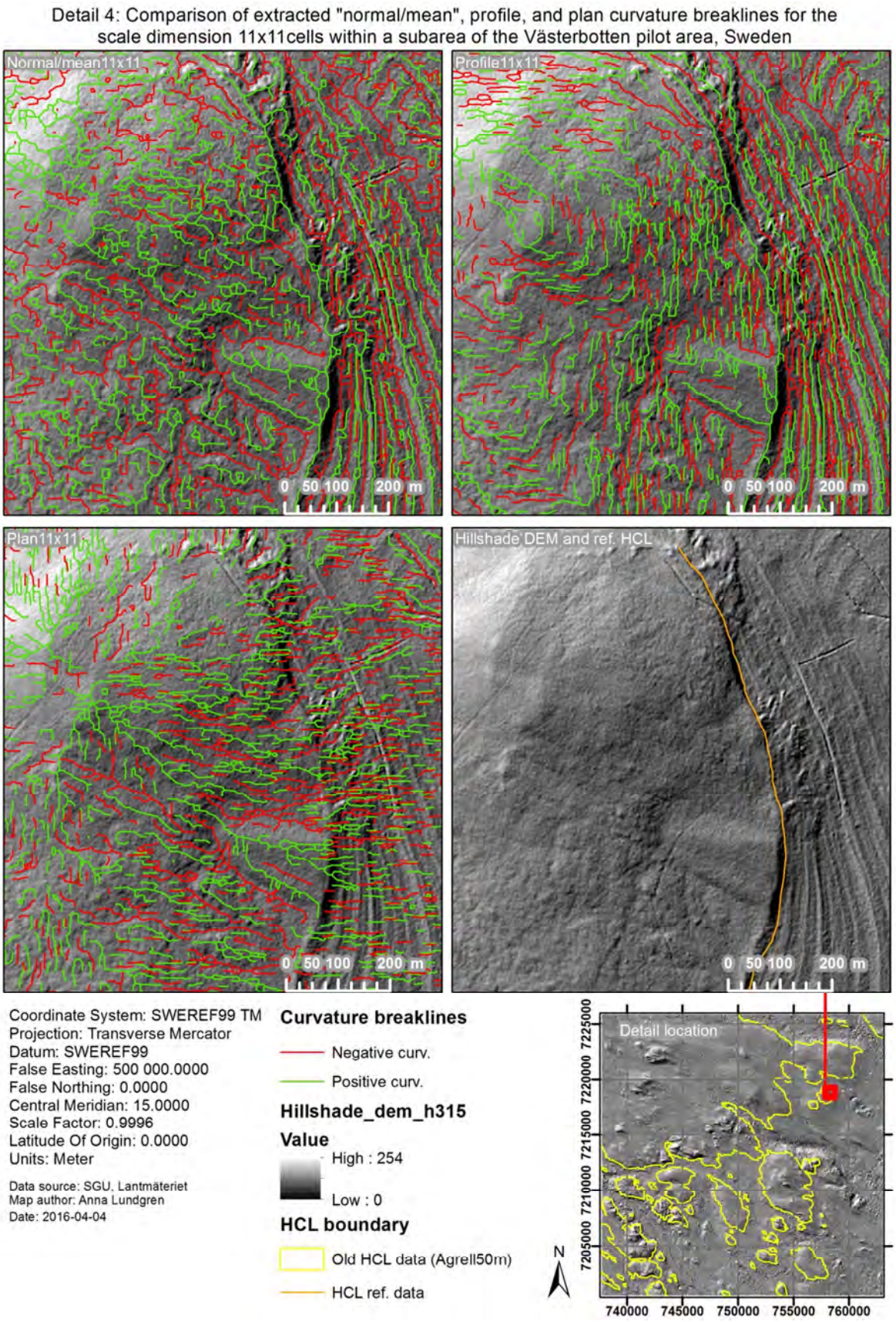

Figure B6. Detail 4 of extracted negative and positive "normal/mean", profile, and plan curvature breaklines for the Västerbotten pilot area.

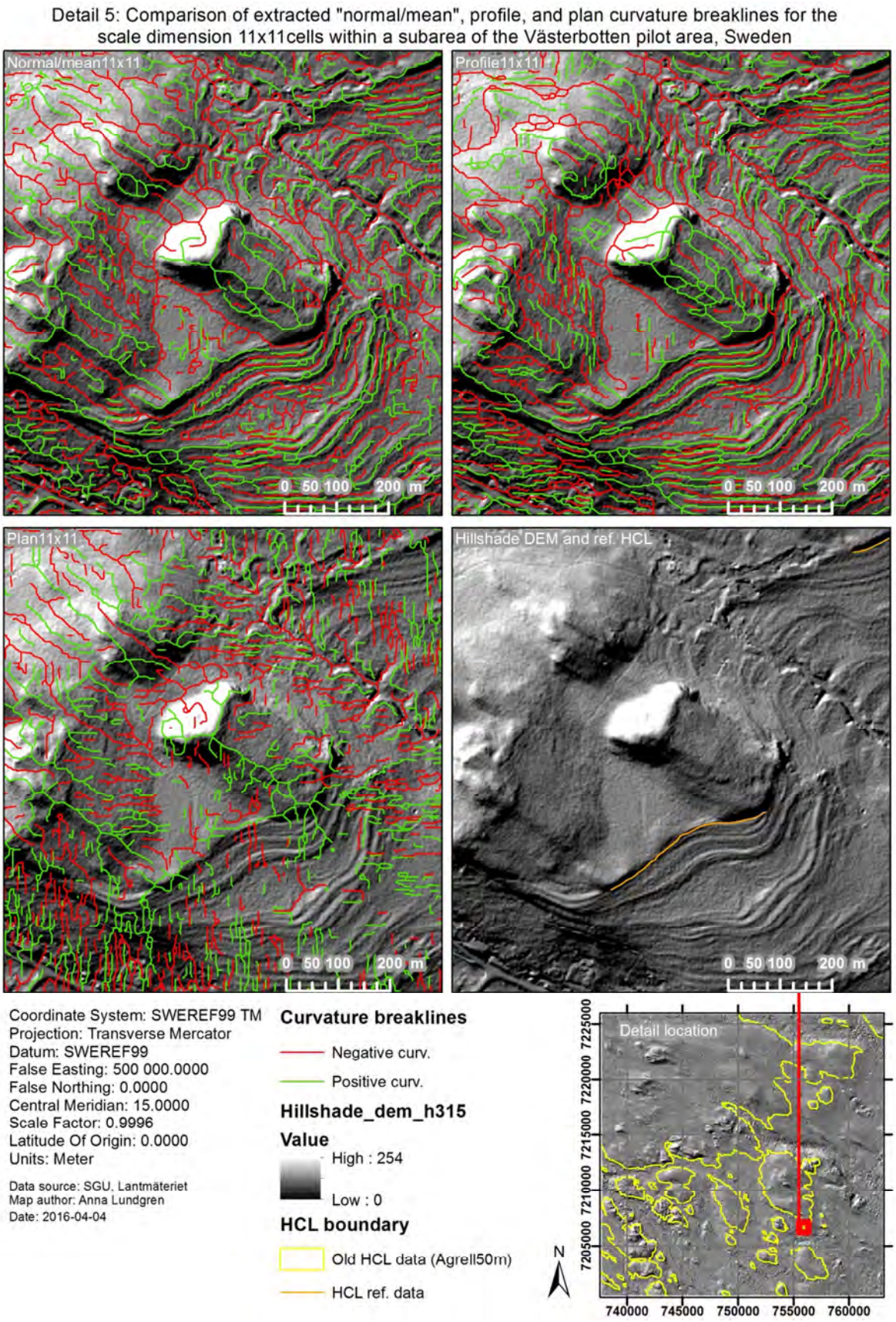

Figure B7. Detail 5 of extracted negative and positive "normal/mean", profile, and plan curvature breaklines for the Västerbotten pilot area.

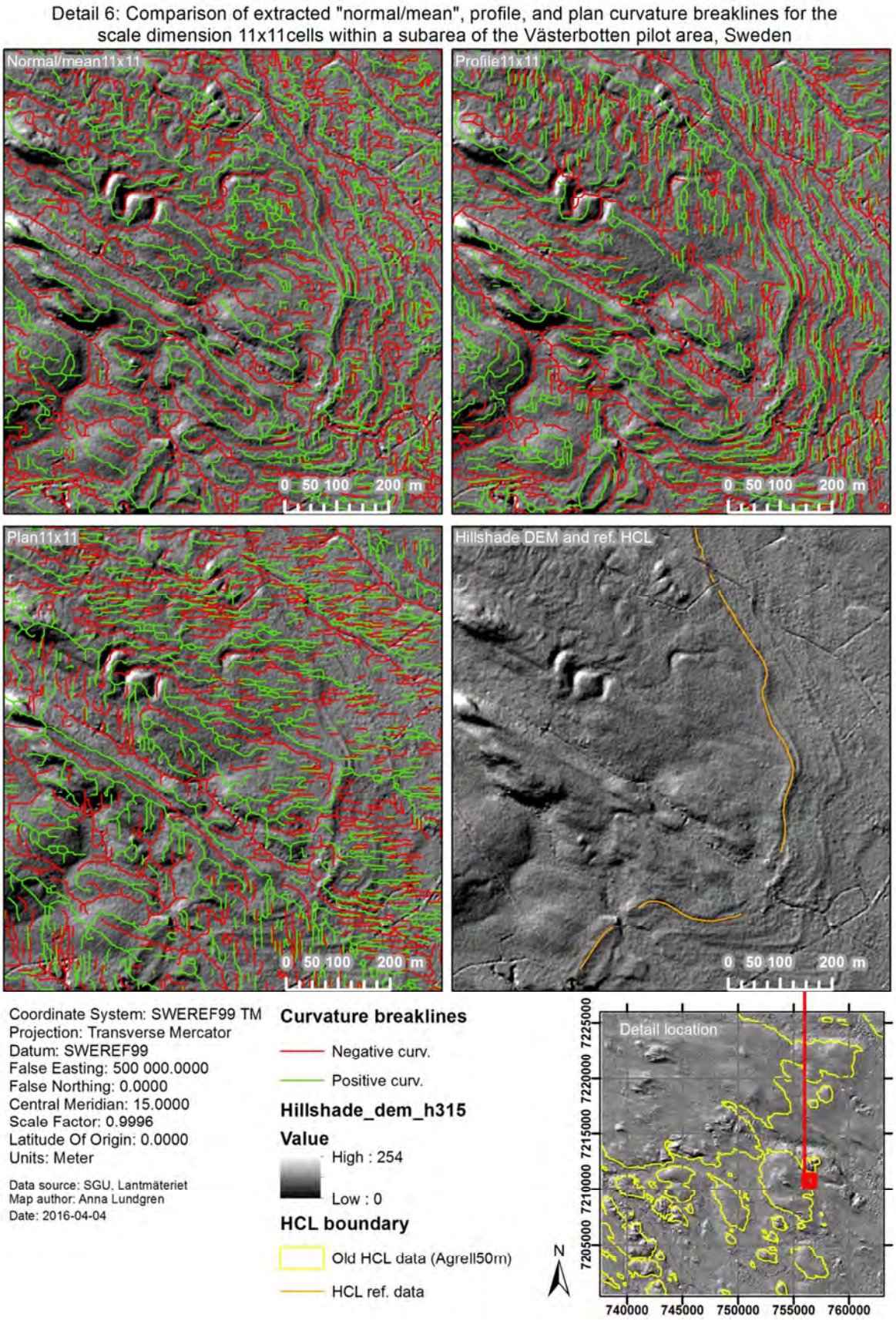

Figure B8. Detail 6 of extracted negative and positive "normal/mean", profile, and plan curvature breaklines for the Västerbotten pilot area.

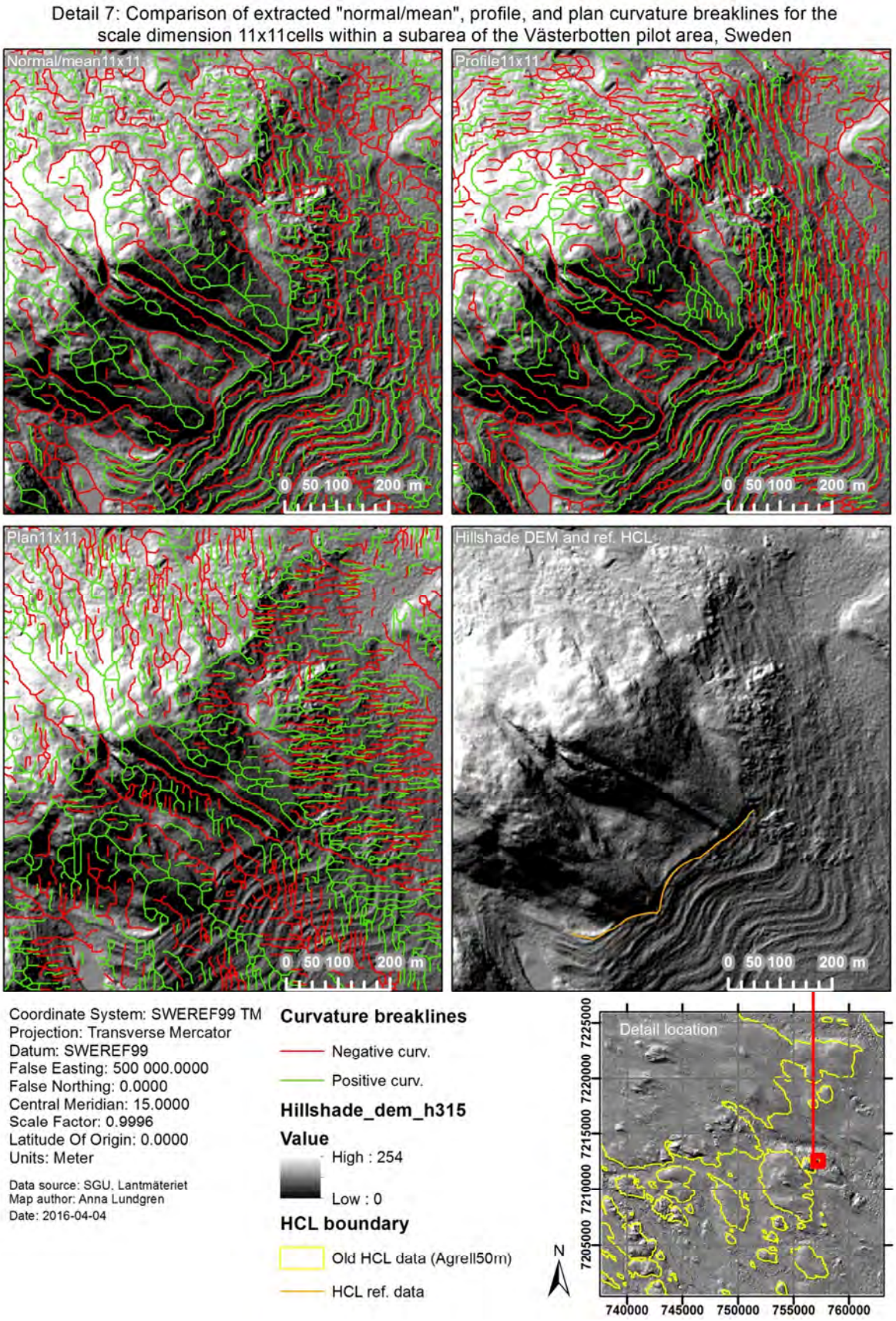

Figure B9. Detail 7 of extracted negative and positive "normal/mean", profile, and plan curvature breaklines for the Västerbotten pilot area.

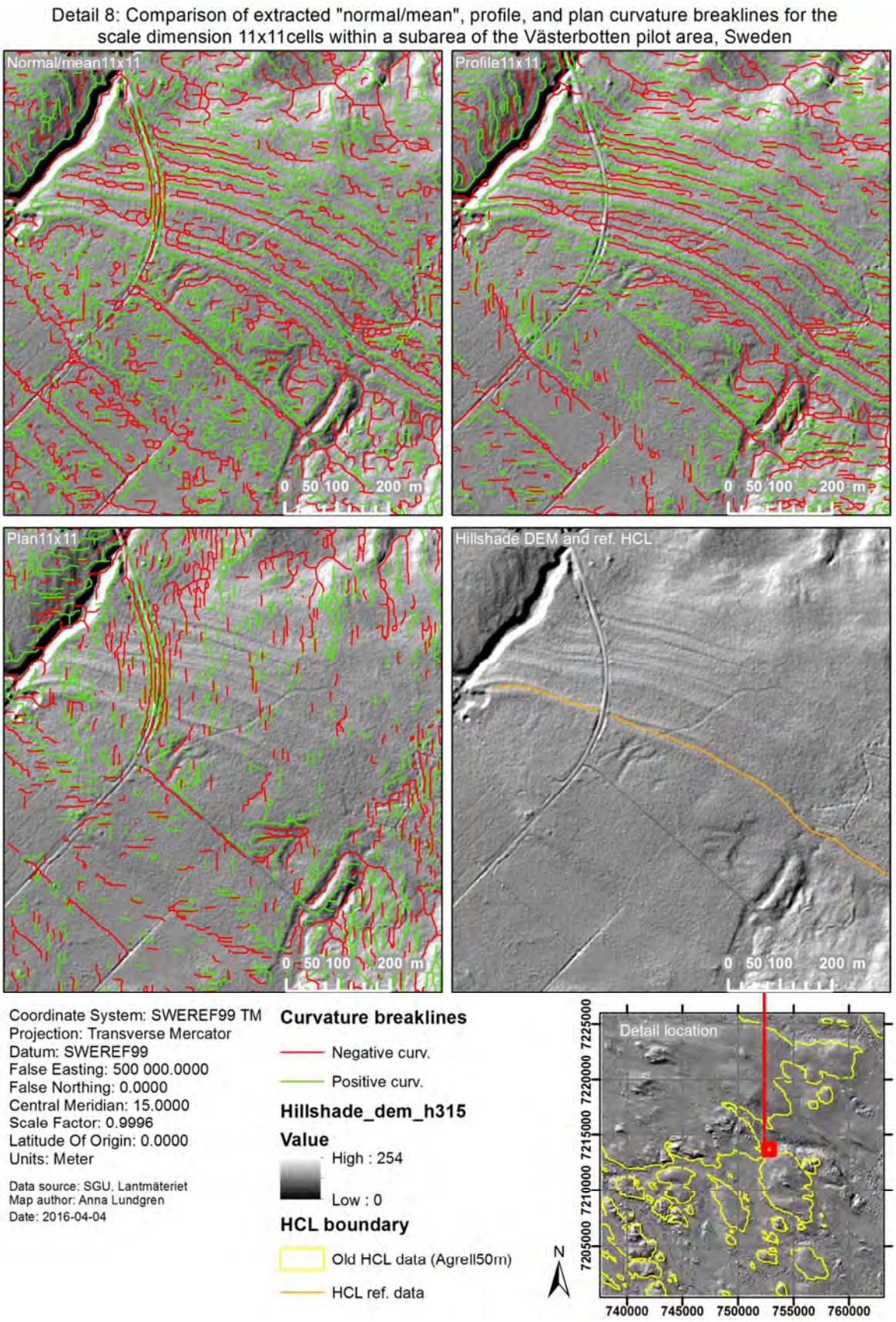

Figure B10. Detail 8 of extracted negative and positive "normal/mean", profile, and plan curvature breaklines for the Västerbotten pilot area.

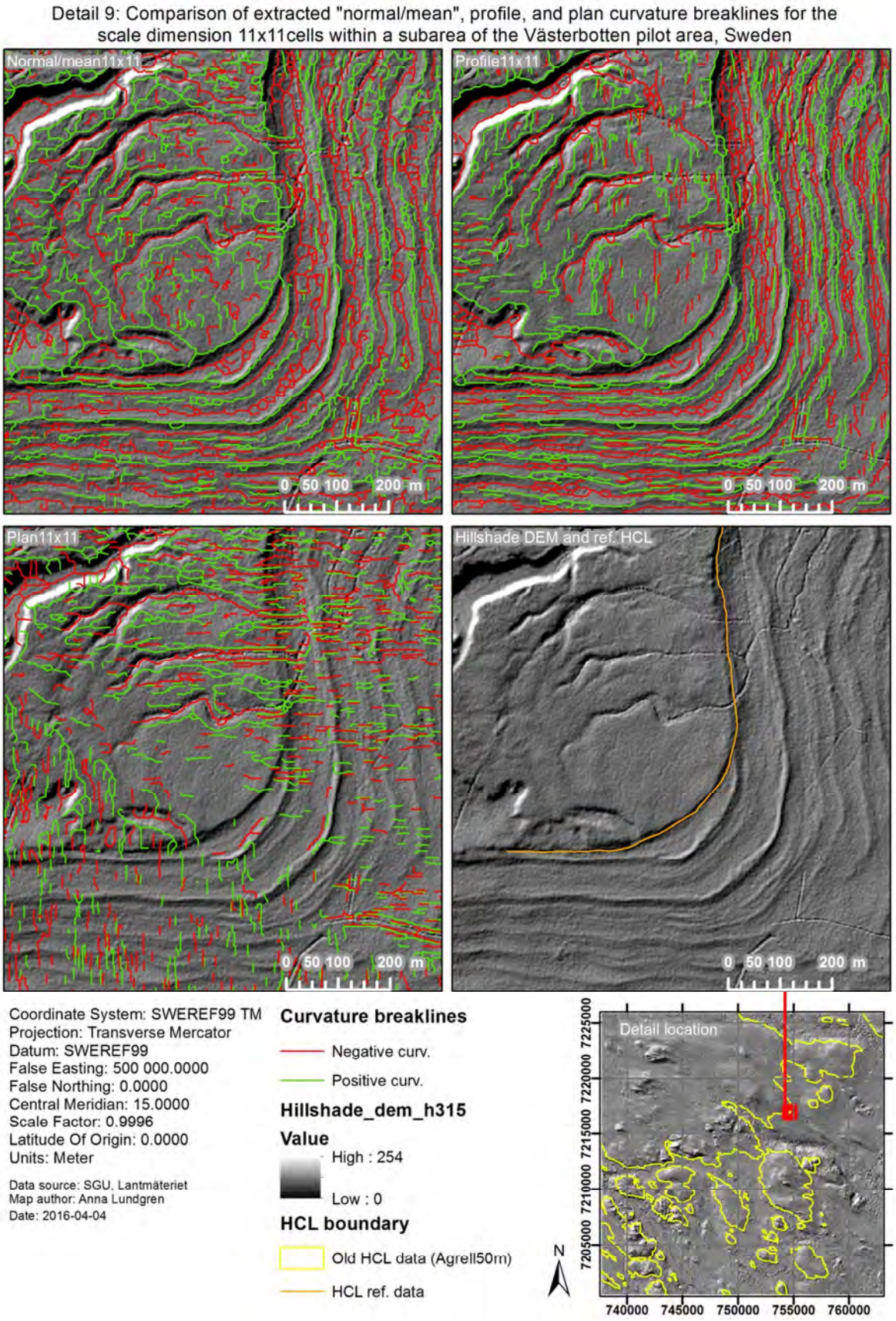

Figure B11. Detail 9 of extracted negative and positive "normal/mean", profile, and plan curvature breaklines for the Västerbotten pilot area.

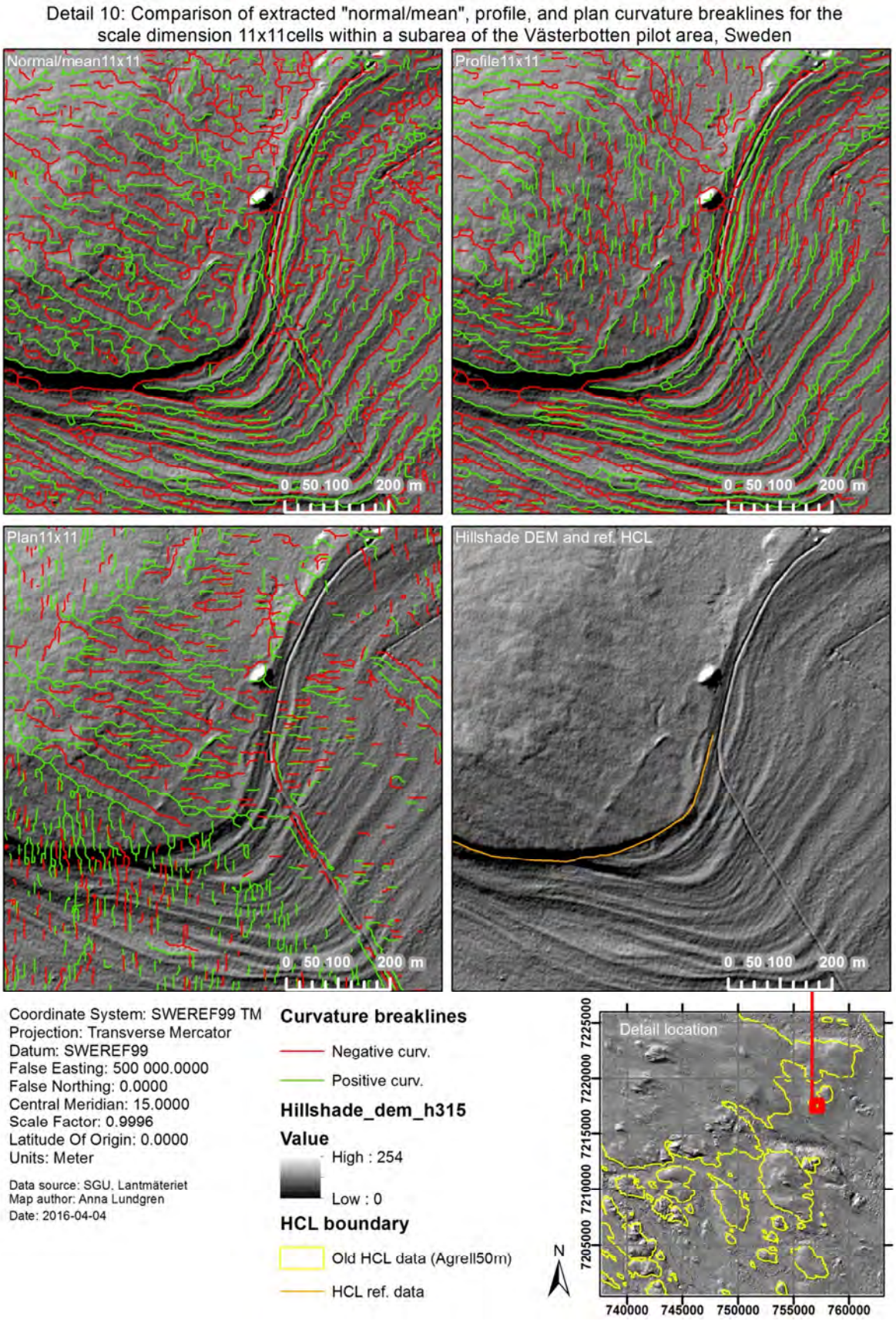

Figure B12. Detail 10 of extracted negative and positive "normal/mean", profile, and plan curvature breaklines for the Västerbotten pilot area.

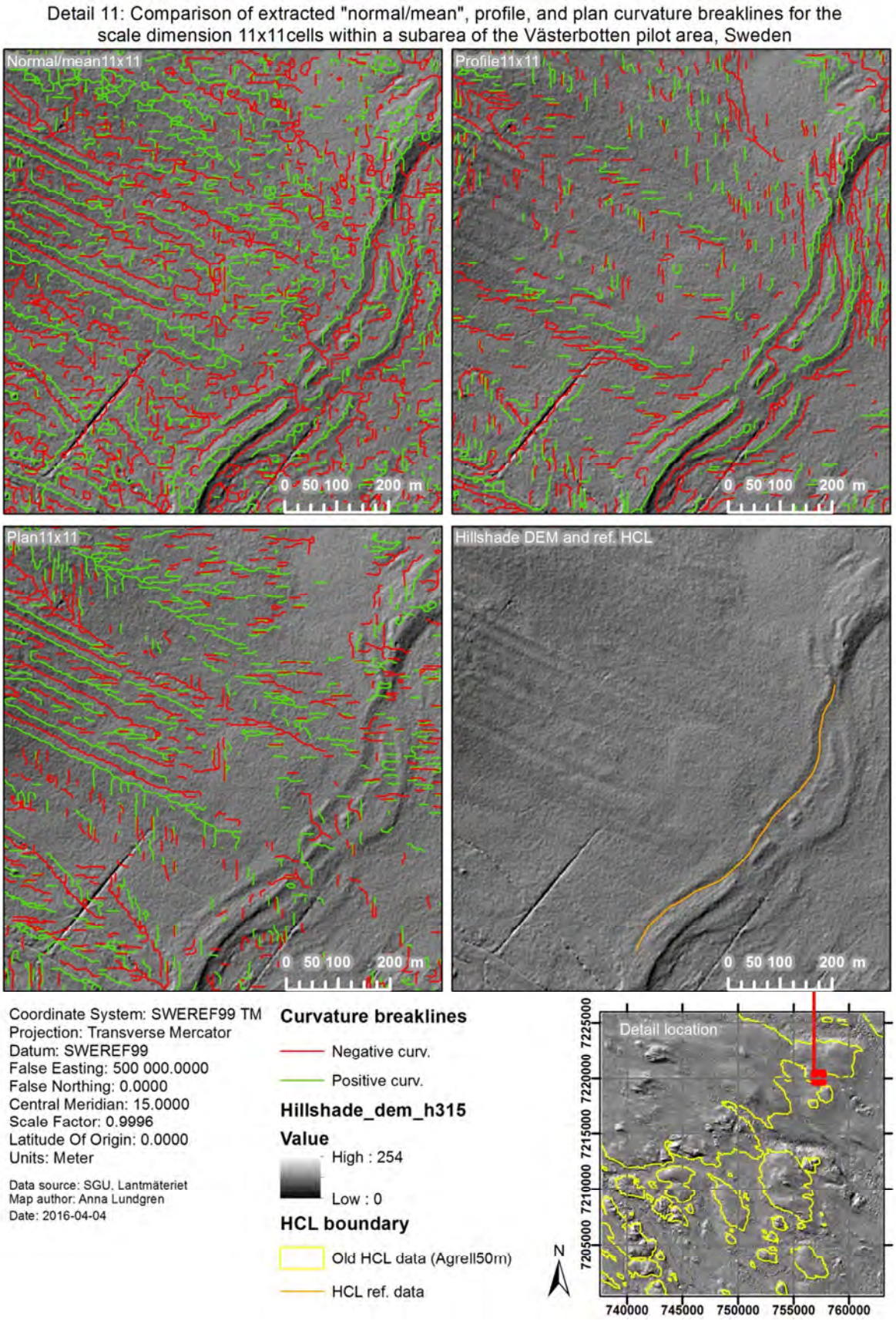

Figure B13. Detail 11 of extracted negative and positive "normal/mean", profile, and plan curvature breaklines for the Västerbotten pilot area.

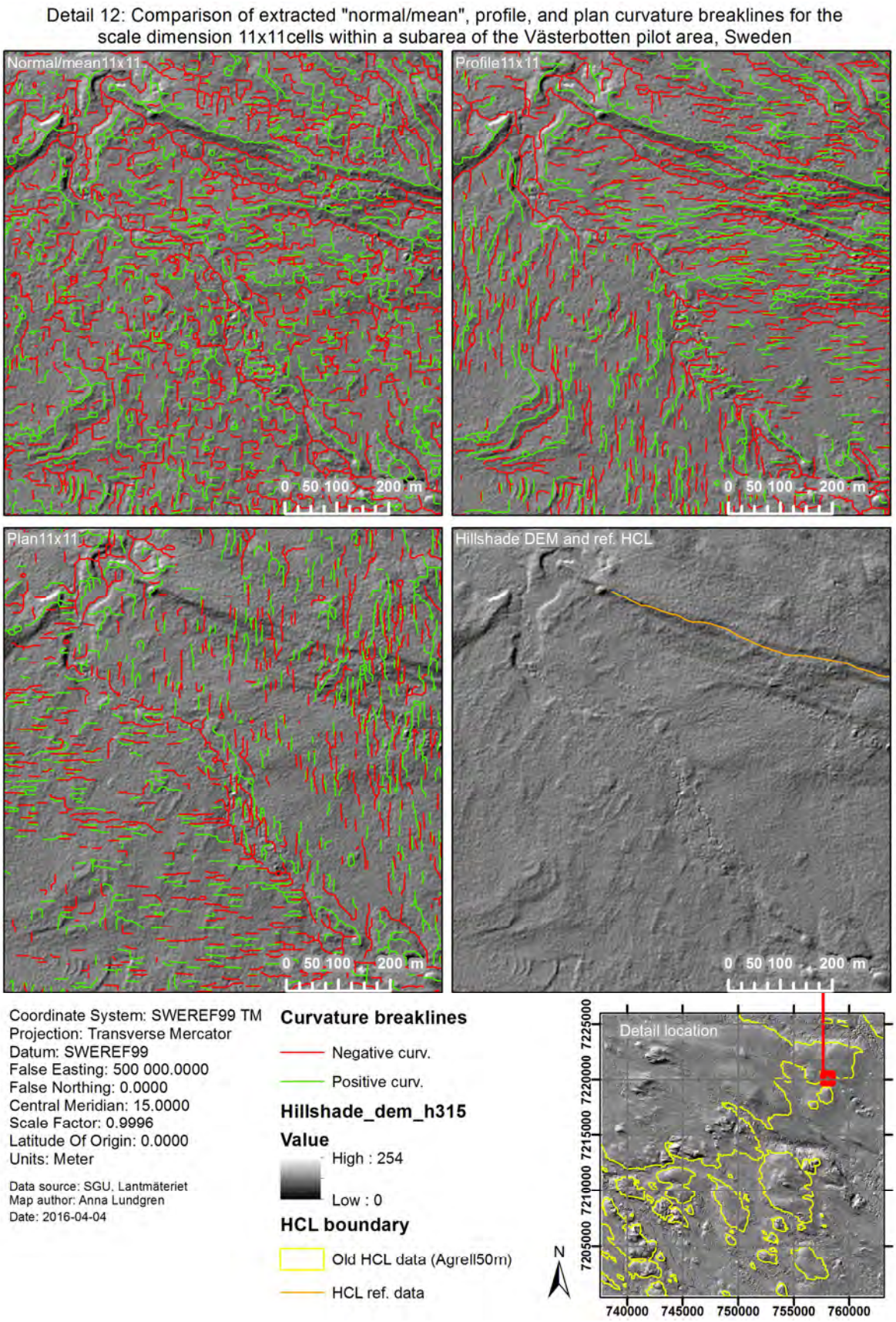

Figure B14. Detail 12 of extracted negative and positive "normal/mean", profile, and plan curvature breaklines for the Västerbotten pilot area.

9.3 Appendix C

Normal Quantile plots of elevation error for the model methods

The normal Quantile plots for the 100 random samples of elevation error for each model method is presented in Figures C1-C7.

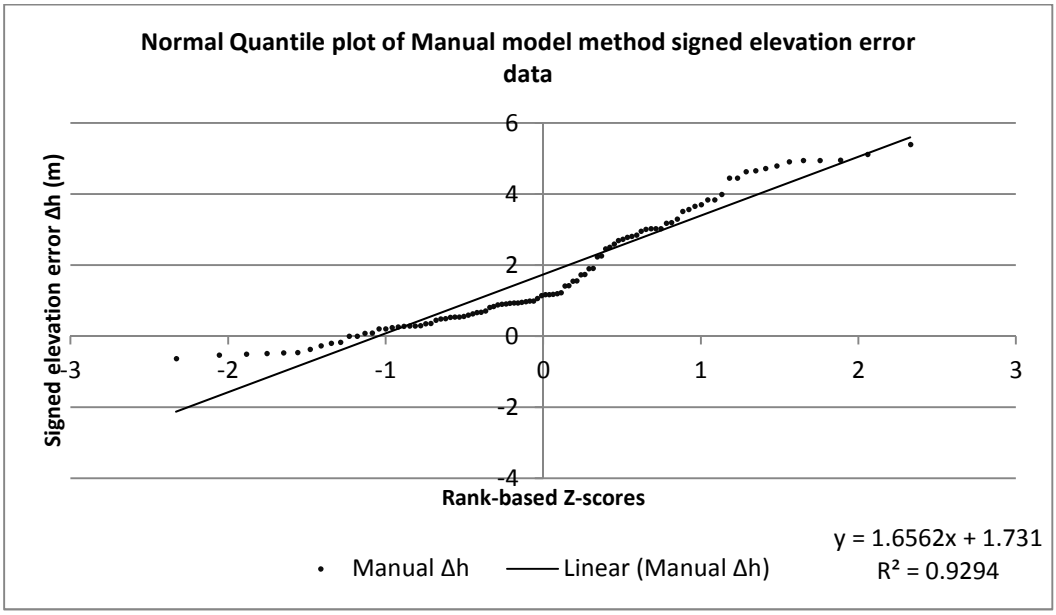

Figure C1. Normal Quantile plot of elevation errors for the 100 random samples along the HCL boundary generated by the Manual model method.

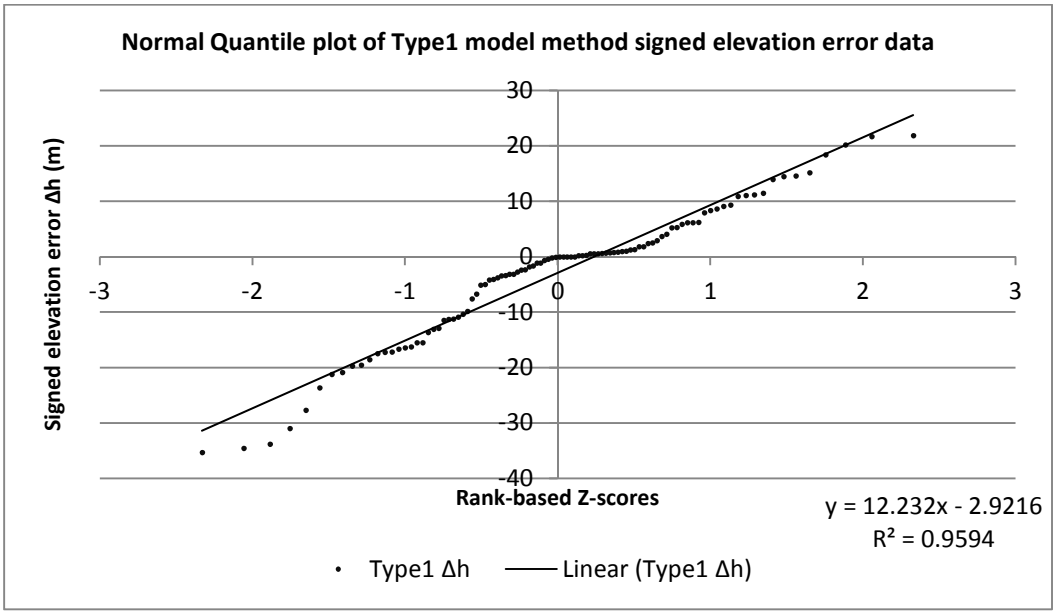

Figure C2. Normal Quantile plot of elevation errors for the 100 random samples along the HCL boundary generated by the Type1 model method.

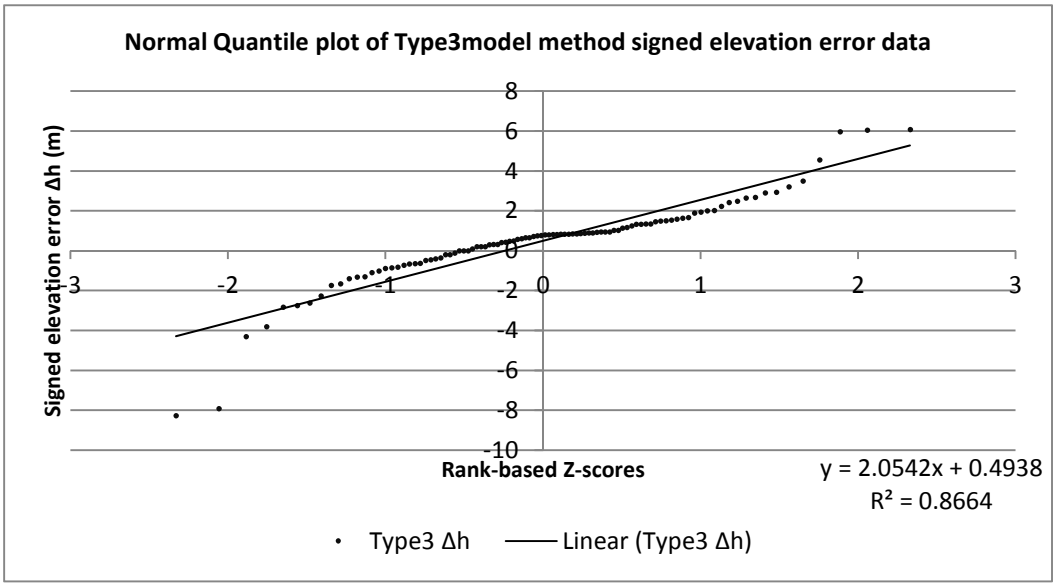

Figure C3. Normal Quantile plot of elevation errors for the 100 random samples along the HCL boundary generated by the Type3 model method.

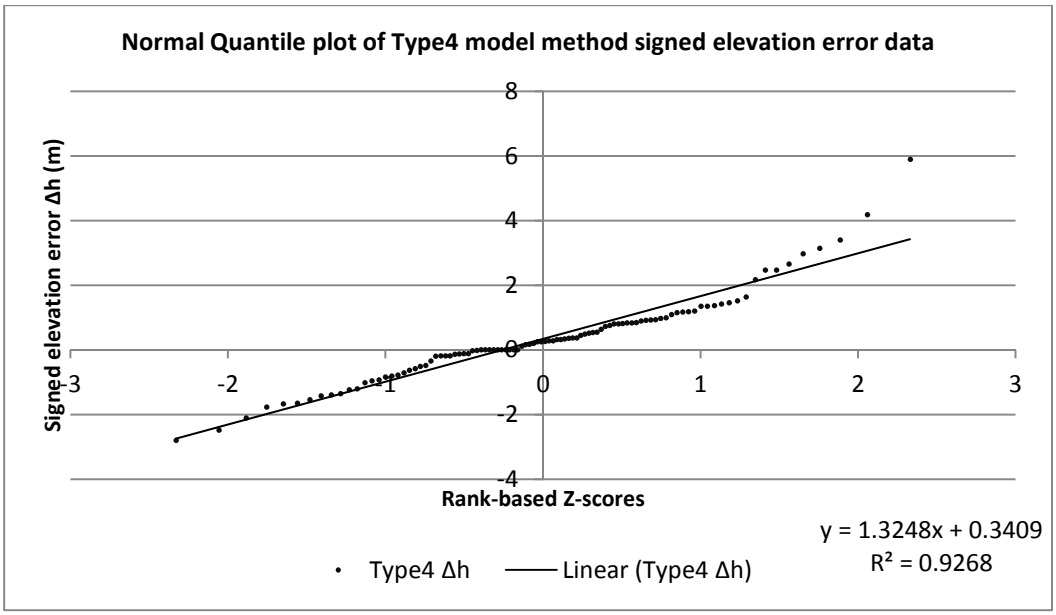

Figure C4. Normal Quantile plot of elevation errors for the 100 random samples along the HCL boundary generated by the Type4 model method.

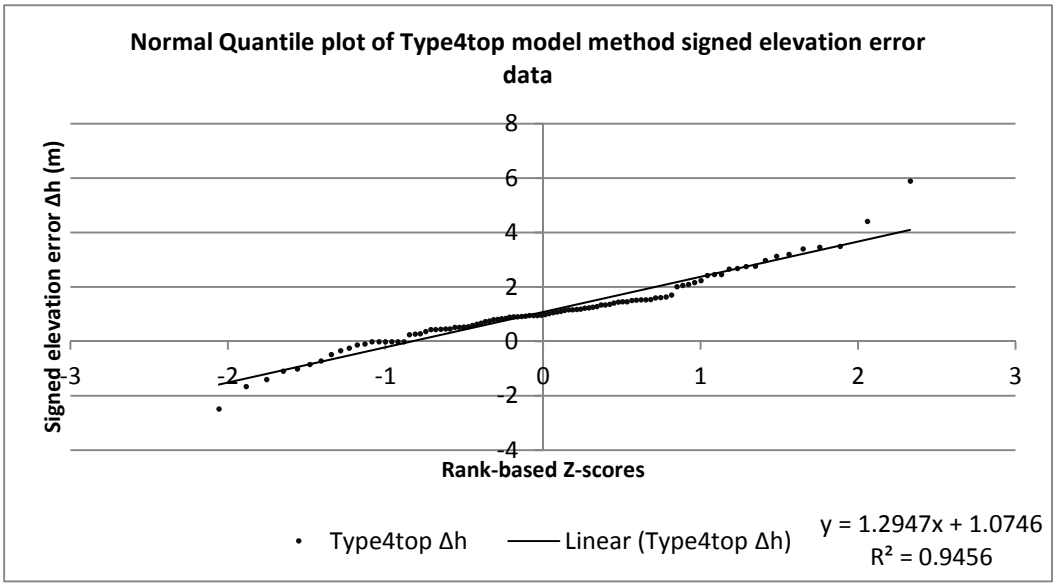

Figure C5. Normal Quantile plot of elevation errors for the 100 random samples along the HCL boundary generated by the Type4top model method.

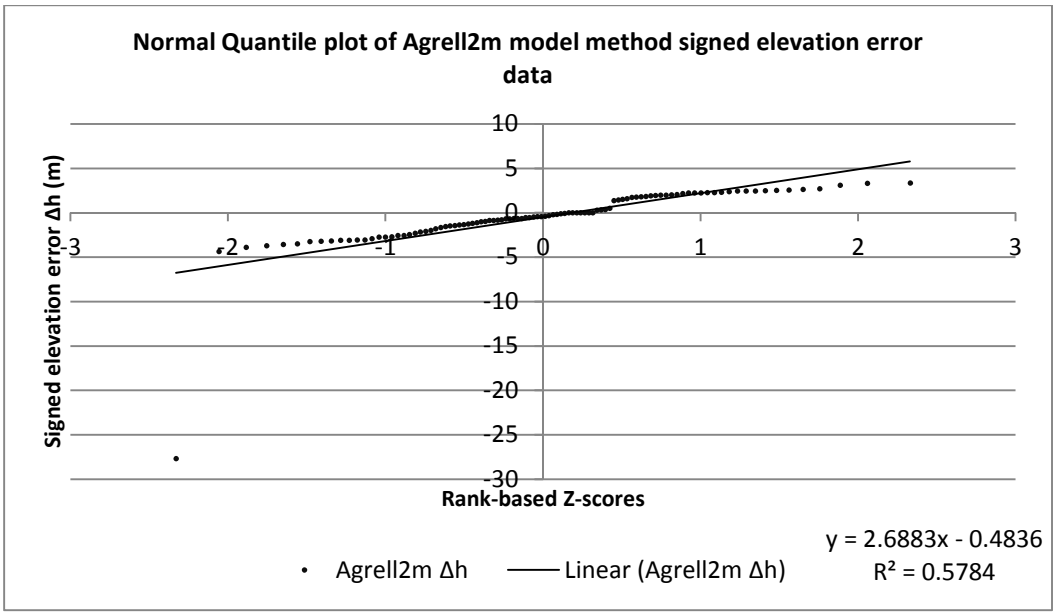

Figure C6. Normal Quantile plot of elevation errors for the 100 random samples along the HCL boundary generated by the Agrell2m model method.

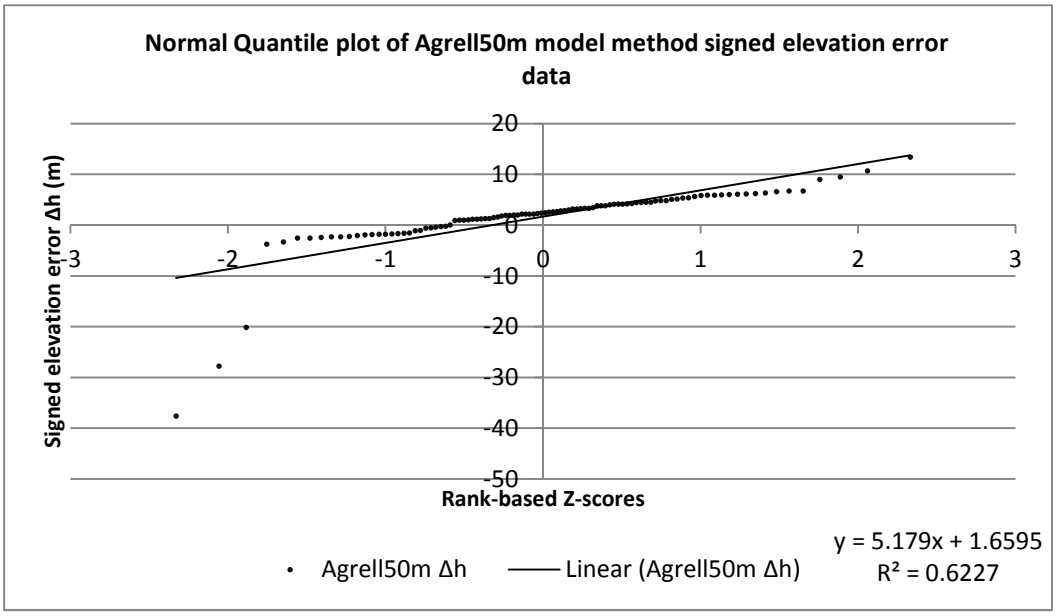

Figure C7. Normal Quantile plot of elevation errors for the 100 random samples along the HCL boundary generated by the Agrell50m model method.

9.4 Appendix D

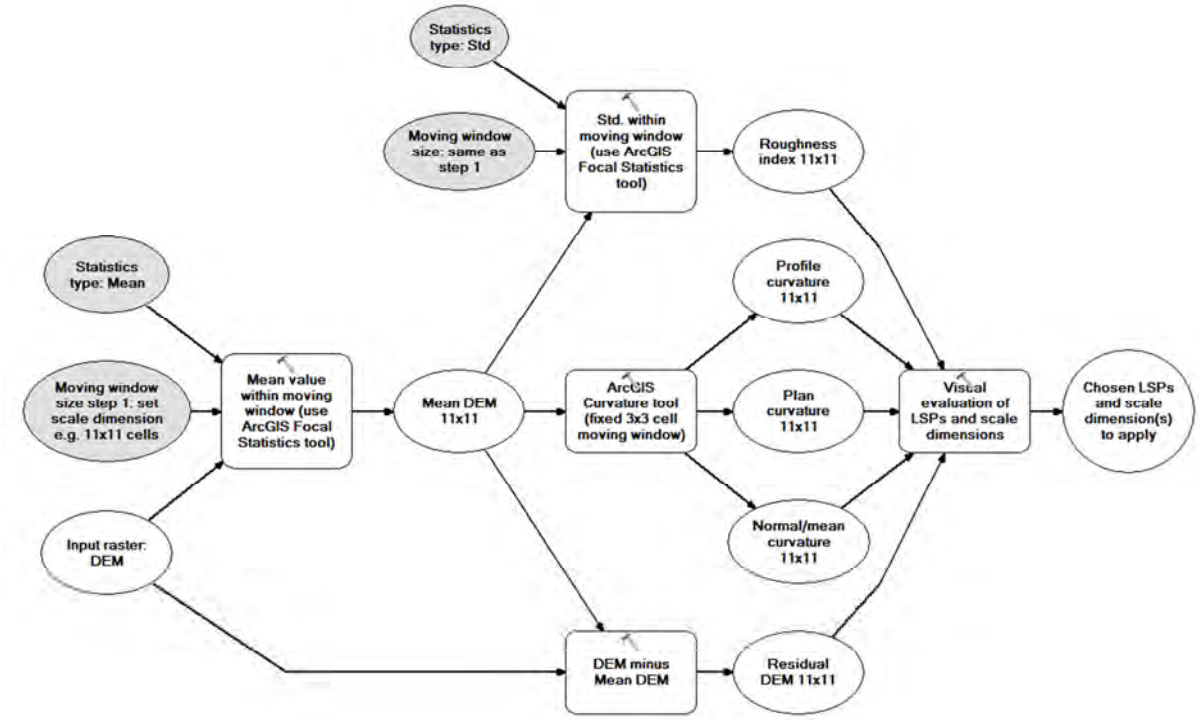

Figure D1 Workflow sketch for the generation of the LSP raters: residual DEM, roughness index, "Normal/mean" curvature, profile curvature, and plan curvature; and the visual scale evaluation. The example is for scale dimension 11x11 cells. Rounded rectangle represent ArcGIS tools used, white ovals represent input and output data, and shaded ovals represent tool settings (ArcGIS 10.2 2015o).

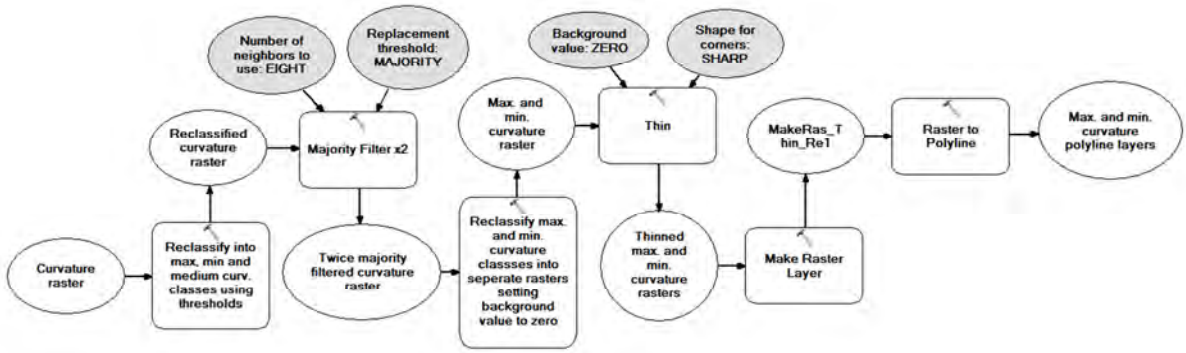

Figure D2 Workflow used for breakline extraction from curvature LSP rasters. Rounded rectangle represent ArcGIS tools used, white ovals represent input and output data, and shaded ovals represent tool settings (ArcGIS 10.2 2015o).

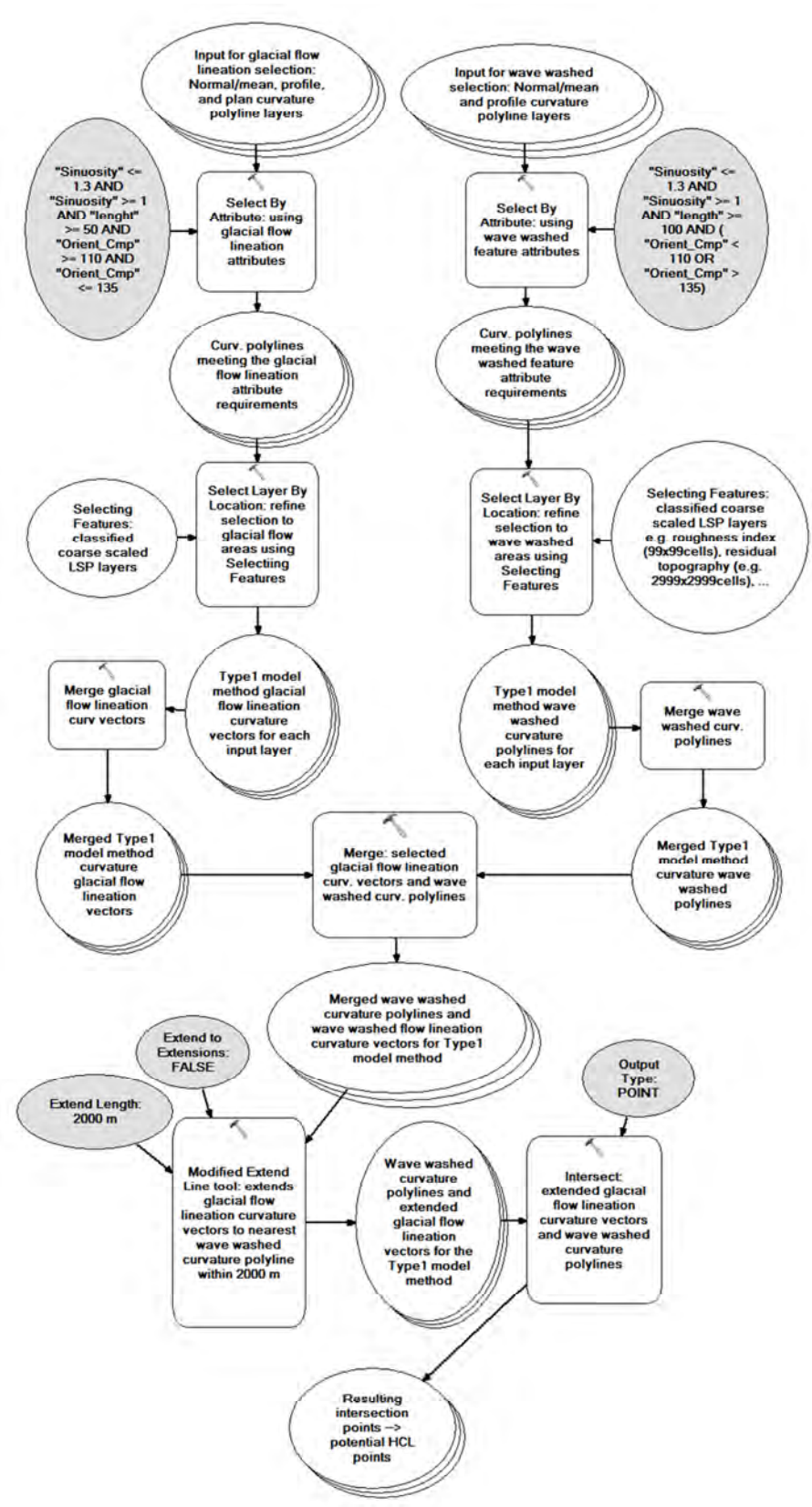

Figure D3 The Type1 model method workflow used for classifying curvature polylines into wave washed and glacial flow lineation breaklines and elongating glacial flow lineation breakline vectors to find intersection points (potential HCL points) with wave washed feature breaklines. Rounded rectangle represent ArcGIS tools used, white ovals represent input and output data, and shaded ovals represent tool settings (ArcGIS 10.2 2015o).

9.5 Appendix E

Ground truth data – digitized and interpolated

Figures E1 and E2 presents the HCL reference data used for the evaluation of the model methods in the Västerbotten pilot area.

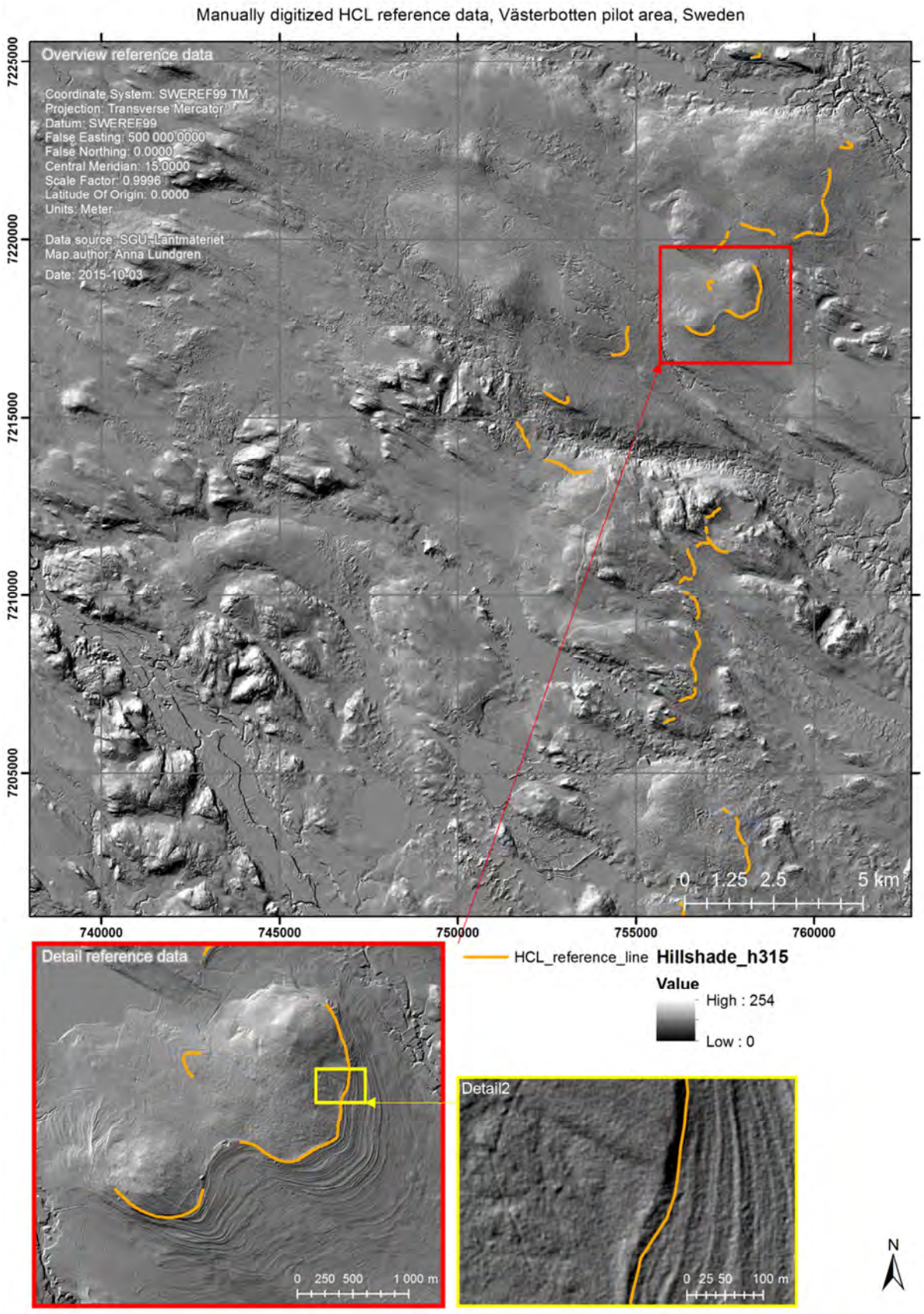

Figure E1. HCL reference data manually digitized using high resolution hillshade maps.

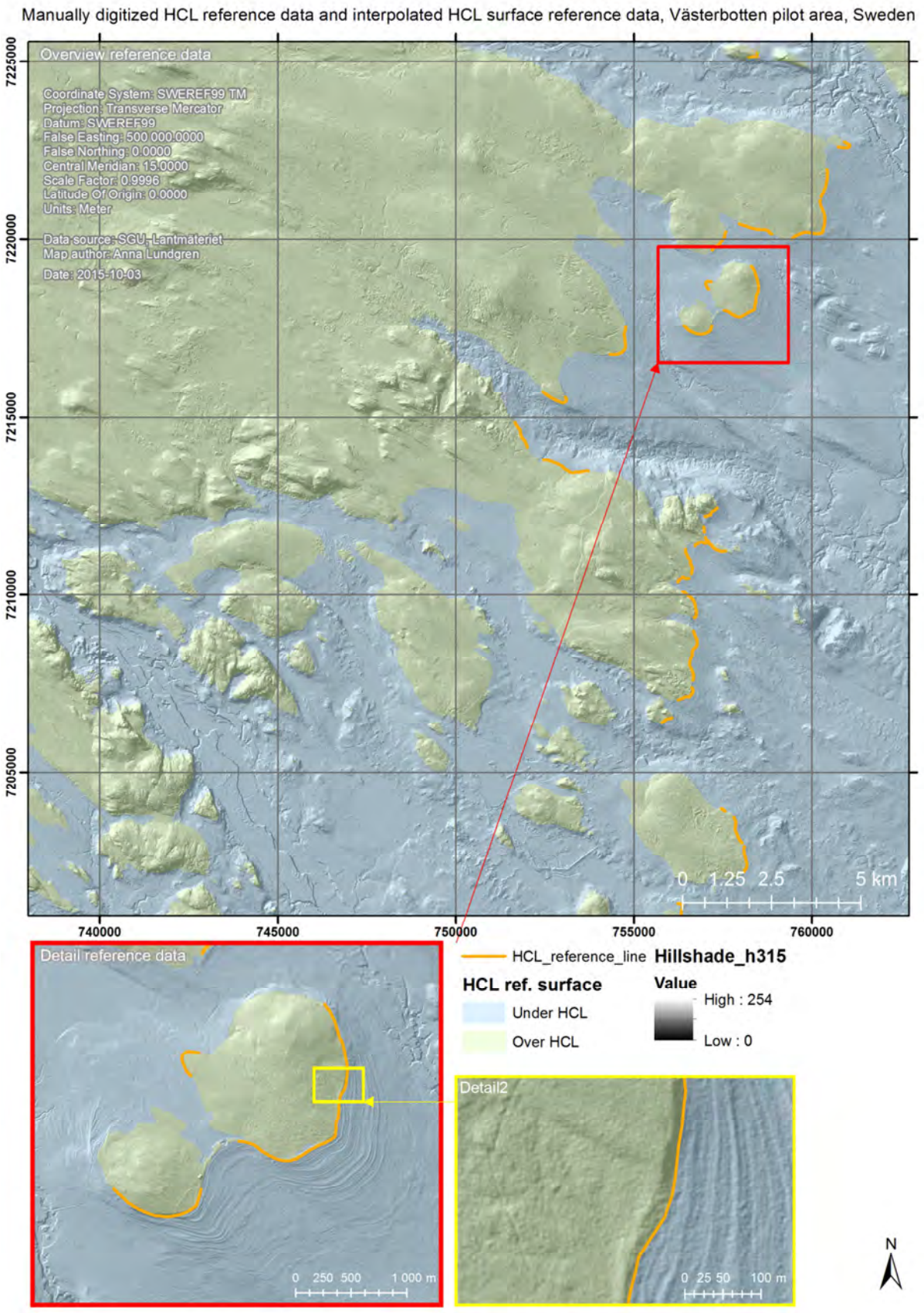

Figure E2. HCL surface reference data interpolated from manually digitized HCL reference data.

9.6 Appendix F

Table F1 Overall Kappa estimation values for model methods Manual, Type1, Type3, Type4, Type4top, Agrell2m, and Agrell50m for each evaluated area size (indicated by buffer) around the reference data. The lowest values are highlighted in red, the intermediate values are highlighted in yellow, and the highest values are highlighted in green.

Evaluation area	**Overall Kappa estimation for model methods:**						
	Manual	*Type1*	*Type3*	*Type4*	*Type4top*	*Agrell2m*	*Agrell50m*
Buff. 11 m	0.376	0.090	0.274	0.324	0.247	0.215	0.050
Buff. 50 m	0.604	0.253	0.658	0.734	0.694	0.533	0.289
Buff. 100 m	0.718	0.338	0.793	0.846	0.826	0.696	0.488
Buff. 1500 m	0.947	0.583	0.954	0.967	0.968	0.953	0.912
'Whole area'	0.952	0.381	0.956	0.962	0.960	0.974	0.946

Table F2 Estimated individual Kappa values for class 1 and class 2 within the evaluation areas: buff 11m, 50m, 100m, 1500m, and 'whole area'. The lowest values are highlighted in red, the intermediate values are highlighted in yellow, and the highest values are highlighted in green.

Evaluation area	**Individual Kappa estimation for class 1: land area under HCL**						
	Manual	*Type1*	*Type3*	*Type4*	*Type4top*	*Agrell2m*	*Agrell50m*
Buff. 11 m	0.784	0.081	0.351	0.394	0.646	0.207	0.113
Buff. 50 m	0.903	0.217	0.672	0.780	0.929	0.527	0.532
Buff. 100 m	0.946	0.298	0.783	0.868	0.953	0.713	0.766
Buff. 1500 m	0.997	0.585	0.929	0.955	0.968	0.963	0.976
'Whole area'	1.000	0.666	0.962	0.970	0.964	0.987	0.988
Evaluation area	**Individual Kappa estimation for class 2: land area over HCL**						
	Manual	*Type1*	*Type3*	*Type4*	*Type4top*	*Agrell2m*	*Agrell50m*
Buff. 11 m	0.248	0.101	0.225	0.275	0.152	0.224	0.032
Buff. 50 m	0.453	0.302	0.644	0.693	0.554	0.540	0.198
Buff. 100 m	0.579	0.392	0.804	0.826	0.728	0.680	0.358
Buff. 1500 m	0.901	0.581	0.981	0.980	0.967	0.943	0.857
'Whole area'	0.908	0.267	0.950	0.955	0.956	0.961	0.908

Table F3 Areal difference values for model methods Manual, Type1, Type3, Type4, Type4top, Agrell2m, and Agrell 50m within the evaluation areas: buff. 11m, buff. 50m, buff. 100m, buff. 1500m, and whole area. The highest values are highlighted in red, the intermediate values are highlighted in yellow, and the lowest values are highlighted in green.

Evaluation area	**Areal difference estimation for class 1: land area under HCL**						
	Manual	*Type1*	*Type3*	*Type4*	*Type4top*	*Agrell2m*	*Agrell50m*
Buff 11	0.5213	-0.1130	0.2185	0.1782	0.6200	-0.0395	0.5553
Buff. 50m	0.3000	-0.1524	0.0203	0.0549	0.2302	-0.0109	0.4104
Buff. 100m	0.2092	-0.1240	-0.0123	0.0222	0.1175	0.0216	0.3113
Buff. 1500m	0.0339	0.0027	-0.0187	-0.0091	0.0004	0.0071	0.0431
'Whole area'	0.0470	0.4170	0.0060	0.0078	0.0042	0.0128	0.0414
Evaluation area	**Areal difference estimation for class 2: land area over HCL**						
	Manual	*Type1*	*Type3*	*Type4*	*Type4top*	*Agrell2m*	*Agrell50m*
Buff 11	-0.5194	0.1126	-0.2177	-0.1775	-0.6177	0.0394	-0.5532
Buff. 50m	-0.3477	0.1767	-0.0235	-0.0636	-0.2669	0.0126	-0.4757
Buff. 100m	-0.2599	0.1541	0.0152	-0.0275	-0.1460	-0.0268	-0.3869

Buff. 1500m	-0.0661	-0.0052	0.0364	0.0177	-0.0008	-0.0139	-0.0840
'Whole area'	-0.0489	-0.4332	-0.0063	-0.0081	-0.0044	-0.0133	-0.0430

Table F4 Completeness, correctness, quality, and redundancy measures for the evaluation of the classification accuracy of the total HCL boundary and the HCL boundary within the 200 m flat buffer around the reference data for the Västerbotten pilot area. For the completeness, correctness, and quality measures the highest values are highlighted in green, the second highest values are highlighted in yellow, the second lowest values are highlighted in orange, and the lowest values are highlighted in red.

"Buffer method" measures for total HCL boundary							
	Manual	*Type1*	*Type3*	*Type4*	*Type4top*	*Agrell2m*	*Agrell50m*
Completeness	0.302	0.090	0.167	0.263	0.237	0.260	0.077
Correctness	0.302	0.001	0.151	0.241	0.213	0.275	0.133
Quality	0.176	0.018	0.086	0.147	0.126	0.154	0.044
Redundancy	-0.022	0.038	-0.003	0.046	0.003	-0.007	-0.276
"Buffer method" measures for HCL boundary within 200 m flat buffer around reference HCL							
	Manual	*Type1*	*Type3*	*Type4*	*Type4top*	*Agrell2m*	*Agrell50m*
Completeness	0.419	0.156	0.435	0.660	0.429	0.212	0.063
Correctness	0.451	0.078	0.320	0.413	0.314	0.245	0.108
Quality	0.267	0.055	0.224	0.348	0.222	0.125	0.032
Redundancy	-0.096	-0.004	-0.032	0.130	0.007	-0.064	-0.473

Series from Lund University

Department of Physical Geography and Ecosystem Science

Master Thesis in Geographical Information Science

1. *Anthony Lawther:* The application of GIS-based binary logistic regression for slope failure susceptibility mapping in the Western Grampian Mountains, Scotland. (2008).

2. *Rickard Hansen:* Daily mobility in Grenoble Metropolitan Region, France. Applied GIS methods in time geographical research. (2008).

3. *Emil Bayramov:* Environmental monitoring of bio-restoration activities using GIS and Remote Sensing. (2009).

4. *Rafael Villarreal Pacheco:* Applications of Geographic Information Systems as an analytical and visualization tool for mass real estate valuation: a case study of Fontibon District, Bogota, Columbia. (2009).

5. *Siri Oestreich Waage:* a case study of route solving for oversized transport: The use of GIS functionalities in transport of transformers, as part of maintaining a reliable power infrastructure (2010).

6. *Edgar Pimiento:* Shallow landslide susceptibility – Modelling and validation (2010).

7. *Martina Schäfer:* Near real-time mapping of floodwater mosquito breeding sites using aerial photographs (2010)

8. *August Pieter van Waarden-Nagel:* Land use evaluation to assess the outcome of the programme of rehabilitation measures for the river Rhine in the Netherlands (2010)

9. *Samira Muhammad:* Development and implementation of air quality data mart for Ontario, Canada: A case study of air quality in Ontario using OLAP tool. (2010)

10. *Fredros Oketch Okumu*: Using remotely sensed data to explore spatial and temporal relationships between photosynthetic productivity of vegetation and malaria transmission intensities in selected parts of Africa (2011)

11. *Svajunas Plunge:* Advanced decision support methods for solving diffuse water pollution problems (2011)

12. *Jonathan Higgins:* Monitoring urban growth in greater Lagos: A case study using GIS to monitor the urban growth of Lagos 1990 - 2008 and produce future growth prospects for the city (2011).

13. *Mårten Karlberg:* Mobile Map Client API: Design and Implementation for Android (2011).

14. *Jeanette McBride:* Mapping Chicago area urban tree canopy using color infrared imagery (2011)

15. *Andrew Farina:* Exploring the relationship between land surface temperature and vegetation abundance for urban heat island mitigation in Seville, Spain (2011)

16. *David Kanyari*: Nairobi City Journey Planner An online and a Mobile Application (2011)

17. *Laura V. Drews:* Multi-criteria GIS analysis for siting of small wind power plants - A

case study from Berlin (2012)

18. *Qaisar Nadeem:* Best living neighborhood in the city - A GIS based multi criteria evaluation of ArRiyadh City (2012)

19. *Ahmed Mohamed El Saeid Mustafa:* Development of a photo voltaic building rooftop integration analysis tool for GIS for Dokki District, Cairo, Egypt (2012)

20. *Daniel Patrick Taylor*: Eastern Oyster Aquaculture: Estuarine Remediation via Site Suitability and Spatially Explicit Carrying Capacity Modeling in Virginia's Chesapeake Bay (2013)

21. *Angeleta Oveta Wilson:* A Participatory GIS approach to *unearthing* Manchester's Cultural Heritage '*gold mine'* (2013)

22. *Ola Svensson:* Visibility and Tholos Tombs in the Messenian Landscape: A Comparative Case Study of the Pylian Hinterlands and the Soulima Valley (2013)

23. *Monika Ogden:* Land use impact on water quality in two river systems in South Africa (2013)

24. *Stefan Rova:* A GIS based approach assessing phosphorus load impact on Lake Flaten in Salem, Sweden (2013)

25. *Yann Buhot:* Analysis of the history of landscape changes over a period of 200 years. How can we predict past landscape pattern scenario and the impact on habitat diversity? (2013)

26. *Christina Fotiou:* Evaluating habitat suitability and spectral heterogeneity models to predict weed species presence (2014)

27. *Inese Linuza:* Accuracy Assessment in Glacier Change Analysis (2014)

28. *Agnieszka Griffin:* Domestic energy consumption and social living standards: a GIS analysis within the Greater London Authority area (2014)

29. *Brynja Guðmundsdóttir:* Detection of potential arable land with remote sensing and GIS - A Case Study for Kjósarhreppur (2014)

30. *Oleksandr Nekrasov:* Processing of MODIS Vegetation Indices for analysis of agricultural droughts in the southern Ukraine between the years 2000-2012 (2014)

31. *Sarah Tressel:* Recommendations for a polar Earth science portal in the context of Arctic Spatial Data Infrastructure (2014)

32. *Caroline Gevaert:* Combining Hyperspectral UAV and Multispectral Formosat-2 Imagery for Precision Agriculture Applications (2014).

33. *Salem Jamal-Uddeen:* Using GeoTools to implement the multi-criteria evaluation analysis - weighted linear combination model (2014)

34. *Samanah Seyedi-Shandiz:* Schematic representation of geographical railway network at the Swedish Transport Administration (2014)

35. *Kazi Masel Ullah:* Urban Land-use planning using Geographical Information System and analytical hierarchy process: case study Dhaka City (2014)

36. *Alexia Chang-Wailing Spitteler:* Development of a web application based on MCDA

and GIS for the decision support of river and floodplain rehabilitation projects (2014)

37. *Alessandro De Martino:* Geographic accessibility analysis and evaluation of potential changes to the public transportation system in the City of Milan (2014)

38. *Alireza Mollasalehi:* GIS Based Modelling for Fuel Reduction Using Controlled Burn in Australia. Case Study: Logan City, QLD (2015)

39. *Negin A. Sanati:* Chronic Kidney Disease Mortality in Costa Rica; Geographical Distribution, Spatial Analysis and Non-traditional Risk Factors (2015)

40. *Karen McIntyre:* Benthic mapping of the Bluefields Bay fish sanctuary, Jamaica (2015)

41. *Kees van Duijvendijk:* Feasibility of a low-cost weather sensor network for agricultural purposes: A preliminary assessment (2015)

42. *Sebastian Andersson Hylander:* Evaluation of cultural ecosystem services using GIS (2015)

43. *Deborah Bowyer:* Measuring Urban Growth, Urban Form and Accessibility as Indicators of Urban Sprawl in Hamilton, New Zealand (2015)

44. *Stefan Arvidsson:* Relationship between tree species composition and phenology extracted from satellite data in Swedish forests (2015)

45. *Damián Giménez Cruz*: GIS-based optimal localisation of beekeeping in rural Kenya (2016)

46. *Alejandra Narváez Vallejo:* Can the introduction of the topographic indices in LPJ-GUESS improve the spatial representation of environmental variables? (2016)

47. *Anna Lundgren:* Development of a method for mapping the highest coastline in Sweden using breaklines extracted from high resolution digital elevation models. (2016)